July 2017

A Landscape of Thermal Inequity: Social Vulnerability to Urban Heat in U.S. Cities

Bruce Coffyn Mitchell
University of South Florida, bmitchell@ncrc.org

A Landscape of Thermal Inequity:

Social Vulnerability to Urban Heat in U.S. Cities

by

Bruce Coffyn Mitchell

A dissertation submitted in partial fulfillment
of the requirements for the degree of
Doctor of Philosophy Geography, Environment, and Planning
School of Geosciences
College of Arts and Sciences
University of South Florida

Co-Major Professor Jayajit Chakraborty, Ph.D.
Co-Major Professor M. Martin Bosman, Ph.D.
Kamal Alsharif, Ph.D.
Timothy W. Collins, Ph.D.
Sara E. Grineski, Ph.D.
Ruiliang Pu, Ph.D.

Date of Approval:
May 12, 2017

Keywords: urban geography, environmental justice, climate justice, climate change, urban heat island (UHI), social vulnerability

ACKNOWLEDGEMENTS

First and foremost, I wish to thank my family for their patience and understanding during the process of researching and writing this work. My wife, Olivia has tirelessly "filled-in" for me, supporting the effort to finish this project. My daughter Zoe is always a gem and provided an occasional excuse to take a walk, helping me to refresh my thinking. Also my mother, Lili Coffyn, has been a cheerful sounding board for ideas. Special thanks to my advisor and co-author, Dr. Jayajit Chakraborty, who provided me with a wealth of information as the methodology was developed to test these ideas. He has been a steadfast support through graduate school and a constant example of dedication, clear thinking, and methodological rigor. Thanks to my co-advisor Dr. Martin Bosman. Our many discussions have been a great joy, which have balanced my quantitative approaches with theoretical insight. Many thanks to Dr. Ruiliang Pu who patiently taught me remote sensing techniques, and provided the mono-window algorithm for calculating land surface temperature. Also my thanks to Dr. Kamal Alsharif, Dr. Timothy Collins, Dr. Joni Firat and Dr. Sara Grineski whose knowledge of the subject matter has been very valuable. Finally, I want to thank my employer, the National Community Reinvestment Coalition, and my director Jason Richardson for material support which was critical as I finished this work. NCRC is one of the organizations at the forefront of the fight for greater equity and social justice.

TABLE OF CONTENTS

LIST OF TABLES

LIST OF FIGURES

ABSTRACT

A combination of the urban heat island effect and a rising temperature baseline resulting from global climate change inequitably impacts socially vulnerable populations residing in urban areas. This dissertation examines distributional inequity of exposure to urban heat by socially disadvantaged groups and minorities in the context of climate justice. Using Cutter's hazards-of-place model, variables indicative of social vulnerability and biophysical vulnerability are statistically tested for their associations. Biophysical vulnerability is conceptualized utilizing a urban heat risk index calculated from summer 2010 LANDSAT imagery to measure land surface temperature , structural density through the normalized difference built-up index, and vegetation abundance through the normalized difference vegetation index. A cross-section of twenty geographically distributed metropolitan statistical areas (MSAs) in the U.S. are examined using census derived variables at the tract level. The results of bivariate correlation analysis, ordinary least squares regression, and spatial autoregression analysis indicate consistent and significant associations between greater social disadvantage and higher urban heat levels. Multilevel modeling is used to examine the relationship of MSA-level segregation with tract-level minority status and social disadvantage to higher levels of urban heat. Segregation has a significant but varied relationship with the variables, indicating that there are inconsistent associations with urban heat due to differing urban ecologies. Urban heat and social vulnerability present a varying landscape of thermal inequity in different urban areas, associated in many cases with residential segregation.

CHAPTER ONE:

INTRODUCTION

The combined effects of two global trends, urbanization and climate change, have generated considerable concern regarding their adverse and disproportionate impacts on the health of urban populations. Urbanization increases population density and leads to the spatial expansion of cities, replacing vegetation with built structures of generally lower albedo, greater impervious surface area, and higher thermal mass (Golden 2004). Conventional methods of urban development which alter the thermal exchange between the land surface and lower atmosphere at a local scale, result in higher urban heat levels, a phenomenon referred to as the urban heat island (UHI) effect (Oke 1992). Urban heat is an important example of anthropogenic impact on the environment, specifically human/earth interaction through urbanization, which has received scant attention from urban geographers. On the other hand, the UHI has been a long-standing topic of investigation by urban climatologists (Stewart 2010). Their efforts have been directed toward modeling the complex dynamics of the UHI at the lowest levels of the atmosphere, where surface, canopy, and boundary layers interact. Consequently, a descriptive approach to urban heat characterizes the work of urban climatologists and physical geographers. With a few exceptions, the study of the adverse health impacts of urban heat and heat waves has remained within the domain of public health or natural hazards research.

There are multiple social and physical factors which increase the risk from urban heat including urbanization, shifting demographic patterns, and climate change. Worldwide, the patterns of human habitation have become increasingly urbanized, exceeding 50 percent urbanization around 2008 (UNDESA 2011). Meanwhile, the population age structure, particularly those of post-industrial nations, is expected to become older as birthrates decrease and life spans increase (UNDESA 2002). These demographic shifts are occurring simultaneously as a higher global temperature baseline changes the climate of areas, causing weather to become more variable and subject to extremes (IPCC 2007). Already in North America there have been temperature increases of 0.17 to 0.25 degrees Celsius per decade since the 1970's (USEPA 2013). The increasing temperature baseline and greater extremes in high temperature seem related to a higher incidence of heat waves (Gaffen and Ross 1998; Hales et al. 2003; Meehl and Tebaldi 2004).

Social Vulnerability

Excessive heat, especially during heat waves, is among the foremost natural hazards related cause of fatality in the U.S. (NOAA NWS 2013). While urban climatologists and atmospheric scientists have defined a heat wave in multiple ways, it can be considered as two or more days of abnormally and uncomfortably hot and unusually humid weather conditions (NOAA NWS 2012). Urban heat is a causal factor in increased morbidity and mortality from heat exposure, and also contributes to other health issues, like cardiovascular and respiratory illnesses (Hales et al. 2003). Numerous empirical studies have reported increased rates of morbidity and mortality among socially vulnerable populations during heat waves in urban areas

(Kalkstein and Davis 1987; Kalkstein and Greene 1997; Whitman et al. 1997; O'Neill 2003; Sheridan, Kalkstein, A.J., and Kalkstein, L.S. 2008). The empirical evidence suggests that the oldest and youngest, least educated, economically disadvantaged, and racial/ethnic minority residents are particularly vulnerable to the effects of urban heat in U.S. metropolitan areas (Ellis 1978; McGeehin and Mirabelli 2001; Basu and Ostro 2008). The concept of social vulnerability is established in natural hazards research (Cutter et al. 1997; 2009), and here refers to an increased sensitivity to hazards depending on demographic, socioeconomic, or housing characteristics of people in communities. Urban heat highlights the issue of social vulnerability to a hazard which is distributed inequitably across urban areas and populations.

The distribution of vulnerability to hazards in different places is a central topic in the hazards research literature. Cutter (1996) proposed a hazards-of-place model of vulnerability which focuses on specific place-based interaction between biophysical vulnerability and social vulnerability. As shown in Figure 1, risk is directly impacted by efforts to mitigate it in this model. Both risk and mitigation establish the hazard potential which in turn has a geographic context and impacts the social fabric of communities. The geographic context impacts biophysical vulnerability; and the social fabric, social vulnerability. Both components (biophysical and social vulnerability) collectively affect overall place vulnerability which goes full circle to impact risk and mitigation. This is a highly dynamic model in which Cutter has operationalized a cascading series of relationships to examine issues like community resilience (Cutter et al. 2008). This dissertation concerns itself with the evaluation of hazards-of-place by examining the interplay of biophysical and social vulnerability in U.S. urban areas at the census tract level, which are used as a proxy for neighborhoods.

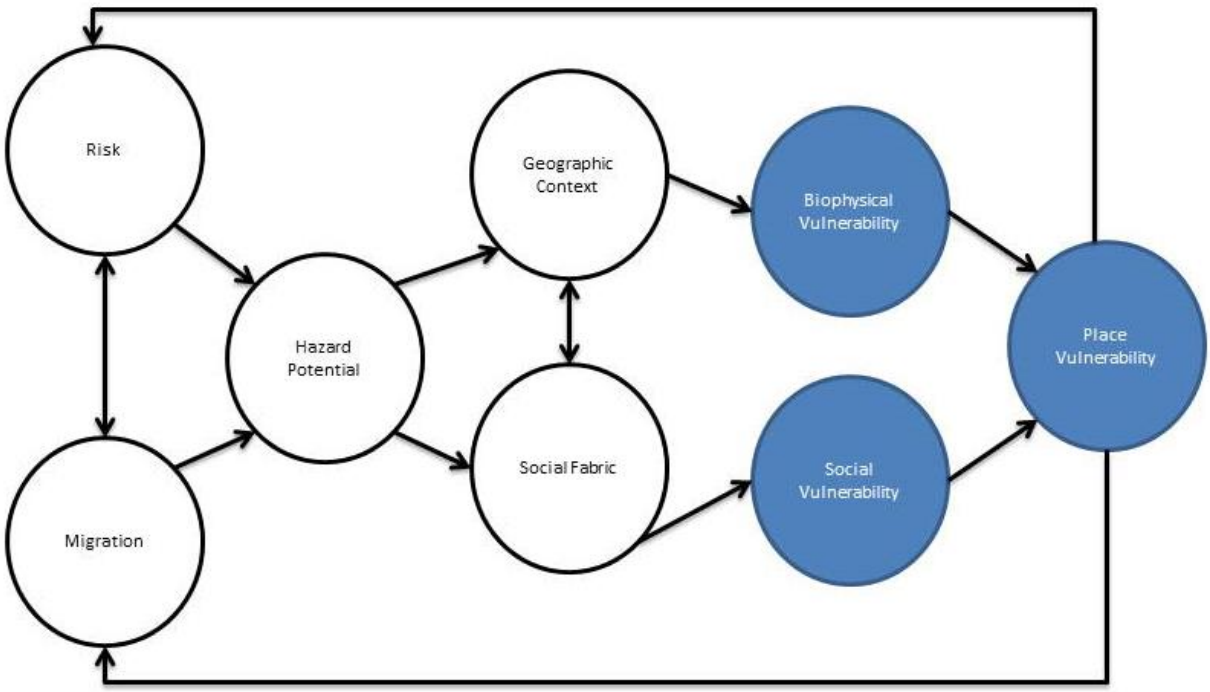

Figure 1. Cutter's hazards-of-place model of vulnerability. *Source:* Author's rendering after Cutter (1996).

A similar, but less complex, model of the relationship of risk (R) with hazards (H) and vulnerability (V) is offered by Wisner et al. (2004) in the equation $R = H * V$. For Wisner et al., people's exposure to risk is evaluated by the impact of hazards. Wisner's risk equation was operationalized by Collins et al. (2013) as a way of evaluating the level of risk children experience from biophysical vulnerability and social vulnerability to climate change. The association of biophysical vulnerability and social vulnerability may also be an indicator of environmental inequities related to socioeconomic status, race, ethnicity, or age. Consequently, the relative vulnerability of different places defined through the hazards-of-place model is a useful concept when examining claims of environmental injustice regarding inequitable exposure to the biophysical factors of elevated temperature, sparse vegetation, and dense urban structure and their association with socially vulnerable groups of people in different urban areas.

Thermal Inequity

Urban heat, and the combination of the UHI and increases in the temperature baseline, has not attracted the level of attention that other hazards impacted by global climate change have. Since it does not leave a path of material destruction like other weather related hazards, urban heat has been called the "silent killer" (Luber and McGeehin 2008). However, several high casualty events have generated media attention about the destructive capacity of heat waves on urban populations. The 1995 Chicago heat wave, 2003 European heat wave, and 2010 Moscow heat wave and associated fires were mass casualty events, drawing public attention to the health impacts of heat waves. Consequently, urban heat is seen primarily as a public health issue which can be managed through improved emergency preparedness like warning systems (Kalkstein 1991) and cooling shelters (Semenza et al. 1996). Others call for UHI mitigation through alteration of the built environment, which includes structural measures like cool and green roofs, increased green space and permeable land cover (Harlan et al. 2006; Johnson et al. 2012). Because of its episodic occurrence, lack of material damage, and impact on socially vulnerable groups that often lack political power, urban heat was not framed as an environmental justice issue until recently.

Although heat waves have been understood by most scholars concerned with urban climatology and public health as a natural hazard, urban heat should also be considered an issue of environmental equity, specifically, a climate justice concern. It is a hazard that combines elevated urban temperatures from the UHI with increasing numbers of days of extreme heat, signifying greater heat wave frequency and intensity, one of the many effects ascribed to global climate change (Meehl and Tebaldi 2004). The contribution of anthropogenic factors transforms the common understanding of heat waves as natural hazards that prevailed until the late 20th

century (Klinenberg 1999). Like hurricanes, tornadoes, and drought, heat waves were once considered an "act of God" or nature with little or no human causality. However, increasing urban heat differs from these other natural hazards because it arises from multiple anthropogenic causes. It is a consequence of higher urban density and changes to land cover combined with increasing global temperature baseline and climate variability due to greenhouse gas emissions. These factors combined with social issues make urban heat a hazard which is socio-technical in origin and could have substantial adverse impacts on populations living in developed nations located in mid-latitude regions. Additionally, vulnerability to this hazard is not distributed equitably across society. As mentioned earlier, some individuals are especially vulnerable to elevated urban heat both because they live in hotter areas and also because of neighborhood effects like inadequate social ties or economic resources (Browning et al. 2003; Harlan et al. 2013). These individuals constitute socially vulnerable groups which may have limited abilities to cope with or mitigate the hazard.

Environmental justice advocates and scholars emphasize that disproportionate exposure to a hazard, coupled with an inability to mitigate its negative effects, is fundamentally unjust. Since environmental inequities are socially produced, environmental justice research seeks to uncover the structural dynamics which underpin inequality (Brulle and Pellow 2006). Extensive analysis of morbidity and mortality during heat waves indicate that there is considerable disparity in the distribution of risk among populations with several factors indicative of social vulnerability (Ellis 1978; Kalkstein and Davis 1989; O'Neill 2003; Semenza et al. 1996; Whitman et al. 1997). *Who you are,* and *where you live* are critical factors when assessing vulnerability to the threat of urban heat. With urban heat the central question is: are socially vulnerable groups consisting of young children, older adults, racial/ethnic minorities, and

individuals of lower socioeconomic status who live in the structurally densest and least vegetated parts of U.S. metropolitan areas disproportionately exposed to the adverse impacts of urban heat and heat waves? If this is the case, then many U.S. metropolitan areas may collectively represent a "landscape of thermal inequity," which is both a physical and cultural landscape of differential exposure and social vulnerability to urban heat.

Outline of this Dissertation

The goal of this dissertation is to address several major gaps in the growing research literature on the adverse social impacts of urban heat and situate urban heat as an issue relevant to climate justice. Using a geographic approach in three case studies, this dissertation comprehensively and systematically examines urban heat and social vulnerability in a spatially diverse selection of localities including many of the largest U.S. cities, which are facing the risk of heat waves indicated by increased extreme heating days by 2050. Previous empirical studies of this topic have been confined to only one or two cities as study sites. For instance, Phoenix is often chosen as a study area due to its high summer temperatures and status as a population center. Limiting study areas allows depth of analysis, and also a historical consideration of urban development, but it makes it difficult to assess the differential impacts of place. How does the association between exposure to urban heat and social vulnerability differ from city to city? This dissertation takes a broad approach by studying multiple urban areas at the metropolitan level across the nation so that differences in associations of the variables can be compared. Additionally, several methodological limitations of the previous research are addressed through the consideration of spatial autocorrelation and use of an urban heat risk index (UHRI) which

accounts for a larger set of factors than simply LST. Finally, this dissertation examines the association of racial and ethnic segregation and exposure to urban heat using a multilevel modelling method (MLM), also known as hierarchical linear modeling. In this way the relevance of segregation in establishing the urban ecology of different cities of the U.S. can be examined. These theoretical and methodological improvements should advance research in this field, establishing it as an issue of climate justice warranting academic study in the fields of urban geography, natural hazards, and environmental justice.

The three articles comprising this dissertation explore urban heat and the exposure of socially vulnerable groups at the census tract level. The first paper in chapter 2 examines the association between land surface temperature (LST), commonly used as a measure the surface urban heat island (SUHI), and the location of socially vulnerable communities. The second, in chapter 3, extends the work by establishing a new index of urban heat to account for the relationship of built structural density, vegetation, and LST. This urban heat risk index (UHRI) is then used to investigate the association with social vulnerability in different neighborhoods. An expanded set of explanatory variables is used in three different cities with varying urban ecologies. Finally, in chapter 4 the association of urban heat with socioeconomic status and the interaction of segregation with minority residential patterns are investigated in different urban areas throughout the U.S. The three articles can be understood in the theoretical context of place vulnerability (Cutter 1996). The dependent variable of LST or the UHRI is indicative of biophysical vulnerability, while the explanatory variables are indicators of social vulnerability in that theoretical context.

Each paper expands on the spatial scale of the study areas, increasing the scope of analysis of this dissertation. The first paper is a small scale-study set in the geographically

bounded peninsula of Pinellas County, Florida in the southeastern region of the U.S. Pinellas County is the most densely populated county in Florida and has been fully residentially developed, having reached a "built-out" status (Mitchell and Chakraborty 2014). Here, the urban processes of sprawling suburbanization in the post-war period were followed by recent gentrification and demographic inversion resulting in a changing urban ecology. The second paper encompasses larger geographic scale than the first, examining the three most populous urban areas of the U.S.: Chicago, Los Angeles, and New York City (Mitchell and Chakraborty 2015). The differing urban ecologies of these cities allow for an analysis of the varying spatial distributions of minority and lower-income neighborhoods. While the methodology of the first two articles implement spatial autoregressive models (SAR), the third utilizes multi-level modeling (MLM). The application of MLM allows an examination of the associations between urban heat, minority, and low socioeconomic status neighborhoods, and then segregation in twenty of the largest urban areas distributed throughout the U.S. defined by their MSA boundaries. Overall, the approach of these three studies is to move to increasing scales and complexity of urban form.

The principal aim of these articles is to frame the environmental equity concerns related to urban heat as an issue of climate justice. They extend the analysis of how urban heat is inequitably distributed in U.S. cities. Urban heat arises from the built structure of cities – the reconfiguration of the natural landscape and its replacement by built structures with different thermal characteristics and capacities. The UHI effect is augmented by an elevated temperature baseline and an increase in heating days caused by global climate change. The UHI creates a differentiated heat structure in cities, resulting in urban heat patterns which do not uniformly impact areas where people live and work. The studies hypothesize that the physical and social

landscape of U.S. cities are places of unequal exposure and unequal vulnerability for residents. This thermal landscape is constructed by social and technological processes which shape U.S. cities. These processes form the context of varying exposure. While extreme heat events, or heat waves, have broad spatial coverage effecting MSAs, their exurbs, and often larger regions, their intensity is spatially variable due to the impact of micro-urban heat islands, which effect neighborhoods differentially (Aniello et al. 1995).

This doctoral dissertation draws from the fields of urban climatology, natural hazards research, and urban geography for an interdisciplinary examination of urban heat with the goal of establishing urban heat and thermal inequity as an environmental justice issue. First, it contributes to the evolving climate justice literature by presenting a methodology based on UHI studies for determining census tract level patterns of urban heat vulnerability. Second, it makes a theoretical contribution by defining thermal inequity as an issue arising out of the social and technological processes of urban formation. Third, it examines the association of a major social problem, segregation, and its relationship with inequitable exposure to urban heat. The final chapter outlines both the conclusions of this research and its effort to link urban heat to social factors like socioeconomic inequality and segregation, and the limitations established by the focus on urban areas of a developed nation like the U.S.

CHAPTER TWO:

URBAN HEAT AND CLIMATE JUSTICE: A LANDSCAPE OF THERMAL INEQUITY IN PINELLAS COUNTY, FLORIDA[1]

Introduction

The combined effects of two global trends, urbanization and climate change, have generated considerable concern regarding their adverse and disproportionate impacts on the health of urban populations (Grimmond 2007; Luber and McGeehin 2008; McCarthy et al. 2010). Urbanization increases population density and leads to the spatial expansion of cities, replacing vegetation with built structures of generally lower albedo, greater impervious surface area, and higher thermal mass (Golden 2004). This pattern of urban development alters the thermal exchange between the land surface and lower atmosphere at a local scale, resulting in higher urban heat levels, a phenomenon referred to as the urban heat island (UHI) effect. In addition to the UHI, global climate change (GCC) is predicted to continue to raise the global temperature baseline and cause greater climate variability (IPCC 2007), increasing the intensity and duration of heat waves (Gaffen and Ross 1998; Meehl and Tebaldi 2004). The predicted increase in heat waves has prompted public health concern regarding rising levels of heat-related illness and mortality, especially in densely populated urban areas where heat is amplified by the UHI (Kalkstein and Greene 1997; McGeehin and Mirabelli 2001; Sheridan, Kalkstein, A.J., and

[1] Portions of this chapter have been previously published in *Geographical Review*, 2014, *104*(4), 459-480, and have been reproduced with permission under Creative Commons licensing.

Kalkstein, L.S. 2008). The analysis of elevated levels of urban heat is an emerging research area in which human-environmental interactions occurring at a global scale such as GCC are linked with regional scale hazards and disasters such as extreme weather events and heat waves.

Mortality rates during heat waves have been studied at least since the 1930s, but attracted increased attention after several high mortality events in the U.S. (1980, 1988, 1995, and 1999) and Europe (2003, 2010) that disproportionately impacted socially vulnerable groups. Social vulnerability is a well-established concept within natural hazards research, which emphasizes demographic, socioeconomic, and housing characteristics that make people more susceptible to the adverse impacts of hazards. In the context of this study, social vulnerability refers to the increased sensitivity to heat waves by specific subgroups such as racial/ethnic minorities and low-income residents in urban areas. Socioeconomic status is an important determinant in the ability to access or afford to operate amenities such as air-conditioning (Basu and Samet 2002), or increased landscaping which moderates temperature extremes (Jenerette et al. 2011). Studies of past heat waves suggest that populations with diminished adaptive capacity to heat are particularly affected, including older people (Ellis 1978; Whitman et al. 1997), African-Americans (Kalkstein and Davis 1989; Whitman et al. 1997; O'Neill 2003; CDC 2012), individuals living alone (Klinenberg 2002), and people lacking the economic resources to mitigate and adapt to elevated urban heat (Semenza et al. 1996). The disproportionate health effects on socially vulnerable populations raise the question whether elevated urban heat is an environmental injustice concern.

Environmental justice scholarship in the U.S. has traditionally focused on the inequitable distribution of disamenities such as air pollution, hazardous waste, and undesirable land uses, with respect to racial/ethnic minorities and economically disadvantaged groups. Environmental

justice advocates and scholars have emphasized the role of race, ethnicity, and socioeconomic status as powerful determinants of the spatial layout of urban areas, influencing the siting of industry, commercial development, transportation, and housing (Bullard 2000; Pulido 2000). Recent studies have extended the traditional environmental justice framework by examining social inequities in the distribution of environmental amenities such as parks (Heynen et al. 2006; Boone et al. 2009), playgrounds (Talen and Anselin 1998), and street trees (Landry and Chakraborty 2009) that provide direct and indirect health benefits to local residents. Climate justice is an emerging subfield of environmental justice, concerned with the inequitable distribution of the impacts of GCC. While climate justice recognizes that the spatial scale of GCC impacts range widely it has tended to operationalize these concerns at an international level (Walker 2012). The adverse and disproportionate impacts of urban heat on socially vulnerable groups represent a hazard that integrates the effects of GCC with the UHI, thus combining the global with the local. Since social inequities associated with these impacts stem from the varying spatial distribution of heat across different communities in urban areas, they require an examination of the urban built structure with its varying thermal capacity. The two factors of physical infrastructure and the spatial clustering of population subgroups are entwined in the disproportionate distribution of heat across urban areas creating *a landscape of thermal inequity* within our cities.

Recent empirical studies have examined social disparities in exposure to elevated levels of urban heat in several metropolitan areas such as Chicago, Phoenix, and Philadelphia (Harlan et al. 2006; Uejio et al. 2011; Chow et al. 2012). Although these studies have made important strides in identifying specific inequities with respect to urban heat, certain limitations have not been consistently addressed. Specifically, previous research has not comprehensively assessed

the spatial pattern of urban heat within study areas, nor has it consistently used geostatistical techniques to account for spatial dependence in the data. Our article seeks to address these methodological limitations of previous work and extend climate justice research through a case study that examines social and spatial inequities in the distribution of urban heat in Pinellas County, Florida. Our study uses high-spatial-resolution and remotely sensed thermal data to systematically analyze the geographic distribution of land surface temperature (LST), a key parameter used in urban climate studies (Voogt and Oke 2003), with respect to socially vulnerable populations. The analysis also incorporates cutting-edge geostatistical techniques that account for spatial autocorrelation. These research enhancements should enable improved identification of the hazard's spatial pattern with respect to neighborhoods with greater social vulnerability. Identifying areas of greater thermal potential and their overlap with vulnerable communities is critical to mitigation efforts for this growing problem, allowing more efficient and equitable allocation of resources when restructuring the urban environment. This capability of resolving temperature at the neighborhood scale combined with geostatistical analysis of socio-demographic variables can be used to establish the presence of a landscape of thermal inequity in urban areas, and determine its geographic variation and extent.

Urban Heat and Thermal Inequity

A review of the literature pertaining to heat waves and urban heat indicates a growing emphasis on social disparities in the spatial distribution of this hazard. While studies of heat waves and mortality have a long history, links between urban land use, the UHI, and mortality came later in the work of Buechley et al. (1972) and Clark (1972). Exposure to excessive heat, regardless of the causal factor, is considered to be, on average, the greatest cause of weather-

related fatalities in the U.S. (CDC 2012). High mortality rates from heat waves during the summer of 1980, and especially as a result of a 1995 Chicago, Illinois heat wave, increased public health awareness of the issue. The shocking death toll in Chicago, which by official count resulted in 536 deaths (ILDPH 1997), compelled public officials to recognize social disparities in the impact of urban heat on vulnerable groups. In his book titled *Heat Wave: A Social Autopsy of Disaster in Chicago*, Klinenberg (2002) argued that socially vulnerable groups including African-Americans, people living on annual incomes below the poverty level, older people living alone, and people with medical conditions were particularly exposed to the risk of urban heat. The inability to recognize this vulnerability represented a massive public policy failure, in which the most helpless members of society were invisible to the municipal emergency planning structure of the time.

Since 1995, greater attention has been devoted to the topic of urban heat and social disparities in its adverse health effects. Several studies have taken a quantitative approach to examine the spatial pattern of urban heat and its differential impact on communities in various metropolitan areas. A study by Harlan et al. (2006) was the first to emphasize disproportionate exposure to urban heat as an environmental justice issue. Comparing the patterns of urban heat in the city of Phoenix and the socio-demographic composition of the city, this research found significant associations between increased temperature and neighborhoods with weaker social networks, lower median income, and higher proportions of Hispanic residents. The study also noted that structural and historical forces had left "poor and minority populations" in "deteriorated urban spaces" which were not amenable to environmental improvement (Harlan et al. 2006). A subsequent study by Jenerette and Harlan et al. (2011) suggested that lack of environmental amenities and cooling vegetation in warmer urban areas of Phoenix amounted to a

"heat riskscape" with varying risk exposure and human vulnerability in the urban environment. Chow et al. (2012) extended Harlan et al's. methodological approach in their Phoenix study, calculating summer maximum and minimum temperatures and an index of vegetation abundance for two periods: 1990 and 2000. Their findings supported the previous evidence that higher temperatures and lower amounts of vegetation were associated with higher numbers of Hispanic and elderly residents, as well as lower socioeconomic status. Chow et al. concluded that economically affluent Phoenicians were better able to manipulate their environment through lower structural density, increased landscaping, and the use of air conditioning (2012). Each of these studies have moved toward a more comprehensive framing of urban heat and the factors associated with social vulnerability as environmental justice concerns.

The studies conducted in the city of Phoenix have relied on the development of an extensive atmospheric temperature data collection system. While atmospheric temperature is the most direct way of assessing exposure to elevated heat, there are other environmental factors that indicate areas of elevated temperature due to the UHI, including the amount and density of vegetation and built structures, the sky view factor of areas, and the geometry of the urban environment (Voogt and Oke 2003). Areas of elevated LST are also an indicator of the spatial boundaries of the surface urban heat island (SUHI) .Other studies have used land surface temperature to assess areas of elevated urban heat. Uejio et al. (2011) analyzed the health impacts of urban heat in both Phoenix and Philadelphia by utilizing LST and impervious surface data in conjunction with a generalized linear mixed model approach to correct for temporal autocorrelation in the data. Additionally, recent studies in the U.S.-Mexico border cities of El Paso, TX and Juárez, Mexico have examined LST as a factor of neighborhood hazard evaluation for climate change (Grineski et al. 2012; Collins et al. 2013). Using Landsat imagery and spatial

regression modeling to correct for spatial autocorrelation, Grineski et al. and Collins et al. applied a social vulnerability index to assess areas of elevated urban heat exposure and climate change risk.

Several studies in the city of Philadelphia have noted significant and positive correlations between elevated LST and higher rates of heat related mortality or health risk in urban areas (Johnson et al. 2009; Johnson and Wilson 2009; Hondula et al. 2012), establishing a precedent for the use of this indicator for measuring urban heat exposure. By directly examining biophysical factors of the SUHI and UHI such as LST and its statistical relationship with socially vulnerable population groups, it may be possible to discern whether a landscape of thermal inequity exists in urban areas.

Study Area

As shown in Figure 2, Pinellas County is located on the west-central coast of Florida and is part of the Tampa–St. Petersburg–Clearwater Metropolitan Statistical Area (MSA), commonly referred to as the Tampa Bay MSA. This county has a humid subtropical climate, typified by hot, wet summers and cool, drier winters. Its peninsular geography, bounded by the Gulf of Mexico to the west and Tampa Bay to the east, has constricted growth and development, and it is now considered "built-out" with the last commercially available green space having been developed in the last decade. Pinellas is the most densely populated county in Florida, with 1,264 persons per square km and a total population of 916,542 (U.S. Census 2010). About 76 percent of its land area is urbanized, while the remainder consists mostly of publicly held parks and preserves.

In addition to its relatively high level of urban density in a state characterized by suburban sprawl, Pinellas County has several distinctive socio-demographic characteristics that

make it suitable for environmental justice research, in general, and climate justice, in particular. It is highly segregated residentially for White and African-American residents, relative to surrounding counties. The White/African-American dissimilarity index for Pinellas is 0.625, compared to 0.437 for neighboring Hillsborough County (USDHHS 2010). Historically, Pinellas County developed as a winter resort and haven for retirees. In 2010, residents aged 65 and older comprised 21 percent of the population compared to 17 percent statewide (U.S. Census 2010). The poverty rate was slightly below the state average of 13.8 percent, at 12.1 percent (U.S. Census, ACS 2010). In addition, Pinellas County has the second largest community of Southeast Asian residents in the state of Florida (U.S. Census 2010). Vietnamese and "Other Asians" including Cambodian, Hmong, and Laotian people comprise almost 45% of the Asian population of the county, and are concentrated in the cities of East and West Lealman and Pinellas Park in the south-central portion of the peninsula. In the 2000 U.S. Census, educational attainment levels were lower and poverty rates higher among the Vietnamese, Cambodian, Hmong, and Laotian groups. Pinellas County's history of rapid growth and development from 1960 to 2000, its recent built-out status, its population loss between 2000 and 2010, and a diversifying population make its demographic patterns similar to those of many mature cities of the Sunbelt region (Hollander 2011). Both the large older population and diversity of minority groups in Pinellas were key factors in choosing it as a study area.

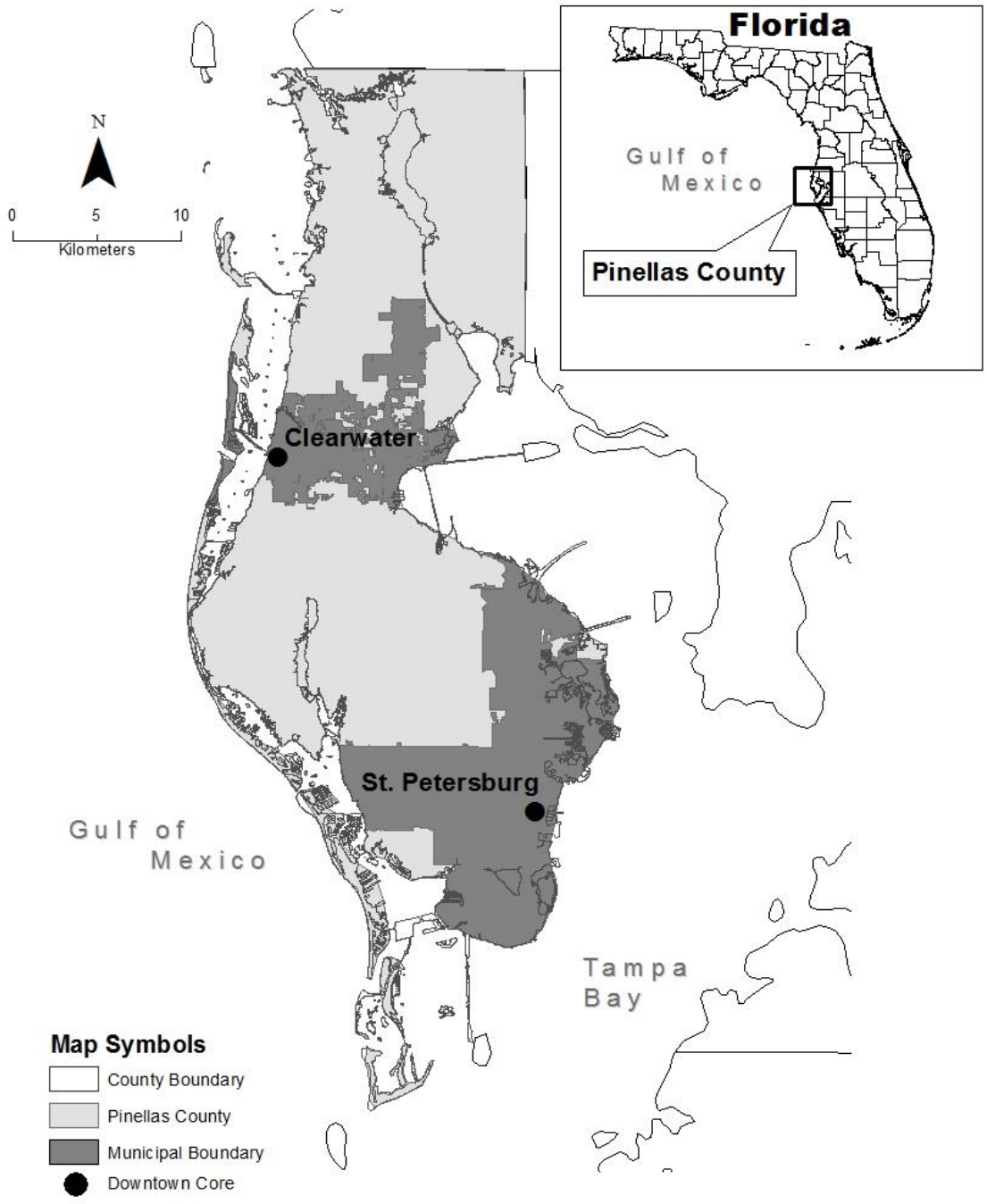

Figure 2. Pinellas County, Florida.

Pinellas County's pattern of development has been centered on a few small urban cores consisting mainly of low-rise buildings. These urban areas are linked by a grid-like pattern of commercial thoroughfares and surrounded by sprawling residential suburbs. Because of its peninsular shape, the urban core areas are generally near the waterfront, creating high density areas near the coast, sometimes buffered from the water by narrow strips of beach or parkland. Waterfront areas are considered an amenity and are preferred sites of residence for the region's economically affluent residents, as demonstrated by higher median household income and median housing values in cooler coastal census tracts. Commercial districts stretch inland, toward the center of the peninsula, where less affluent residential areas are located. This creates a general spatial pattern with residences of higher income population groups located in the cooler waterfront areas, while commercial sites and housing for lower income residents tend to be located toward the interior of the peninsula where the UHI effect is most pronounced. This is a historical pattern of settlement that can be traced back to the early 1900s in the two principal cities of Clearwater and St. Petersburg. Desirable waterfront locations of urban areas were sites of income-producing tourist housing and were also purchased by affluent residents. Areas inland became sites of commercial or light industrial activity and housed the economically disadvantaged residents, among them the African-American community who served as domestic servants and laborers for the burgeoning tourist trade and construction industry. This established a spatial pattern of settlement that largely holds true to the present.

It is difficult to accurately gauge the adverse health effects of urban heat on the population of Pinellas County. The climate is humid subtropical and air-conditioning use is widespread, two factors that may indicate greater acclimatization and adaptation to heat by the population (Medina-Ramón and Schwartz 2007; Zanobetti and Schwartz 2008). Although

Florida is ranked seventh of U.S. states in the overall number of fatalities from excessive heat with 170 deaths from 1999 to 2009 (CDC 2012), the numbers are questionable due to different practices used by physicians and medical examiners in diagnosing heat as a primary or contributing factor in cause of death (Dixon et al. 2005). In terms of hospitalization and illness, the Florida Department of Health reports that between 2005 and 2009, there were 16,523 hospital admissions in the state (rate of 18.3/100,000) for heat related illness (HRI) for residents age 16 or older, and an additional 2,198 admissions for occupational HRI (FL Dept. of Health 2011). Pinellas County ranks lower in terms of occupational HRI admissons than counties located in rural parts of the state where agriculture is still a major economic activity. Despite its lower occupational risks for heat related illness or injury, Pinellas is a densly populated county with a large number of of elderly residents in a state that is ranked high nationally for heat related fatalities.

Data and Methods

This study uses remote sensing techniques, U.S. Census and American Community Survey (ACS) data, and both conventional and spatial regression analysis to evaluate socio-demographic inequities in the geographic distribution of urban heat in Pinellas County, Florida. A workflow summary of methods is presented in Figure 3. The following sections provide a detailed description of specific data sources and methods utilized for this analysis.

Dependent Variable: LST

Land surface temperature (LST) was chosen as the dependent variable in this study because of its status as a key parameter in urban climate studies, and its positive statistical

association with rates of heat-related morbidity and mortality (Johnson and Wilson 2009; Johnson et al. 2009; Hondula et al. 2012), and utilization in environmental justice studies which have considered disparities in the exposure to environmental hazards, including urban heat (Grineski et al. 2012). LST from two types of remote sensing data were first examined in order to determine whether a UHI pattern was present in the study area. MODIS and LANDSAT satellite imagery provided indications of the UHI pattern at different spatial and temporal scales. One kilometer spatial resolution MODIS satellite imagery was acquired to assess whether a diurnal surface urban heat island pattern existed in the study area (NASA LP DAAC). Several MODIS 8-day LST composite images were processed and examined, but due to seasonal weather patterns few cloud-free images were available during the summer months. An image from the period of September 14-21, 2010, which had high average temperatures and the fewest missing pixels was selected. Figure 4 depicts a pronounced diurnal thermal cycle in this study area. The afternoon image, in particular, shows differences between lower coastal and higher inland temperatures, with the greatest contrast in the south-central portions of the Pinellas peninsula. This pattern reverses at night as land with its lower thermal inertia cools more rapidly than wetlands and water, causing the coastal areas to have higher relative temperatures by 1:30 AM (Price 1977).

Although the MODIS imagery allows clear visualization of the diurnal UHI pattern throughout the area, its coarse spatial resolution is poorly suited for finer scale analysis of urban heat. Higher spatial resolution (120 meter) LANDSAT 5 Thematic Mapper (TM) satellite imagery was selected to analyze the dependent variable, LST. This level of spatial resolution allows clear determination of neighborhood differences in LST. An image acquired on 16 July

2010 at 11:53 EDT, a day of high daily average atmospheric temperature (31.7° C) with no precipitation and minimal cloud cover was selected.

Several steps were involved in processing the LST image. The USGS *Earthexplorer* portal was used to export the tagged image file format (TIFF) image, which had been processed to level 1 standard including radiometric correction and georectification. LANDSAT 5 TM captures spectral data in seven bands, and three of these were used to process an image: bands 3 (red) and 4 (near-infrared), and the thermal band, 6. Moderate spatial resolution images like those from LANDSAT 5 TM are suitable for general urban studies and have been used to identify neighborhood level effects, like micro-urban heat islands (Aniello et al. 1995). LST was calculated using the mono-window algorithm as described by Qin et al. (2001) and Pu et al. (2006). Processing involved deriving two images: the thermal image and an emissivity image. The surface emissivity image was produced using bands 3 and 4 to calculate the Normalized Difference Vegetation Index (NDVI) value for each pixel. Using the NDVI, the pixels were then categorized by predominant land cover into water, vegetated, and impervious types. Atmospheric data from the time, including near surface temperature and precipitable water acquired at the National Weather Service station in Ruskin, Florida, were used for MODTRAN 4 atmospheric correction. The emissivity and atmospheric data are then used with the LANDSAT TM thermal data to produce an LST image of the area. Several pixels in the northern part of the peninsula were obscured by clouds and therefore excluded from mean temperature calculations. Their exclusion created minimal differences in temperature (2.32 percent) from the same areas of the July 2011 image. Calibration of the LST image was achieved by using in-situ surface water temperature measurements from National Ocean Service, Clearwater Beach station (CWBF1) (NOAA 2010). After that, water pixels were eliminated from aggregated census tract LST value.

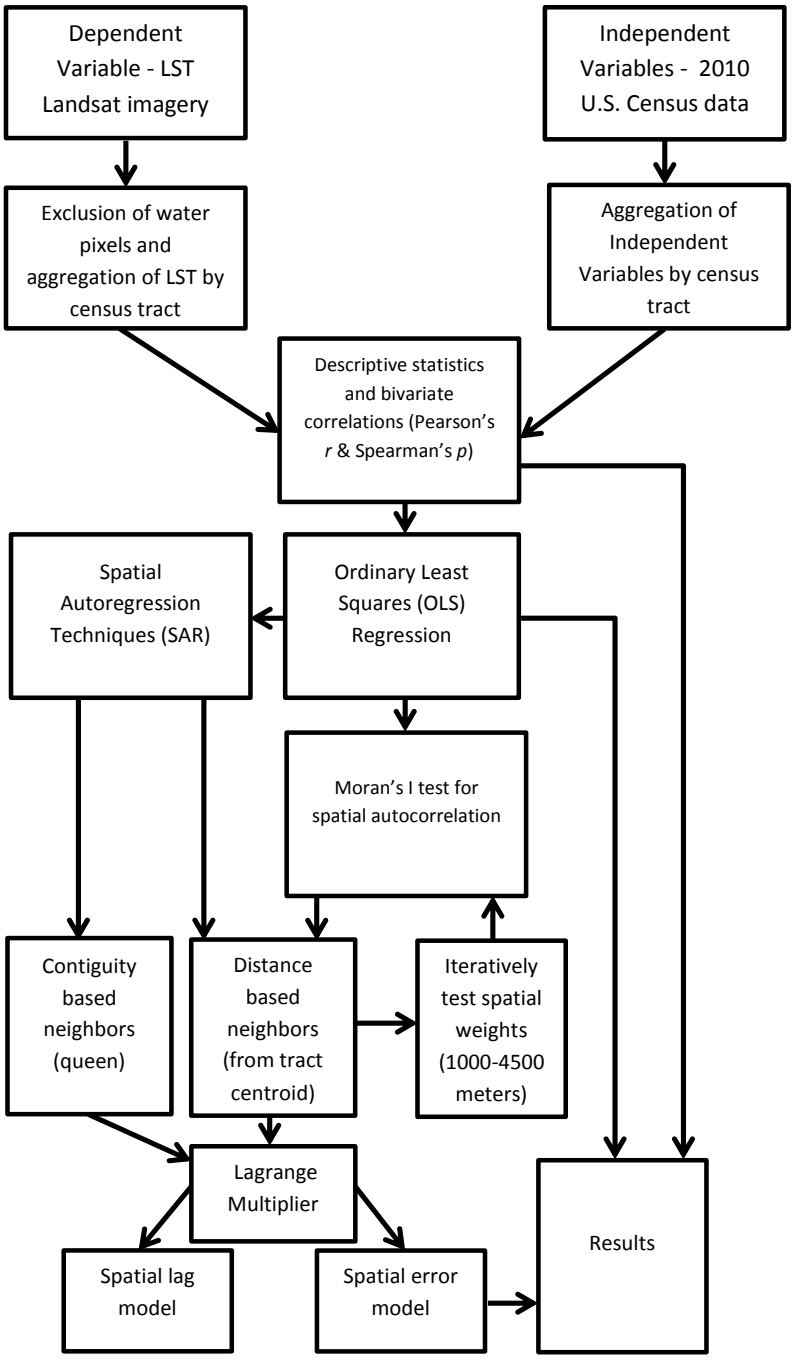

Figure 3. Workflow of statistical methods used in this study.

The LANDSAT TM processed image displayed thermal patterns which were generally consistent with the MODIS image of higher daytime temperatures in the south and central regions of the peninsula. Figure 4 shows the distribution of LST in this region. Higher temperature urban core areas and transportation corridors are clearly evident on this map. The generally cooler temperatures of parks and preserved areas close to lakes, Tampa Bay, and the Gulf of Mexico are also discernible.

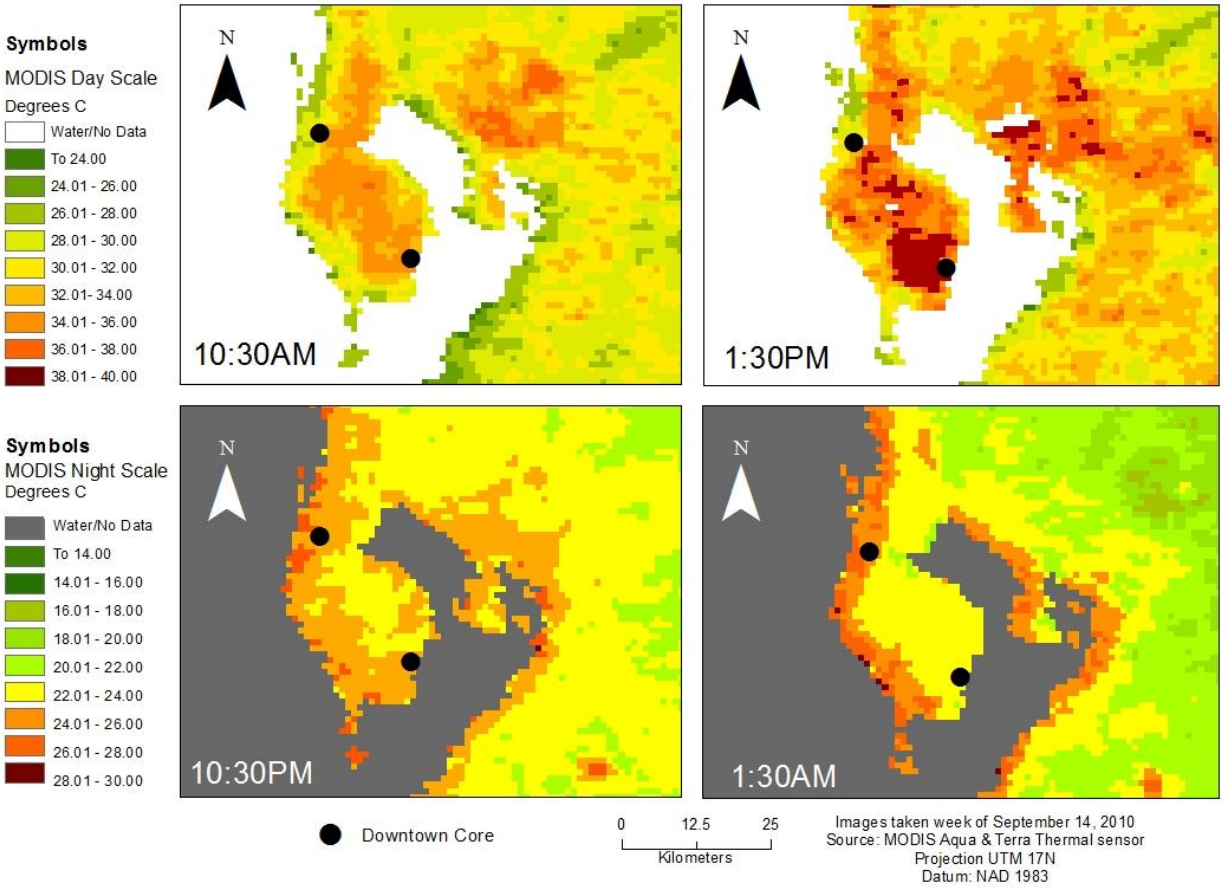

Figure 4. MODIS Aqua and Terra satellite 8-day composite land surface temperature (LST) image of Tampa Bay area with 1km spatial resolution for September 14-21, 2010.

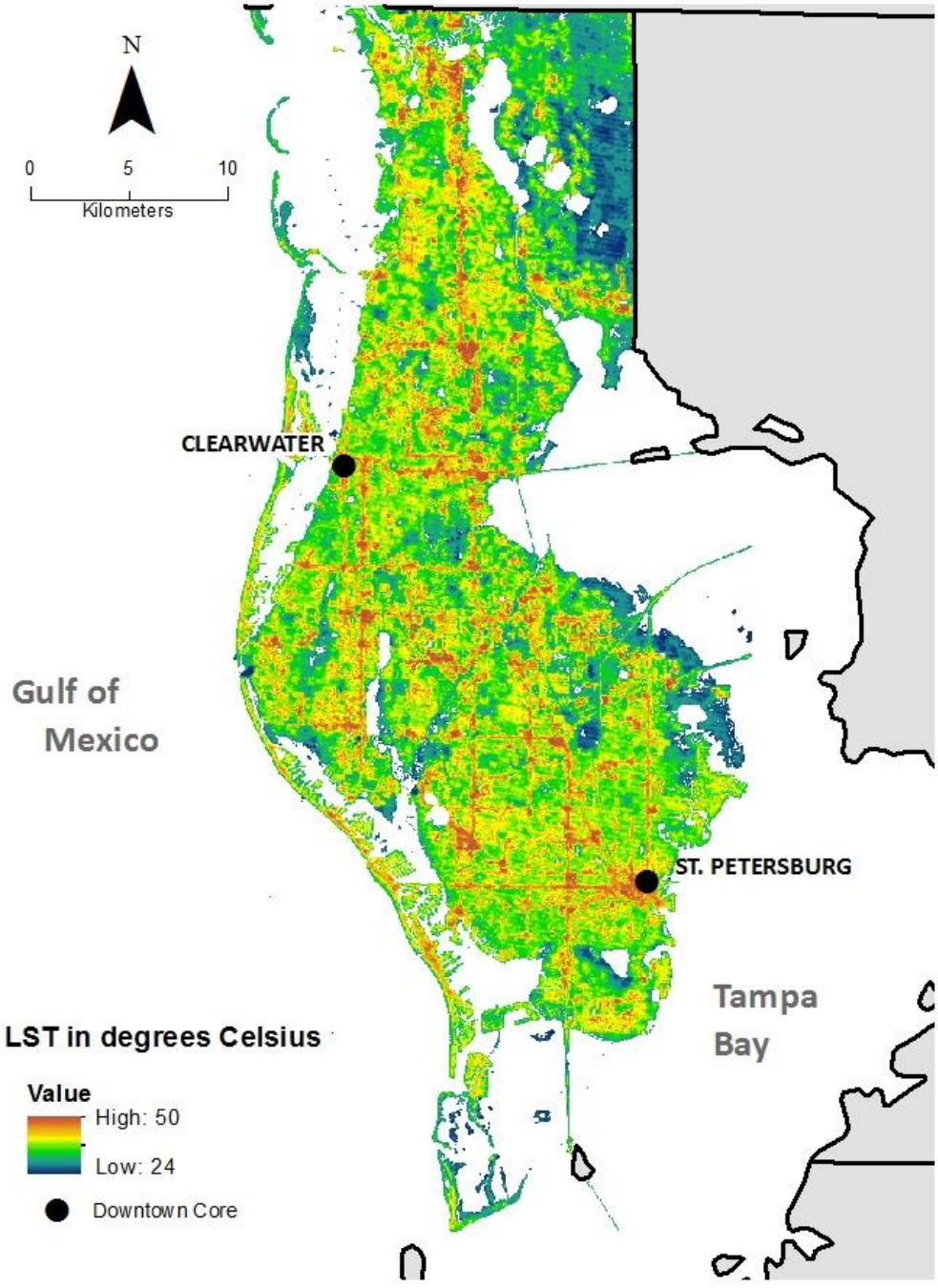

Figure 5. Land surface temperature (LST) remotely sensed by LANDSAT 5 TM sensor satellite, Pinellas County, 16 July, 2010.

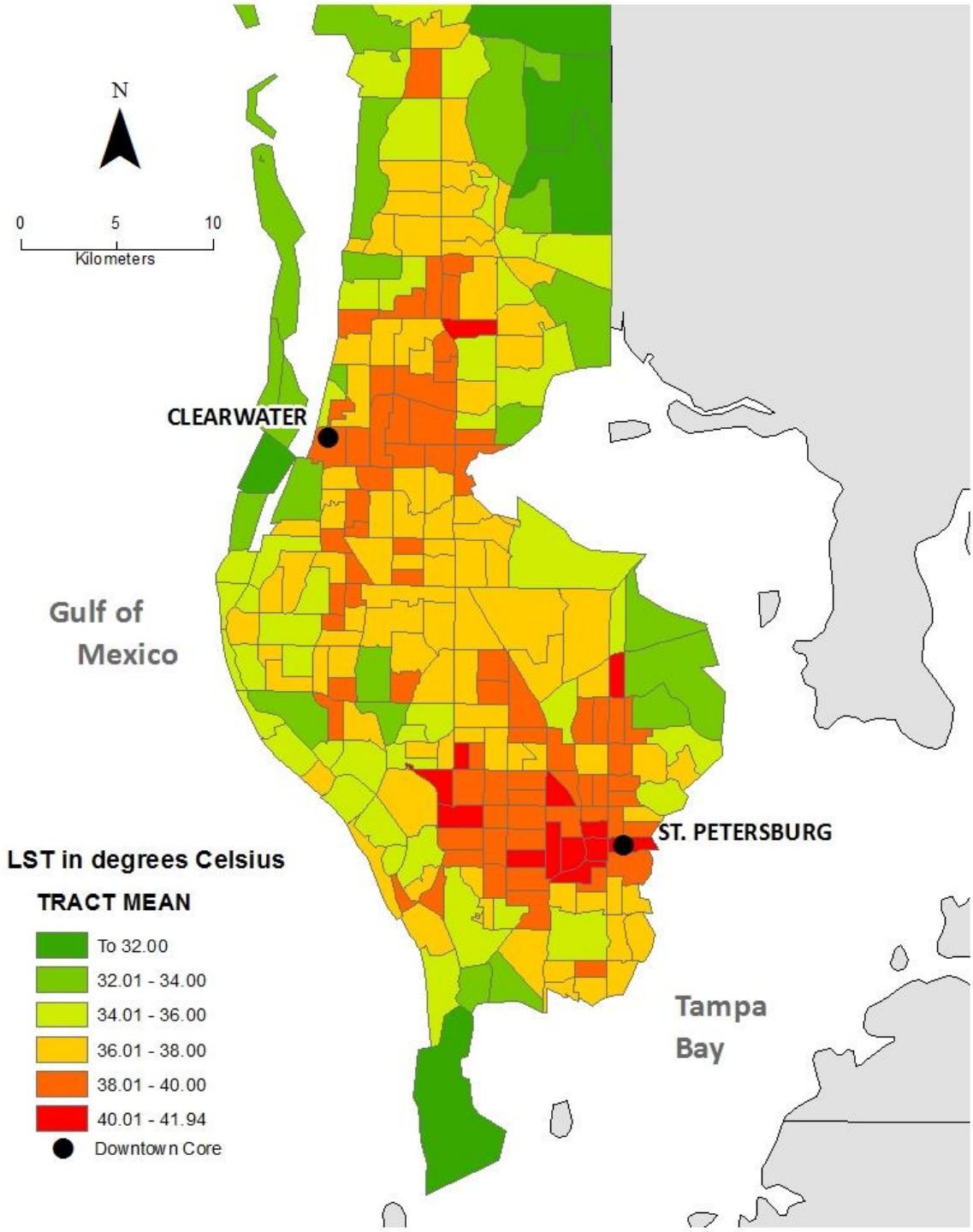

Figure 6. Mean land surface temperature (LST) by census tracts, Pinellas County, 16 July, 2010.

The mean LST for all pixels within each census tract was calculated based on Census 2010 tract boundaries and used to represent the dependent variable for the statistical analysis. The spatial distribution of mean LST values at the census tract level is depicted in Figure 6. The map shows a similar geographic pattern of LST to those in Figures 4 and 5: generally warmer late morning afternoon temperatures for the inland areas and for the densest coastal tracts, with other coastal and wetland areas being cooler.

Independent Variables

Inequities in the distribution of LST were analyzed using a set of demographic and socioeconomic variables from U.S. Census 2010 and 2006-2010 ACS five-year estimates for Pinellas County, Florida, at the census tract level. Our selection of variables was guided, in part, by previous studies of urban heat mortality (Kalkstein and Davis 1989; McGeehin and Mirabelli 2001; O'Neill 2003; Harlan et al. 2006; Basu et al. 2008). In this literature, individuals of lower socioeconomic status, the very young or old, and racial/ethnic minorities have been identified as being particularly vulnerable to the health effects of urban heating. Consequently, the percentage of families at or below the federal poverty level (income in past 12 months below poverty level) and the percentage of all housing that is owner-occupied (home ownership), based on the 2006-2010 ACS estimates, were chosen to evaluate socioeconomic status. Although the U.S. Census provides no reliable measures of family wealth at the tract level, home ownership has been used as a general indicator of wealth and assets in previous environmental justice research (Cutter 2009; Chakraborty 2011). Demographic variables were obtained from the 2010 U.S. Census, Summary File 1. We included both the percentage of population aged 5 years and under, as well as those aged 65 or more years. For race and ethnicity, we focused on the three largest minority

groups in this county: the percentage of the tract population identifying themselves as non-Hispanic Black, Hispanic or Latino of any race, and Asian. Additionally, population density was considered as a control variable, and calculated as the number of people per square kilometer of the land area of census tracts. Finally, all variables were standardized before inclusion in the correlation and regression analysis.

Statistical Methods

To explore basic statistical associations between the dependent variable (mean LST) and each of the independent variables, we began by conducting parametric and non-parametric tests for bivariate correlation, based on Pearson's correlation coefficient, respectively. We then used multivariate regression analysis to evaluate the relationship between urban heat and all independent variables in a single model, based on a three-step process. First, we constructed a multiple regression model based on the ordinary least squares (OLS) method, using LST as the dependent variable. This method is typical of conventional statistics and assumes that observations and regression errors are independent. This assumption, however, is unlikely to be valid if there is clustering of similar values in space or spatial autocorrelation in the data. Spatial autocorrelation is typically caused when observations at proximate locations are more similar or different than would be expected of a random distribution (Kissling and Carl 2008; Chakraborty 2011). This phenomenon has the potential to cause spatial dependence of regression model residuals, thus violating the classical OLS assumption of independence. The second research step thus consisted of determining whether spatial dependence in the data influenced the OLS regression model results. We used the global univariate Moran's *I*-statistic to examine the presence of residual spatial autocorrelation (Anselin and Bera 1998).

In order to test for autocorrelation, it is necessary to specify for each spatial unit which other units are "neighbors" and may influence its values (Cliff and Ord 1981). There are two approaches for defining the neighbors of a spatial unit: contiguity-based or distance-based. For the contiguity-based approach, we utilized first-order "queen-based" contiguity. All adjacent census tracts, including those sharing vertices with the tract of interest were included as neighbors. In contrast, the distance-based method relies on Euclidean distance between tract centroids for the selection of neighbors. The distance for selecting spatial neighbors was determined through an iterative process, involving calculation of weights matrices for a series of distances between centroids, ranging from 1,000 to 4,500 meters. The Moran's *I*-statistic associated with regression model residuals for the various distances was assessed and the distance at which this value ceased to be statistically significant (2,400 meters) at the $p<.10$ level was chosen as the reference value.

Finally, when we detected spatial dependence in the residuals of the OLS model, appropriate spatial regression models were specified to extend the standard regression equation and account for residual spatial autocorrelation. Simultaneous autoregressive (SAR) models are statistical models that consider spatial autocorrelation as an additional variable in the regression and estimate its effect simultaneously with the effects of other independent variables (Chakraborty 2011). This additional term (λ) is implemented with a (distance-based or contiguity-based) spatial weights matrix which accounts for patterns in the dependent variable that are not predicted by independent variables, but are instead related to values of proximate observations. We used the Lagrange Multiplier (LM) and the Robust LM diagnostic tests to determine whether the spatial lag or spatial error model specification should be used (Anselin 2005). Spatial lag models assume that spatial autocorrelation is present in the dependent variable;

spatial error models assume that regression errors exhibit spatial dependence. For our case study, the LM tests indicated that the spatial error specification was appropriate for both contiguity-based and distance-based models.

Results

A pattern of generally warmer LST inland, with cooler areas along the water is evident in both Figures 3 and 4. This pattern, visually detected, represents LST levels throughout the county on the observation date; indicative of clear-sky, summer daytime temperatures. Table 1 provides summary statistics for the entire set of variables, with data for the dependent variable calculated from the tract level values represented in Figure 6. Average LST varies considerably across census tracts within the study area, ranging from 29.55° to 41.94° C, with a mean of 36.92° C. Independent variables such as percent below poverty level, percent owner-occupied, percent age 5 and younger, and percent age 65 and older show substantial range across tracts. This is especially true for the percentage of non-Hispanic Black residents, which ranges from only 0.3 to 95.7 percent, corroborating the high dissimilarity index between this racial group and the White population this suggests a high level of residential segregation. Tract level values of percent below poverty range from 0.70 to 58.0 percent, indicating wide economic disparity. Rates of home ownership also vary greatly, from 11 to almost 96 percent.

Table 1. Descriptive statistics for mean land surface temperature (LST) and explanatory variables.

Variable	Minimum	Maximum	Mean	Std. Dev.
Mean LST (°C)	29.55	41.94	36.92	2.15
Population per sq. km	944.00	8,922.00	3,697.30	1,432.01
% African-American	0.30	95.70	10.34	18.71
% Hispanic	1.40	32.30	7.48	4.69
% Asian	0.00	17.50	2.84	2.55
% Age: ≤ 5 years	0.30	12.60	4.48	1.89
% Age: ≥ 65 years	2.10	74.20	22.31	12.69
% Below Poverty	0.70	58.00	12.11	8.67
% Owner-Occupied	11.40	95.60	67.44	17.05

$N = 244$ census tracts.

Bivariate Correlation Analysis

Our analysis begins with an examination of bivariate parametric and non-parametric correlations to analyze the strength and direction of the statistical relationship between mean LST and each independent variable at the census tract level. Pearson's (*r*-values) correlation coefficients for each variable are presented in Table 2.

Table 2. Bivariate correlation of mean land surface temperature (LST) with explanatory variables.

Variable	Pearson's *r*
Population per sq. km	.414***
% African-American	.133***
% Hispanic	.159***
% Asian	.083**
% Age: ≤ 5 years	.148***
% Age: ≥ 65 years	-.002
% Below Poverty	.322***
% Owner-Occupied	-.288***

$N = 244$ census tracts; $*p < 0.10$; $**p < 0.05$, $***p < 0.01$

The Pearson's correlation coefficient indicates statistically significant and positive linear associations between LST and population density, the percent below poverty level, percent age 5

or younger, as well as the non-Hispanic Black, Hispanic, and Asian percentages, with population density showing the strongest positive correlation. The percentage of owner-occupied homes is the only variable that shows a significantly negative linear correlation with LST. These results suggest that areas of higher LST in this county are associated with significantly higher population density, poverty rates, and racial/ethnic minority proportions, as well as lower levels of home ownership.

Conventional Regression Analysis: Ordinary Least Squares Model

The next step of the analysis uses a traditional ordinary least squares (OLS) regression model to investigate the simultaneous effects of the eight independent variables on mean LST in Pinellas County. The regression results are summarized in Table 3.

Table 3. Ordinary Least Squares (OLS) and Spatial Error Regression of mean land surface temperature (LST).

Variable	OLS	Spatial Error: Contiguity-Based (1st order queen)	Spatial Error: Distance-Based (2400m)
Constant	0.000	0.007	- 0.194
Population per sq. km	0.334***	0.255***	0.283***
% African-American	-0.049	-0.027	0.010
% Hispanic	0.033	0.016	0.052
% Asian	0.126*	0.193***	0.183**
% Age ≤ 5 years	-0.012	-0.081	-0.100
% Age ≥ 65 years	0.086	0.094	0.096
% Below Poverty	0.227***	0.175**	0.132*
% Owner-Occupied	-0.126*	-0.199***	-0.271***
Spatial error parameter (λ)	N/A	0.540***	0.621***
F - Statistic	10.054***	N/A	N/A
Moran's *I* (queen)	0.362***	-0.018	N/A
Moran's *I* (2400 meters)	0.317***	N/A	0.008
Adjusted/Pseudo *R-squared*	0.229	0.473	0.467
Akaike Information Criterion (AIC)	637.615	575.689	580.799

N = 244 census tracts;*$p < 0.10$; **$p < 0.05$; ***$p < 0.01$.

The ANOVA *F*-test indicates overall significance ($p < 0.01$) and the adjusted *R*-squared (0.229) suggesting a reasonable goodness-of-fit for this multiple regression model. The multicollinearity condition index is 4.775, confirming low levels of multicollinearity among the standardized independent variables. Variable coefficients for both non-Hispanic Black and Hispanic percentages do not remain significant ($p>.10$) after controlling for age and socioeconomic status in a multivariate model. However, population density, percent Asian, and percent below poverty level are significantly positive, while percent owner-occupied is significantly negative. The next step was to determine if the regression residuals (errors) from this OLS model satisfy the classical linear regression assumption of independence, or if they exhibit significant spatial autocorrelation. The residual Moran's *I* statistic associated with the contiguity-based and distance-based approaches for selecting spatial neighbors were 0.362 and 0.367, respectively. Both these positive values are statistically significant ($p<.01$), confirming that the residuals are spatially dependent with respect to their values in neighboring tracts. Since this is a serious violation of the assumption of independence, the OLS regression model is inadequate for analyzing the association between the dependent and independent variables.

Spatial Regression Analysis: Spatial Error Model

Spatial autoregressive (SAR) modeling was employed to account for the significant and positive spatial autocorrelation indicated by the OLS regression residuals. Results of SAR analysis, using a spatial error model specification, indicate several improvements from the OLS model (Table 3). For both SAR models (contiguity-based and distance-based), the Moran's *I*-statistic is near zero and statistically non-significant ($p<.10$), while the spatial error term (λ) is

highly significant (p<.001). This implies that the effects of spatial autocorrelation have been mostly eliminated from this regression model using either the contiguity or distance-based methods. Additionally, the pseudo *R*-squared (0.473 and 0.467) shows an improvement in goodness-of-fit compared to the OLS model. Finally, the Akaike Information Criterion (AIC) scores from the spatial error models are also lower than the AIC from the OLS model, indicating considerable improvement in model performance.

Differences between the two methods of neighbor selection for the SAR models, contiguity (queen) and distance (2,400 meters) are evaluated by comparing the relative value of the Moran's *I*-statistic. While both measures are non-significant (p> .10), the distance-based weights matrix of the SAR model yields only a slightly lower Moran's *I* (0.008 versus -0.018). Consequently, both SAR models yield Moran's *I* values close to zero, and reduce spatial autocorrelation when compared to the OLS model.

Results of both SAR models indicate that several independent variables are significantly and positively associated with LST (p<.10). Census tracts with higher average LST are characterized by significantly greater population density and poverty rates, as well as a higher percentage of Asian residents. Coefficients for non-Hispanic Black and Hispanic percentages in the spatial error model are positive, but non-significant in presence of the other variables. Rates of home ownership show a negative association with mean LST, and this relationship was also statistically significant (p < .01) in the SAR models. The results of the SAR distance model are consistent with the OLS model in which population density, percent Asian, percent below poverty, and percent home owner-occupied were all significantly related to LST.

Concluding Discussion

Climate justice has focused primarily on the inequitable distribution of the adverse impacts of climate change on economically, politically, and socially marginalized communities around the world. In the case of urban heat, the effects of the UHI are compounded by climate change. Socially vulnerable groups in cities are inequitably exposed to a hazard which amplified by human induced climate change and the built structure of urban environments. As this important subfield of environmental justice research continues to develop, a rigorous empirical methodology is required to examine the interconnection between the built urban environment, urban heat, and socio-demographic characteristics of urban residents.

From an empirical perspective, our case study reveals significant statistical relationships between *where* particularly vulnerable groups live and their *level of exposure* to elevated urban heat. Specifically, the findings clearly indicate that urban heat is distributed inequitably with respect to race, ethnicity, and socioeconomic status in the study area of Pinellas County, Florida. The results of bivariate correlation analysis revealed that mean LST to be significantly greater in neighborhoods with higher population density, higher proportions of non-Hispanic Black, Hispanic, Asian (especially Southeast Asian), and elderly residents, as well as those with higher poverty and lower home ownership rates. Multiple regression analysis confirmed that LST is significantly greater within census tracts that contain higher percentages of certain minority subgroups, higher poverty rates, and lower percentages of home ownership, even after controlling for contextual factors such as population density and the effects of spatial autocorrelation. Taken together, this indicates higher urban heat levels in impoverished and racially segregated census tracts which may be considered more socially vulnerable. Many of these socially vulnerable neighborhoods are located in areas away from the coast and toward the

center of the peninsula, where LST levels are substantially higher. Central Pinellas (cities of East and West Lealman, and Pinellas Park), with higher percentages of residents of Southeast Asian origin, indicating particular social vulnerability, seem especially impacted. Overall, these findings are consistent with prior studies in other metropolitan areas (e.g., Harlan et al 2006; Chow el al. 2012; Hondula et al. 2012) and support the primacy of race, ethnicity, and poverty in explaining patterns of thermal inequity.

Our findings suggest that the urban built environment itself should be considered as an important factor which influences the spatial distribution of urban heat across different, and sometimes more vulnerable demographic and socioeconomic groups. This association of urban heat and socially vulnerable groups reveals the presence of what can be characterized as a *landscape of thermal inequity* within this metropolitan area. The geographic distribution of urban heat and its adverse effects on vulnerable populations is a rapidly growing research area, especially considering the recent pattern of heat waves in North American cities (Gaffen and Ross 1998; Stone et al. 2010). Because of the socio-technical nature of the hazard and its embeddedness within the built structure of the urban environment, comprehensive modes for surveying urban heat provide a tool for enhancing adaptation and mitigation strategies as the impacts of GCC become more pronounced.

CHAPTER THREE:

LANDSCAPES OF THERMAL INEQUITY:

DISPROPORTIONATE EXPOSURE TO URBAN HEAT IN THE THREE LARGEST U.S. CITIES[2]

Introduction

In the past two decades, several high mortality heatwave events have been recorded in developed countries. A 2003 heatwave in Western Europe lead to an estimated 50,000 to 70,000 excess deaths (Robine et al. 2008). In 2010, a heatwave combined with atmospheric pollution caused by fires in the Moscow region of the Russian Federation caused an excess mortality of over 11,000 (Shaposhnikov et al. 2014). While these events were region-wide in scope, the 2003 heatwave affected densely populated urban areas like Paris, France, and its suburbs which suffered the highest rates of mortality (Fouillet et al. 2006). The urban heat island (UHI) effect is the result of several complex factors, including higher structural density and lower amounts of vegetation in urban areas, which create an urban microclimate that is generally hotter than surrounding rural areas (Oke 1992). The relationship between the UHI and elevated mortality has been documented by prior studies (Buechley 1972; Clarke 1972; Smoyer 1998). Additionally, higher rates of heat related mortality have been linked with levels of urbanization and acclimatization, as indicated in an analysis of 50 cities of the U.S. (Medina-Ramón et al. 2007).

[2] Portions of this chapter have been previously published in *Environmental Research Letters*, 2015, *10*(11), 115005 and have been reproduced with permission from IOP Science.

The U.S. is a highly urbanized nation with almost 81 percent of its population living in cities and towns (U.S. Census 2010). This high rate of urbanization increases risks from heat waves for densely situated populations impacted by local climate factors such as the UHI. Urban heat, compounded by periodic and region-wide heat wave events, leads to elevated rates of morbidity and mortality in U.S. cities (Kalkstein and Greene 1997; McGeehin and Mirabelli 2001; Sheridan, Kalkstein, and Kalkstein 2008; Zanobetti et al. 2008). Heat waves are currently the most significant weather-related cause of mortality in the U.S. (NOAA, NWS 2013). Several high mortality events in the U.S. provide examples of the devastating effect of heat waves on urban populations during 1980, 1988, 1995, and 1999. The 1995 Chicago heat wave has been the subject of extensive analysis that found socially vulnerable people, which includes low income, elderly, African-American, and/or socially isolated residents, to be disproportionately exposed (Semenza et al. 1996; Klinenberg 2002). Subsequent studies of different urban areas of the U.S. have confirmed a linkage between urban heat exposure and factors of social vulnerability (McGeehin and Mirabelli 2001; O'Neill et al. 2003; Uejio et al. 2011). Because of the seeming inequitable exposure to the risk posed by urban heat on racial/ethnic minorities and economically disadvantaged populations, the problem is beginning to be framed as an environmental justice issue, specifically one of climate justice.

The environmental injustice implications of exposure to urban heat for individuals of lower socioeconomic status were first discussed in Klinenberg's (2002) sociological analysis of the 1995 Chicago heatwave. This association between heat exposure and social vulnerability was explored in more detail by Harlan et al.'s (2006) quantitative research on "heat-related health inequalities." Jenerette et al. (2011) expanded this work to emphasize the role of land use and land cover in influencing thermal spatial structure and the development of distinct neighborhood

microclimates. These neighborhood level thermal patterns are elements of an "urban heat riskscape" associated with racial/ethnic minority and lower socioeconomic status. Subsequent research by Chow et al. (2012) examined the "spatial distribution of vulnerability" using a wider range of demographic and socioeconomic variables, but focused on the same urban area (Phoenix, Arizona), as Harlan and Jenerette (2006; 2011). Using data related to heat exposure and other climate-based risk factors in conjunction with an expanded set of variables representing socioeconomic status, Grineski et al. (2012 and 2013) examined the bi-national sister cities of El Paso and Ciudad Juarez to find social inequities in exposure to climate change in a study area extending across national boundaries of the U.S. and Mexico, respectively. Both these studies extend the concept of the "climate gap" (Morello-Frosch et al. 2009; Grineski et al. 2012, 2013) by which racial/ethnic minority or lower socioeconomic status residents are both inequitably exposed to climate change and possess inadequate resources to mitigate or adapt to its adverse effects.

The environmental justice concerns outlined in the previously discussed research have been expanded in recent work, but most heat-related studies focus on the U.S. Southwest. The largest U.S. metropolitan areas that are often characterized by higher proportions of African-Americans have not been investigated in this research. While some urban heat studies have been conducted outside the U.S. Southwest (McGeehin and Mirabelli 2001; O'Neill et al. 2003; Uejio et al. 2011), these scholars have not explored the climate justice dimension, or attempted to compare urban areas from different regions of the U.S. A comparative analytical framework that includes a broader range of socially vulnerable groups and allows generalizations across the various urban heat studies is lacking. A systematic and comparative analysis of large urban areas in the U.S. is necessary to provide a foundation for evaluating the association between elevated

urban heat and the location of socially vulnerable populations, and enhance our understanding of the socio-spatial consequences of excess heat exposure.

This article contributes to the emerging environmental justice literature on heat-related inequities by evaluating the spatial and social distribution of urban heat in the three largest U.S. cities: New York, New York; Chicago, Illinois; and Los Angeles, California. By using an index of landscape-related factors collectively related to elevated urban heat, the spatial patterns of association with specific socio-demographic characteristics are examined at the neighborhood level. The objective is to determine if racial/minorities and socioeconomically disadvantaged residents in these three cities are distributed inequitably with respect to an Urban Heat Risk Index, developed by combining three characteristics of the urban thermal landscape: land surface temperature, vegetation abundance, and structural density of the built urban environment. Our use of a single risk indicator that combines three heat-related variables allows us to better develop and evaluate a comparative framework for analyzing patterns of heat-related inequities than what has been previously done. Statistical associations between this Urban Heat Risk Index and multiple indicators of social vulnerability are examined and compared to determine how the socio-spatial distribution of urban heat varies across the three largest cities of the U.S.

Data and Methods

The three study areas were selected based on their large population size and the future risk posed by global climate change. The three most populous metropolitan areas in the U. S. were chosen for analysis: New York City, Los Angeles, and Chicago. Climate change modeling based on the Intergovernmental Panel on Climate Change A2 emissions scenario using National Center for Atmospheric Research mid-century (2045-2059) climate models (NCAR/UCAR

CESM 2013) indicate that all three cities may be substantially impacted in the future by increasing temperatures, with temperature anomalies ranging from 2.0° to 3.0° C. The basic unit of analysis for this study are census tracts defined by 2010 Decennial U.S. Census boundaries. Census tracts are one of the basic spatial units of U.S. census enumeration that are commonly used to represent neighborhoods and include a population that ranges from 2,500 to 8,000 residents. Geographic boundaries for each study area were delineated by selecting contiguous areas of 75% impervious surface, and then including all census tracts within the counties containing those areas of higher ISA. These study area boundaries are depicted in Figure 7, which shows that the counties still include urban and suburban areas of their respective cities. Higher percentages of impervious surface area (% ISA) have been used in prior studies as an indicator of urban land uses (Lu and Weng 2006) and urban cores have been defined as areas with greater than 75% ISA (Imhoff et al. 2010). For this study, areas of high % ISA were identified using the 2006 National Land Cover Dataset before county boundaries were selected. This technique defines the spatial extent of urban areas through their impact to the landscape, rather than arbitrarily selecting the areas included in U.S. Census Metropolitan Statistical Area (MSA) boundaries.

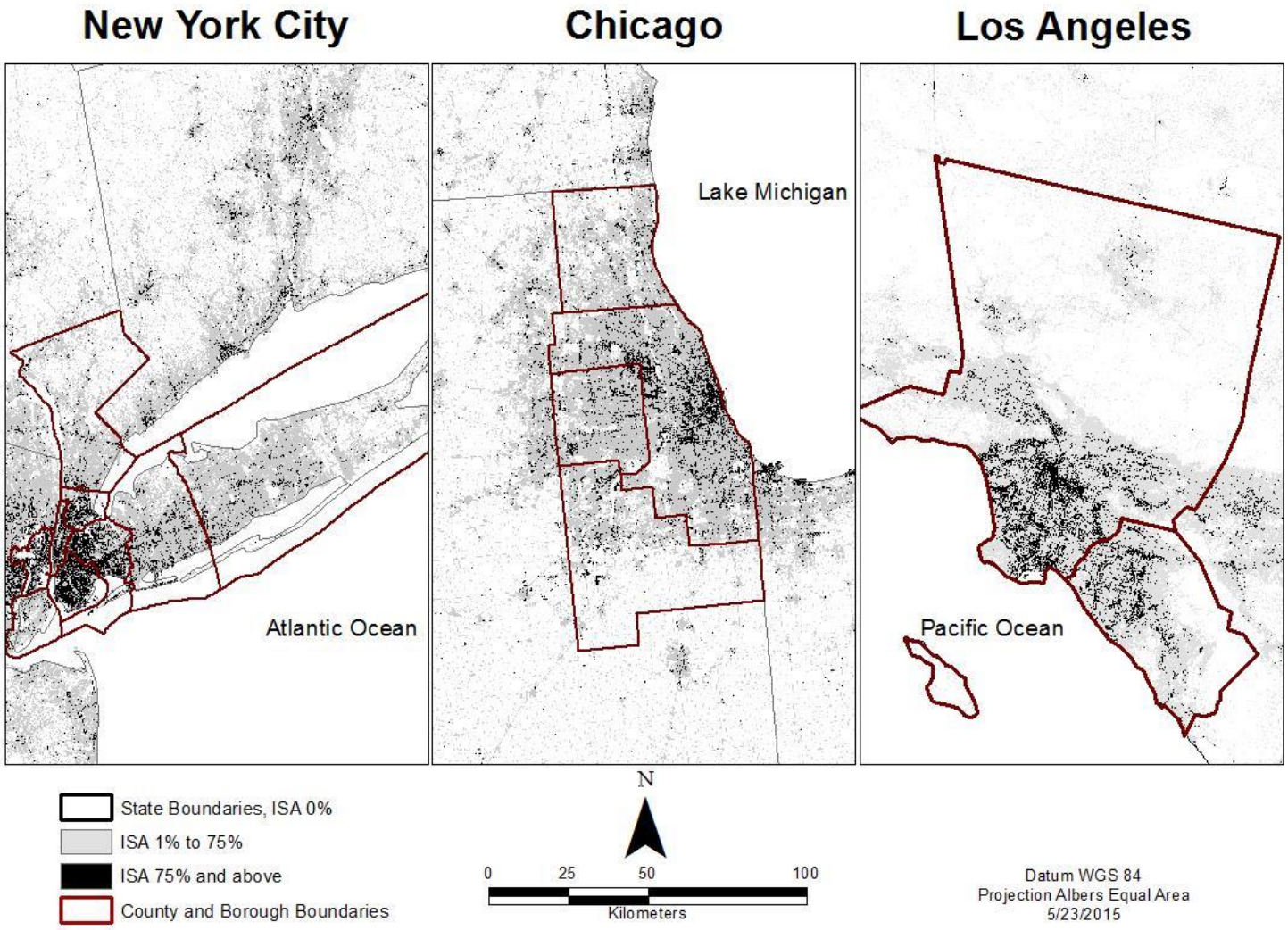

Figure 7. The spatial distribution of percent impervious surface area greater than 75% in New York City, Chicago, and Los Angeles.

This study emphasizes the interaction of physical factors related to urban heat and social vulnerability at the neighborhood level to assess environmental injustice. LANDSAT Thematic Mapper (TM) remote sensing derived data is used to quantify the physical factors of structural density, vegetation abundance, and temperature. Use of LANDSAT data allowed for the representation of urban heat at moderate spatial resolutions of 30 to 120 meters, which are sufficient for neighborhood level measurements. The dependent variable in this study denotes the physical aspects of urban heat-related risk, while the independent variables represent the demographic and socioeconomic characteristics of residents in our study areas.

Dependent Variable: UHRI

A quantitative index of biophysical factors related to urban heat, referred to as the Urban Heat Risk Index (*UHRI*), was developed and used as the dependent variable for our statistical analysis. The values were estimated using the equation:

$$UHRI = (LST + NDBI) - NDVI$$

Where LST is land surface temperature, NDBI is the normalized difference built-up index which assesses built structure density, and NDVI the normalized difference vegetation index, which is an indicator of vegetation abundance. Prior studies have indicated strong correlations between landscape factors of NDBI and NDVI and the UHI (Dousset and Gourmelon 2003; Chen et al. 2003). LST, in particular, has been used to delineate the spatial extent of the surface UHI (Voogt 2000; Voogt and Oke 2003). Additionally, LST has been shown in previous research to have a positive statistical association with rates of heat-related morbidity and mortality (Johnson and Wilson 2009; Johnson et al. 2009; Hondula et al. 2012). We used the equal weighting approach

because there was no logical reason to assume that one of these factors contributes differently to urban heat exposure. The values of LST, NDBI, and NDVI for each pixel in the study areas were derived using LANDSAT satellite Thematic Mapper (TM) 5 remotely sensed imagery. A single clear-sky image from the summer of 2010 was selected for each of the study areas which provided the maximum atmospheric temperature of the available images. In the case of LST, the mono-window algorithm based on the thermal radiance transfer equation was used to extract temperature values from the imagery data (Qin et al. 2001; Pu et al. 2006). The NDBI was calculated using the same imagery with the equation: $DBI = \frac{(SWIR-NIR)}{(SWIR+NIR)}$, where SWIR is the shortwave infrared band and NIR is the near- infrared band, or LANDSAT TM bands 5 and 4 respectively. The NDVI was calculated in the same way using the equation: $NDVI = \frac{(NIR-Red)}{(NIR+Red)}$ using LANDSAT bands 3 and 4. LST, NDBI, and NDVI values were then averaged for the land portion of each census tract, excluding water from calculations of temperature, structural density, and vegetation. The values of these biophysical indicators were then standardized using their z-scores before calculation of the *UHRI* scores for each tract. The tract level distribution of the *UHRI* in our study areas is shown in Figure 8.

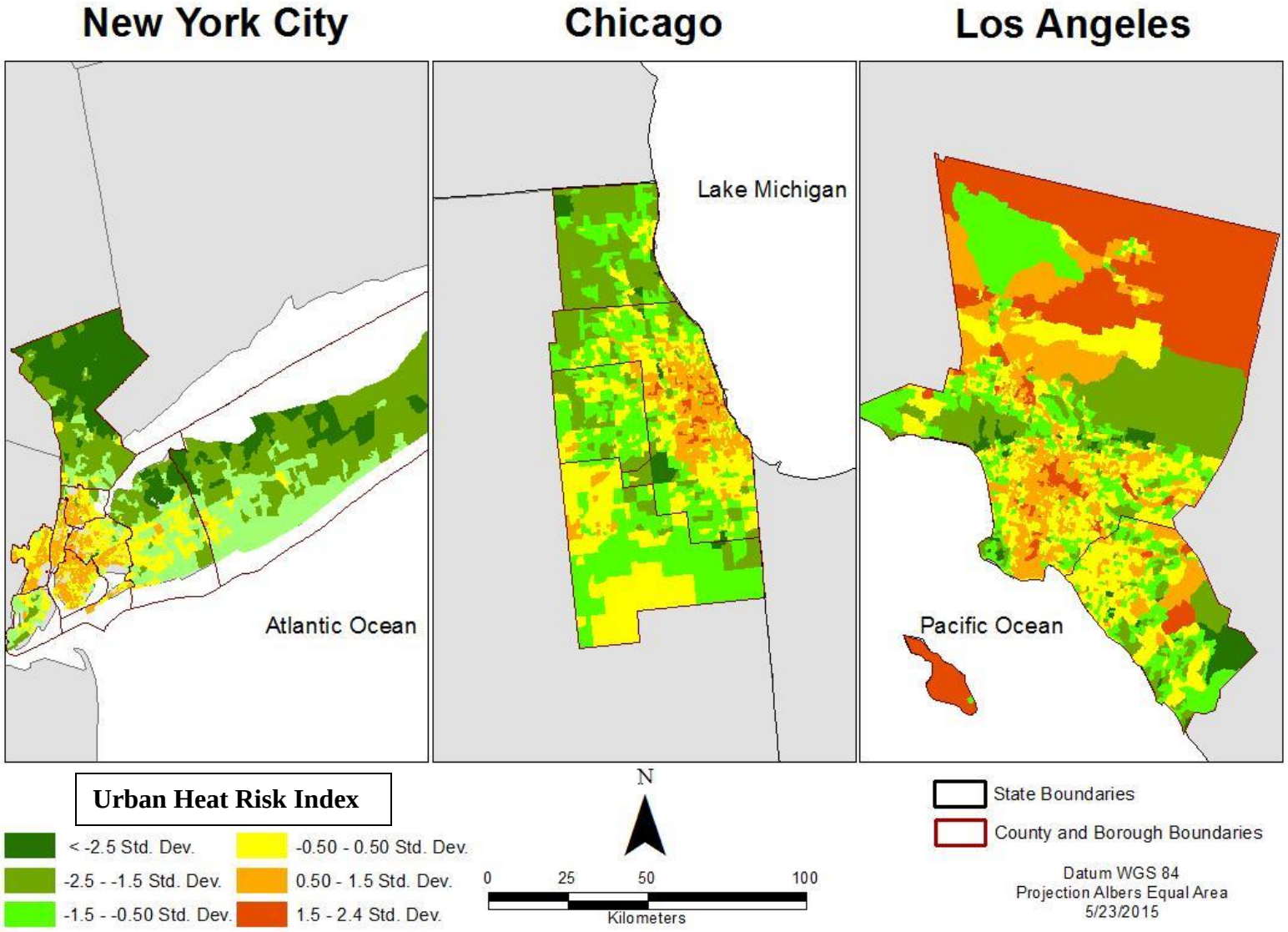

Figure 8. The spatial distribution of the UHRI in New York City, Chicago, and Los Angeles.

Independent Variables

The environmental justice consequences of urban heat were assessed with census tract level socio-demographic data from the 2010 U.S. Census and 2009-2013 five-year American Community Survey (ACS) estimates. Our analysis utilizes variables representing extremes of age (children aged five and under and elderly aged 65 and over), race (Non-Hispanic Black and Asian), ethnicity (Hispanic), median household income, educational attainment (percent 25 and over who are high school graduates), and home ownership (owner-occupied homes), with the addition of the Gini coefficient to measure neighborhood level income inequality. The Gini coefficient from the ACS is a summary measure of income inequality that ranges from 0 to 1. A value of 0 indicates perfect equality where all households in a census tract have equal incomes, while a value of one indicates perfect inequality where only one household has any income. This index has been used as a measure of socioeconomic vulnerability and coping capacity in previous environmental justice studies (Elliott et al. 2004; Chakraborty et al. 2014). Variables representing the percent of disabled persons (disabled for any reason) and linguistic isolation (percent of households in which no one over 14 years of age speaks English) were also included. Disability status and linguistic isolation may reinforce social isolation, potentially diminishing the ability of individuals to understand or respond to public health heat warnings and mitigation measures. The variables indicating social vulnerability can then be assessed for their relevance in specific urban and regional contexts using methodologies that are discussed below. Table 4 includes a list.

Table 4. Variables used in the study of Chicago, Los Angeles, and New York City.

Variable Name	Data Source	Dates
Dependent Variable: Urban Heat Risk Index (*UHRI*)	Calculated as: *(LST+NDVI)-NDBI*	Derived from remotely sensed variables below:
Land Surface Temperature (LST)	LANDSAT 5, TM sensor, 120 meter resolution	New York - July 4, 2010; Chicago - Sept 10, 2010; Los Angeles- Sept 20, 2010
Normalized Difference Built-up Index (NDBI)	LANDSAT 5, TM sensor, 30 meter resolution	
Normalized Difference Vegetation Index (NDVI)	LANDSAT 5, TM sensor, 30 meter resolution	
Independent Variables:		
% Age 5 and under	U.S. Census	2010
% Age 65 and over	U.S. Census	2010
%Non-Hispanic Black	U.S. Census	2010
% Asian	U.S. Census	2010
% Hispanic	U.S. Census	2010
% Disabled	2013 5-year ACS estimates	2009-2013
% High School graduate	2013 5-year ACS estimates	2009-2013
% Non-English speaking	2013 5-year ACS estimates	2009-2013
% Owner-occupied homes	U.S. Census	2010
Median household income	2013 5-year ACS estimates	2009-2013
Gini coefficient	2013 5-year ACS estimates	2009-2013
Population density	U.S. Census	2010

Statistical Methods

Each study area was analyzed separately using all populated census tracts which were not missing data for any of our Independent variables. First, descriptive statistics were used to compare the three different study areas. Next, scatterplots of the *UHRI* and each of our independent variables were examined and natural logarithmic transformations of specific variables were calculated to account for nonlinear relationships. Subsequently, all variable values were standardized and bivariate correlation analysis was conducted using parametric tests, based on Pearson's correlation coefficient.

The relationship between the dependent variable (*UHRI*) and the set of independent variables in each study area were then analyzed using the ordinary least-squares (OLS) regression method. While OLS regression has been used extensively in the analysis of environmental and social inequities, it assumes that the observations and regression errors are independent. This assumption is likely to be invalid due to the clustering of similar values in space, or spatial autocorrelation (Kissling and Carl 2008; Chakraborty 2011). We tested the residuals for spatial autocorrelation using the global and univariate Moran's *I*-statistic (Anselin and Bera 1998). The Moran's *I* for the OLS models associated with all three study areas exhibited significant ($p<.001$) spatial autocorrelation in the residuals, implying that they failed to meet the assumption of independence. Consequently, we used simultaneous autoregressive (SAR) models, which consider the spatial autocorrelation as an additional variable in the regression equation to estimate its influence simultaneously with that of the other variables (Chakraborty 2011). To determine the appropriate SAR model specification, the Lagrange Multiplier (LM) statistic was utilized (Anselin 2005). The LM test indicated that spatial error models should be used in all three study areas.

Spatial regression models are based on the relationship between neighboring analytical units, using either contiguity or distance between tract centroids to define a spatial weights matrix. Both the queen contiguity approach and iterative selection of distance bands were tested, but the distance-based approach was more successful in reducing residual spatial autocorrelation, as measured by global Moran's *I*-statistic, to a statistically non-significant level in each study area. The optimal distances for these bands were determined to be 7,300, 8,500, and 7,400 meters, respectively, for New York City, Chicago, and Los Angeles. Finally, the multicollinearity condition index associated with the regression models were found to be smaller

than 8.0 in all three study areas, ruling out significant correlations between the independent variables.

Results

Differences in the natural and built landscape of each study area greatly impacted the geographic distribution of *UHRI* scores, particularly in Los Angeles with its sparsely populated desert areas. Visual examination of the spatial patterns of percentage impervious surface over 75% and the *UHRI* in Figures 7 and 8 indicate considerable overlap of these two factors in all three study areas, which should be expected since structural density is one of the variables that comprise the *UHRI*. However, in the case of Los Angeles, the relationship changes in the extreme northern desert areas that have relatively higher *UHRI* levels but lower levels of impervious surface. The descriptive statistics for all variables in our three study areas are summarized in Table 5.

Of the three study areas, Los Angeles with its sprawling urban structure and arid region north of the San Gabriel Mountains has the highest mean NDBI, and lowest NDVI, indicating that it is extensively built-up and sparsely vegetated, with areas of exposed rock and soil. One limitation of the NDBI is its inability to delineate areas of barren soil from built urban structure, (Zha et al. 2003). Los Angeles also had the highest mean LST and the date that the remote sensing image was taken (September 20, 2010) coincided with a heatwave in the Los Angeles region during which the daily high atmospheric temperature exceeded 40°C.

Table 5. Descriptive statistics for dependent and independent variables at the census tract level for Chicago, Los Angeles, and New York City.

	New York			Chicago			Los Angeles		
Variable	**Min**	**Max**	**Mean**	**Min**	**Max**	**Mean**	**Min**	**Max**	**Mean**
LST(°C)	22.68	51.61	44.46	25.53	35.24	31.32	30.17	53.20	45.41
NDBI	-0.194	0.233	0.081	-0.094	0.209	0.062	-0.020	0.338	0.138
NDVI	-0.082	0.696	0.184	-0.049	0.562	0.276	-0.074	0.372	0.094
UHRI (standardized)	-9.24	4.75	0	-7.44	5.84	0	-10.76	8.66	0
% Age 5 and under	0	22.70	6.13	0	16.00	6.60	0	15.20	6.42
% Age 65 and over	0	82.60	12.77	0	52.40	11.60	0.10	82.40	11.38
% Non-Hispanic Black	0	96.51	21.95	0.03	99.34	23.53	0	90.75	7.19
% Asian	0	88.13	10.71	0	88.88	5.98	0	87.20	14.28
% Hispanic	0	93.20	26.01	0.10	98.70	20.70	3.00	99.00	44.09
% Disabled	0	74.00	9.42	0	36.00	9.84	0	88.20	9.23
% High school	0	100.00	72.56	28.50	100.00	84.83	23.50	100.00	76.46
% Non-English	0	74.70	12.79	0	53.20	7.69	0	79.10	14.99
% Owner-occupied	0	100.00	45.31	0	100.00	61.71	0	96.70	50.60
Median household	9675	243622	67285	9550	236250	63,840	6406	231648	64,829
Gini coefficient	0.0189	0.6750	0.4325	0.2092	0.7215	0.4204	0.0600	0.7200	0.4154
Population density	5	114639	14610	12	196409	4215	1	36483	4739
Number of tracts	3096			1838			2927		

In contrast to Los Angeles, the cities of Chicago and New York are more extensively vegetated and have lower structural density as measured by the NDVI and NDBI. Chicago had the lowest mean LST, the imagery been taken on September 12, 2010, a day when atmospheric temperature reached only 30°C. Cloud-free LANDSAT TM imagery taken on a day of warmer atmospheric temperatures was not available for Chicago that year. The data for New York revealed a higher mean NDBI and lower NDVI than Chicago, indicative of greater structural density and less extensive vegetation. New York was also much warmer than Chicago, with a mean LST only 1° C cooler than Los Angeles. This is because the New York data was taken on July 4, 2010, with a daily high temperature of 35°C and also because it was a longer summer day, with an hour more insolation at the time of image capture than for either Chicago or Los Angeles. The values of LST, NDBI and NDVI were standardized prior to the calculation of the *UHRI* variable. In the case of LST, this standardization compensated for differences in temperature levels for the dates the remote sensing imagery was taken. The *UHRI* scores indicate the highest mean values for New York, followed by Los Angeles and Chicago. This can be partly explained by the very high LST and low NDVI values for tracts in the desert areas of Los Angeles, some of which were excluded from the study due to their low population values of less than 500. LST in the New York study area ranged widely, and landcover varies from marshes to concrete and asphalt, however unlike Los Angeles, the hottest tracts still contained exposed populations. While the landscape of Los Angeles may have greater extremes in temperature and less vegetation, the manner in which its population is exposed to these risks differs from that of Chicago and New York.

Examination of descriptive statistics for the independent variables (Table 5) reveals considerable differences in socio-demographic characteristics that reflect the diverse urban

ecologies of these study areas. New York City has a much higher population density than the other two study areas, an indicator of the intensity and extent of its residential built urban structure. There are substantial differences in the socioeconomic and racial/ethnic composition of the three cities. Los Angeles has a lower Non-Hispanic Black and higher Hispanic mean population percentages in its tracts than the other cities and also a higher percentage of linguistically isolated households. Chicago had the highest Non-Hispanic Black and lowest Asian mean population, but also the highest mean percentage of high school graduates.

Bivariate correlations of the *UHRI* scores with the independent variables, listed in Table 6, revealed similar statistical relationships across the three study areas for most variables. The age-related variables show consistent significant and positive associations with the *UHRI* for percentage Age 5 and under, and negative for Age 65 and over. This limited exposure appears to be inconsistent with prior research which suggests that elderly adults are not only a particularly vulnerable group, but may have higher levels of exposure (Semenza et al. 1996; Klinenberg 2002; Fouillet et al. 2006). However, socioeconomic status may be a confounding factor since the percentage of individuals aged 65 or more shows a significant and positive relationship with home ownership based on Pearson's correlation coefficient in all three study areas, and with median household income in New York City and Los Angeles. The percentages of Non-Hispanic Black and Hispanic residents are consistently and positively associated with the *UHRI*, suggesting that tracts with higher proportions of these racial/ethnic groups are exposed to higher levels of biophysical risk. The Asian subgroup indicates a significantly positive correlation only in New York City, but significantly negative relationships in the two other areas.

Table 6. Bivariate correlation of Urban Heat Risk Index with census tract level independent variables for Chicago, Los Angeles, and New York City.

	Pearson's *r*		
Variable	**New York**	**Chicago**	**Los Angeles**
% Age 5 and under	.218**	.328**	.426**
% Age 65 and over	-.323**	-.259**	-.416**
% Non-Hispanic Black$_a$	.249**	.216**	.212**
% Asian$_a$	.195**	-.076**	-.099**
% Hispanic$_b$	.222**	.435**	.547**
% Disabled	.207**	.157**	.146**
% High school graduate$_c$	-.130**	-.505**	-.591**
% Non-English speaking$_d$	.430**	.376**	.488**
% Owner-occupied homes	-.671**	-.534**	-.442**
Median household income	-.541**	-.515**	-.625**
Gini coefficient	.175**	.066**	-.181**
Population density$_a$	.537**	.317**	.357**

**$p < .01$ Variables natural log transformed: a= Los Angeles, New York; b= Chicago, New York; c= Chicago, Los Angeles; d= Chicago, Los Angeles, New York

In terms of the other variables, the percentage with a disability shows positive and significant correlations with the *UHRI* in all three areas. Educational attainment measured by percentage of high school graduates was significantly and negatively associated, while linguistic isolation was significant and positive in all three study areas. Relationships were particularly strong, significant, and consistent between the *UHRI* and socioeconomic characteristics. Median household income and home ownership show significant and negative relationships with the *UHRI*, indicating that greater biophysical risk is associated with lower socioeconomic status in all three study areas. Finally, population density is consistently significant and positive across the three study areas.

A spatial error regression analysis (regression coefficients) was run for the three cities, the results of which are summarized in Table 7. The percentage of individuals aged 5 and under was significantly and negatively related with *UHRI* in New York City and Los Angeles, but positively related in Chicago. The significance and direction of relations between *UHRI* and the variable age 65 and over was significant and negative in New York City and Los Angeles, but non-significant in Chicago. The proportion of racial/ethnic minorities was generally higher in areas of greater urban heat risk. Non-Hispanic Black and Hispanics were significantly and positively related to the *UHRI* in Chicago and Los Angeles, while Asians were significantly and positively associated with the *UHRI* in all three study areas. Disability was significant and positive only in Los Angeles, The percentage of high school graduates significant and negative in Los Angeles. Linguistic isolation measured by percent Non-English speaking households was significant and positive in both New York and Chicago.

Table 7. Spatial error regression of Urban Heat Risk Index for Chicago, Los Angeles and New York City.

	New York	**Chicago**	**Los Angeles**
% Age 5 and under	-.048**	.066**	-.092**
% Age 65 and over	-.134**	-.019	-.111**
% Non-Hispanic Black$_a$	-.013	.067***	.095**
% Asian$_a$	.031***	.089**	.169**
% Hispanic$_b$	-.111**	.145**	.297**
% Disabled	.014	-.005	.044***
% HS graduate$_c$	-.007	-.013	-.120**
% Non-English speaking$_d$	.079**	.068**	.011
% Owner-occupied homes	-.269**	-.019	-.211**
Median HH income	-.076**	-.144**	-.259**
Gini coefficient	-.076**	-.135**	-.123**
Population density$_a$	.496**	-.009	-.229**
Spatial error term (*rho*)	.772**	.960**	.906**
Akaike Info Criterion	5237.82	3106.46	5567.99
Pseudo r-squared	0.69	0.70	0.62
Moran's I	-0.001	-0.001	0.001

***$p < .001$; **$p < .01$; *$p < .05$ Variables natural log transformed: a= Los Angeles, New York; b= Chicago, New York; c= Chicago, Los Angeles; d= Chicago, Los Angeles, New York

The socioeconomic variables generally showed the same consistent patterns of significant and negative associations with the *UHRI* that were revealed in the bivariate correlation analysis. Home ownership was significant and negative in New York City and Los Angeles, while median household income showed a significant negative relationship across all three study areas. The Gini coefficient was also significantly negatively associated, indicating greater economic homogeneity for tracts with elevated *UHRI*. These three factors collectively imply that there is a consistent relationship between lower socioeconomic status and increased *UHRI* across our study areas.

Our spatial definition of study regions for this analysis relies on the selection of areas with high percentages of contiguous impervious surface and the political boundaries of the associated counties. This approach results in the inclusion of urban, suburban, and sometimes rural areas within the counties selected for analysis. The final step of our analysis focuses on assessing how the statistical relationships with the *UHRI* observed in Table 7 would change if rural and suburban areas with relatively lower population density were excluded from each of the three study areas. To compare the results of the broader metropolitan areas with those of their core urban areas, restricted and more structurally dense areal extents were chosen and spatial regression models were estimated for these core urban areas. The New York City study area was redefined using data from its five boroughs and Hudson County, New Jersey, Chicago was restricted to the boundaries of Cook County, and only areas south of the San Gabriel Mountains were included in the Los Angeles study area. This resulted in the exclusion of rural areas in north Long Island and Westchester County with higher vegetation and low structural density (New York), rural areas north and west of Cook County (Chicago), and the arid and less vegetated northern areas which produce high NDBI values and yet are not structurally dense (Los

Angeles). For estimating the spatial error models for these core urban areas, spatial weights were recalculated resulting in 5,100, 6,000, and 7,200 meter distance bands for New York City, Chicago, and Los Angeles, respectively. The regression results for both the larger metropolitan and core urban areas are summarized in Table 8. In both Chicago and Los Angeles, the statistical significance and signs for most independent variables are similar in the larger metropolitan and core urban areas, although regression coefficients for a few variables indicate higher values. The results for New York, however, reveal substantial changes when the predominantly rural areas are excluded from the analysis. When the more structurally dense and socio-demographically heterogeneous core area is considered, the signs of the coefficients relating the *UHRI* to the Gini coefficient, median household income, and percent high school graduates all change to become significant and positive, as do the coefficients for the variables percent age 5 and under and percent Hispanic population. Additionally, percent Asian residents becomes non-significant, the percent disabled becomes significant, and home owner-occupancy becomes non-significant in the model for the core area of New York City. These directional changes in statistical associations with the *UHRI* for eight of our 12 independent variables in New York City emphasize the importance of scale and spatial extent when selecting study areas for urban heat analysis. The relatively minor changes in significance of the variables in Chicago and Los Angeles indicates the stability of the *UHRI* model in those areas, though goodness-of-fit as indicated by the *pseudo r-squared* and *Akaike Information Criterion* is smaller in models from the core urban areas when compared to the models based on the larger study area extents for all three study areas.

Table 8. Comparison of spatial error regression model results for broader metropolitan and core urban areas for Chicago, Los Angeles, and New York City.

	New York		Chicago		Los Angeles	
	Broader	**Core**	**Broader**	**Core**	**Broader**	**Core**
% Age 5 and	-.048**	.177**	.066**	.421**	-.092**	-.108
% Age 65 and	-.134**	-.357**	-.019	-.015	-.111**	-.229**
% Non-Hispanic Black$_a$	-.013	-.099	.067***	.387**	.095**	.322**
% Asian$_a$	.031***	-.016	.089**	.315**	.169**	.196**
% Hispanic$_b$	-.111**	.328**	.145**	.575**	.297**	.484**
% Disabled	.014	.113*	-.005	.065	.044***	.204**
% HS graduate$_c$	-.007	.398**	-.013	.0003	-.120**	-.539**
% Non-English speaking$_d$	.079**	.344**	.068**	.179**	.011	.168**
% Owner-occupied homes	-.269**	-.074	-.019	.219*	-.211**	-.285**
Median HH	-.076**	.219**	-.144**	-.165	-.259**	-.567**
Gini coefficient	-.076**	.439**	-.135**	.082	-.123**	-.050
Population	.496**	.498**	-.009	.082	-.229**	-.171**
Spatial error term (*rho*)	.772**	.945**	.960**	.957**	.906**	.161
AIC	5237.82	8803.88	3106.46	4762.67	5567.99	10532.50
Pseudo r-squared	0.69	0.49	0.70	0.61	0.62	0.49
Moran's I	-0.001	0.001	-0.001	<.001	0.001	<.001
N (no. of tracts)	3,096	2,327	1,838	1,318	2,927	2,638

***$p < .001$; **$p < .01$; *$p < .05$

Variables natural log transformed: a= Los Angeles, New York; b= Chicago, New York; c= Chicago, Los Angeles; d= Chicago, Los Angeles, New York

Concluding Discussion

The effects of urbanization and an increasing global temperature baseline make cities important sites for studying racial/ethnic and socioeconomic inequities in heat exposure and its negative consequences. There have been recent indications that urban areas have experienced higher incidences of heat waves, with half of the 217 cities in a recent global study showing

increases in extreme hot days from 1973 to 2012 (Mishra et al. 2015). The current pace of urbanization combined with temperature increases will probably expand the number of people exposed to the adverse health effects of episodic heat waves. In this context, our study focused on documenting and analyzing landscapes of thermal inequity which are developing in the U.S., but exist at a variety of scales across our planet. The dynamic behind this landscape are the anthropogenic modifications to the land surface by urbanization and chemical composition of the atmosphere through industrialization. This landscape of thermal inequity is influenced by aspects of a physical landscape produced by changes in structural density and vegetation discernible in the urban heat island effect and its alteration of urban microclimates. It also manifests as a transformation to the landscape due to changes in regional climate resulting in greater temperature extremes and shifting rainfall patterns. Finally, it is also a social landscape of community location and varying urban ecology.

Our study provides a comparative assessment of urban heat exposure resulting from changes to the physical landscape and factors relating to urban ecology which shape the spatial pattern of social vulnerability in the three largest U.S. cities. By developing a new risk index, our research allows the systematic and comparative analysis of urban heat in different cities. There are, however, certain limitations associated with the evaluation of disproportionate heat risk using urban landscape factors. One limitation is that mitigating or adaptive strategies like air conditioning are not accounted for. Most people in urban areas spend a higher portion of their time indoors, which would be mitigated by the presence or absence of air conditioning, which is itself potentially influenced by socioeconomic status. Additionally, the presence or absence of private backyard shade access can also factor into heat risk. Although these variables were not included in our study, these factors might alter the statistical relationships that we found.

Synthesizing across the three study areas, we find consistent and significant associations between the risk factors of urban heat and lower socioeconomic status of urban residents, which are similar to those reported in previous studies of other U.S. cities. The greatest consistencies in association were present in the socioeconomic variables related to household income and home ownership, and also the Gini coefficient, while the demographic variables suggest that local patterns in the distribution of racial/ethnic minority neighborhoods influence the relationship between heat exposure and social vulnerability. Higher risk burdens imposed on neighborhoods occupied by African-American and Hispanic residents were consistently evident in the bivariate correlations, and in all areas except New York in the multiple regression analysis. Linguistic isolation was also a significant factor in all areas except for Los Angeles. We also found disproportionate exposure to heat risk for neighborhoods that contain a higher proportion of disabled individuals and those who lack high school education. Our comparison of analytical results from the broader metropolitan and core urban areas indicated that scale and spatial extent of the study area is an important consideration for analyzing thermal inequity. The spatial error model estimated for core urban areas revealed several changes in the results for New York City, but indicated relatively minor changes in the significance and signs of variables for Chicago and Los Angeles. These differences are indicative of the varying urban ecologies of the study areas, as well as their relationships with structural and vegetation density and land surface temperature.

In conclusion, our statistical findings point to a climate justice issue that is related to the "climate gap" suggesting that people and households with reduced economic means to adapt to and mitigate the effects of urban heat have greater exposure to its adverse effects (Grineski et al. 2013; Shonkoff et al. 2011). The association between urban heat risk and social vulnerability indicates the need for improved urban heat island and heat wave mitigation strategies. Since the

problem of urban heat exposure is complicated by local factors related to the urban structure and by an increasing global temperature baseline, it demands policy decisions at multiple scales. Structuring effective strategies involves increased research, planning, and resource allocation in areas of cities where minorities and low-income populations are concentrated and more exposed to extreme heat. A major impediment here is the lack of awareness among urban planners and public health officials of the risk burdens imposed on socially vulnerable residents by elevated greenhouse gas and co-pollutant emissions and their amplification by urban heat (Mendez 2015). However, the landscape of thermal inequity found in the three largest U.S. cities represents an important example of climate injustice faced by communities characterized by racial/ethnic minorities and socioeconomically disadvantaged residents and underscores the need to conduct more comparative analyses and develop appropriate policy solutions.

CHAPTER FOUR

EXPLORING THE RELATIONSHIP BETWEEN RESIDENTIAL SEGREGATION AND THERMAL INEQUITY IN TWENTY U.S. CITIES

Introduction

In the U.S., racial, ethnic, and economic segregation has played a crucial role in establishing the life constraints and environmental exposures of minorities and people with incomes below the poverty level. The intertwining of social differences with environmental exposure in different places is a primary component of environmental justice concerns (Walker 2012). Much of environmental justice scholarship has been driven by the insight that the stratification of groups of socially disadvantaged people into segregated neighborhoods presents different environmental exposures leading to inequity: communities of people with the least socioeconomic means and power to adapt to or mitigate their risk are often the most exposed (Lopez 2002; Morello-Frosch et al. 2002; Morello-Frosch and Jesdale 2006; Morello-Frosch and Lopez 2006). At the core of this insight is the realization that environmental exposure is often contingent upon the relative economic and political power of groups within society and the siting of neighborhoods where socially disadvantaged people live within urban areas. However, debate over the "relative predictive power of race and income," and whether one factor is more important than the other in determining environmental exposure has occupied much attention (Downey and Hawkins 2009). Ranking the primacy of one factor over the other, income or race,

overlooks their intertwining, neglecting the fundamental economic and social dynamics of neighborhood segregation. Segregation is a multifaceted social process, involving not only the separation of people based on race or ethnicity, but their clustering, concentration and isolation from other groups (Massey and Denton 1989). As such, it directly affects the inequitable exposure of minorities, especially those with low income, to a wide range of environmental hazards. Segregation is an essential cause of distributive injustices in environmental exposure.

Environmental justice scholars have considered the inequity of exposure to a broad range of hazards, human-made and natural. In the case of climate change, multiple exposures to risk are being presented and much has been written about the natural hazards of sea level rise, increasing storm occurrence and intensity, and the vulnerability of coastal areas (Cutter et al., 2009). Changes to the temperature baseline and the occurrence of temperature anomalies, presents another type of risk driven by climate change (Gaffen and Ross 1998; Hales et al. 2003; Meehl and Tebaldi 2004). Increases in temperature are associated with episodic heatwaves which have a documented history of increasing mortality rates (Ellis and Nelson, 1978; Kalkstein and Davis 1989; Kalkstein and Greene 1997; McGeehin and Mirabelli 2001; Sheridan, Kalkstein, A.J., and Kalkstein, L.S. 2008). Children (Vanos 2015), older adults (Semenza et al. 1999; Whitman et al. 1997), people living with disabilities or of lower socioeconomic status (Curriero et al. 2002; Harlan et al. 2006), and some minorities (O'Neill et al. 2003; Uejio et al. 2011; Whitman et al. 1997) are considered to be socially vulnerable, or at higher risk than the general public from heat waves. In the U.S., the 1995 Chicago heat wave has been cited as an example of social inequity in the distribution of risk (Klinenberg 1999). More recently, two extreme heat events in Europe (2003, 2010) resulted in exceptionally high mortality rates (Poumadere et al. 2005; Shaposhnikov et al. 2014), and the Third National Climate Assessment in 2014 cites

extreme heat events among the key human health concerns associated with global climate change (Melillo et al. 2014). Recent studies present the possibility of an increase in summer temperature anomalies (Christidis et al. 2015), such that over the next two decades, over half the world's population will be exposed to summer mean temperatures in excess of the historically hottest summer (Mueller et al. 2016). The increasing summer mean temperature presents particular risk to urbanized populations, where the twin anthropogenic causes of higher temperatures; climate change and the urban heat island (UHI) places large populations at heightened risk. This exposure is not equally distributed spatially, but can be localized, with specific neighborhoods at greater risk (G. Huang et al. 2011). Social differences to exposure to urban heat is rooted in the sometimes localized spatial distribution of urban heat in micro-urban heat islands (Aniello et al. 1995), the segregated structure of cities where socially vulnerable groups sometimes live in the densest, least vegetated areas with higher heat exposure (Harlan et al 2013), and the difficulty socially vulnerable groups have in adapting to and mitigating their exposure. Aside from passing concern about mass casualties during heatwaves, differential exposure to urban heat and the ability of socially vulnerable groups to cope with it has been overlooked by most environmental justice researchers.

Since environmental justice focuses on racial and ecomnomic disparity in environmental exposure, residential segregation, with its impact on the spatial arrangement of communities, is of critical importance. Numerous studies have examined the role of metropolitan level residential segregation in health outcomes in the public health literature (Hart 1998; Collins 1999; Cooper 2001; Kramer 2008; Osypuk 2008) however, the association between racial/ethnic segregation has not been examined in the same detail. An early study by Lopez (2002) examined the relationship of air toxics exposure and Black/White segregation using the dissimilarity index in

44 U.S. metropolitan areas. Its results suggested that the combination of segregation, Black/White poverty, and higher levels of manufacturing employment within MSAs were significant factors in increased exposure. Another national study of air toxics exposure at the census block group level by Morello-Frosch and Jesdale in 2006 found significant health disparities by economic status and Black/White and Hispanic/White segregation. This was followed by Downey's (2007) study of air toxics exposure and Black/White and Hispanic/White segregation which presented complex findings. There were considerable differences in exposure between the 61 metropolitan areas, with higher levels of exposure for Black populations in some areas and for Hispanics in others, suggesting a complicated relationship between this form of environmental exposure, segregation, and economic inequality. Finally, Jesdale et al. (2013) examined the relationship between heat-risk related land cover, the location of minority communities, and segregation across the nation. Greater minority presence and higher segregation levels corresponded with lower levels of tree canopy, one indicator of higher exposure to urban heat. Aside from the previously mentioned study, the literature relating race/ethnicity, measures of segregation, and exposure to urban heat is mostly undeveloped, leaving questions regarding their role in inequitable exposure to urban heat largely unanswered.

This paper examines social inequities in the distribution of urban heat in twenty of the largest U.S. cities, many of which are typified by conditions of extreme segregation also called "hypersegregation" (Massey and Denton 1989). Previous studies have shown that in many urban areas socially vulnerable groups are associated with greater health risk (McGeehin and Mirabelli 2001; O'Neill et al. 2003) from exposure to urban heat (Huang et al. 2011; Uejio et al. 2011). This association has been found in areas with higher proportions of racial and ethnic minorities (Grineski et al. 2012; Collins et al. 2013) and with populations of lower socioeconomic status

(Harlan et al. 2006; Mitchell and Chakraborty 2015). In fact, this is a global urban problem arising out of the structure of cities and suburbs as Byrne et al. (2016) examined in lower income neighborhoods of Gold Coast City in Australia which have higher exposure to urban heat than wealthier areas. However, aside from Jesdale et al.'s work (2013), the relationship with segregation has not been systematically analyzed.This paper extends the environmental justice literature on urban heat by examining whether cities with higher levels racial and ethnic segregation, and which contain neighborhoods with greater socioeconomic disparity, have heightened exposure. It proposes that socially vulnerable groups are exposed to higher levels of urban heat, then examines whether the segregated social structure of U.S. cities is also associated with inequitable exposure. This paper employs multilevel modeling techniques to examine whether segregation impacts the association of race, ethnicity, and income in exposure to one aspect of climate change: neighborhood level differences in exposure to urban heat by testing two hypotheses:

H1: Within metropolitan areas, higher levels of urban heat as measured by an urban heat risk index (UHRI) are associated with larger proportions of racial and ethnic minorities and with lower socioeconomic status of neighborhoods.

H2: Between metropolitan areas, greater levels of racial and ethnic segregation within a metropolitan area is associated with higher exposure to urban heat as measured by the UHRI.

Both hypotheses are tested using multi-level modeling (MLM) which allows variables nested at different levels of grouping to be statistically tested for their association. In the case of this study H1 will be assessed within metropolitan areas at the census tract level to discern the significance of the relationship between race, ethnicity, socioeconomic status and higher exposure to urban

heat. H2 involves a metropolitan level examination of segregation between 20 metropolitan statistical areas (MSA) widely distributed across the U.S. These hypotheses aim to examine whether lower socioeconomic and racial/ethnic minority status are associated with exposure to higher levels of urban heat, and whether residential segregation influences this association.

Data and Methods

This study utilizes a retrospective, cross-sectional design with two components. The first component is a within MSA analysis of the association of the UHRI and variables indicative of demographic and socioeconomic status. The second component is a between MSA analysis of the UHRI and five indices of segregation identified by Massey and Denton (1989) as indicators of hypersegregation. Segregation has typically been examined using only the well-known dissimilarity index (ID) to quantify the evenness of distribution for two groups (Lopez 2002; Morello-Frosch and Jesdale 2006; Downey 2007). The use of a single index has been criticized because it understates the level and the complexity of segregation, especially for Black neighborhoods, which entail other spatial aspects such as centralization, clustering, concentration, and isolation (Acevedo-Garcia et al. 2003). The aforementioned five indices have been used in different combinations to assess levels of segregation nationally, notably by the U.S. Census Bureau (2002), to evaluate changes in urban segregation over time (Reardon and O'Sullivan 2004; Galster and Cutsinger 2007).

The 20 U.S.cities included as study areas were selected on the basis of their large population size, wide regional distribution, and projected increase in extreme heating days by mid-century due to global climate change. First, MSAs with the highest population sizes were

identified. They were then divided by the four U.S. Census regions. Five cities from each of the four U.S. Census regions were selected, providing a wide distribution of urban areas across the country, representing both coastal and mid-continental areas. No more than one city per state was selected. Consequently, even though Dallas and Houston Texas are two of the largest cities by population, the larger city, Dallas with the greater increase in predicted extreme heating days, was chosen to represent cities most at risk and also prevent the overrepresentation of particular states. The resulting sample of cities listed in Table 9 are home to nearly one-third of the U.S. population. Data on the number of extreme heat events (EHEs) from 1975-1995, and their predicted number in 2050 are displayed (Greene et al. 2011).

Table 9: List of the twenty MSAs selected.

Region	City	Average Extreme Heat Event Days 1975-1995*	Predicted Extreme Heat Event Days 2050	2010 Population
Northeast	New York City	11	55	19,000,000
	Philadelphia	6	54	5,900,000
	Boston	11	51	4,600,000
	Providence	7	38	1,600,000
	Hartford	6	31	1,200,000
South	Dallas	11	22	6,500,000
	Atlanta	5	48	5,400,000
	Tampa	3	36	2,800,000
	Washington D.C.	16	53	5,600,000
	Memphis	9	18	1,300,000
Midwest	Chicago	5	18	9,500,000
	Detroit	9	15	4,300,000
	Minneapolis	8	23	3,300,000
	St. Louis	11	35	2,800,000
	Cincinnati	4	22	2,100,000
West	Los Angeles	1	60	12,900,000
	Phoenix	7	84	4,200,000
	Seattle	2	54	3,500,000
	Denver	9	88	2,600,000
	Portland	4	42	2,300,000
Total	20			101,200,000

*Estimated by Greene et al., 2011 using NCAR, CCM3 climate models

In order to visualize the possible impact of climate change on the sample cities, data predicting increases in high temperature anomalies based on the National Center for Atmospheric Research (NCAR) mid-century (2045-2059) climate models (NCAR/UCAR CESM 2014) was mapped. These models are produced from the Community Climate System Model (CCSM) which simulates a variety of climate change scenarios established by the IPCC Fourth Assessment report. The map in Figure 9 displays a pattern of increasing summer temperature anomalies which affects the entire U.S., but is especially strong in the west and Midwest and for the cities represented in the sample in particular.

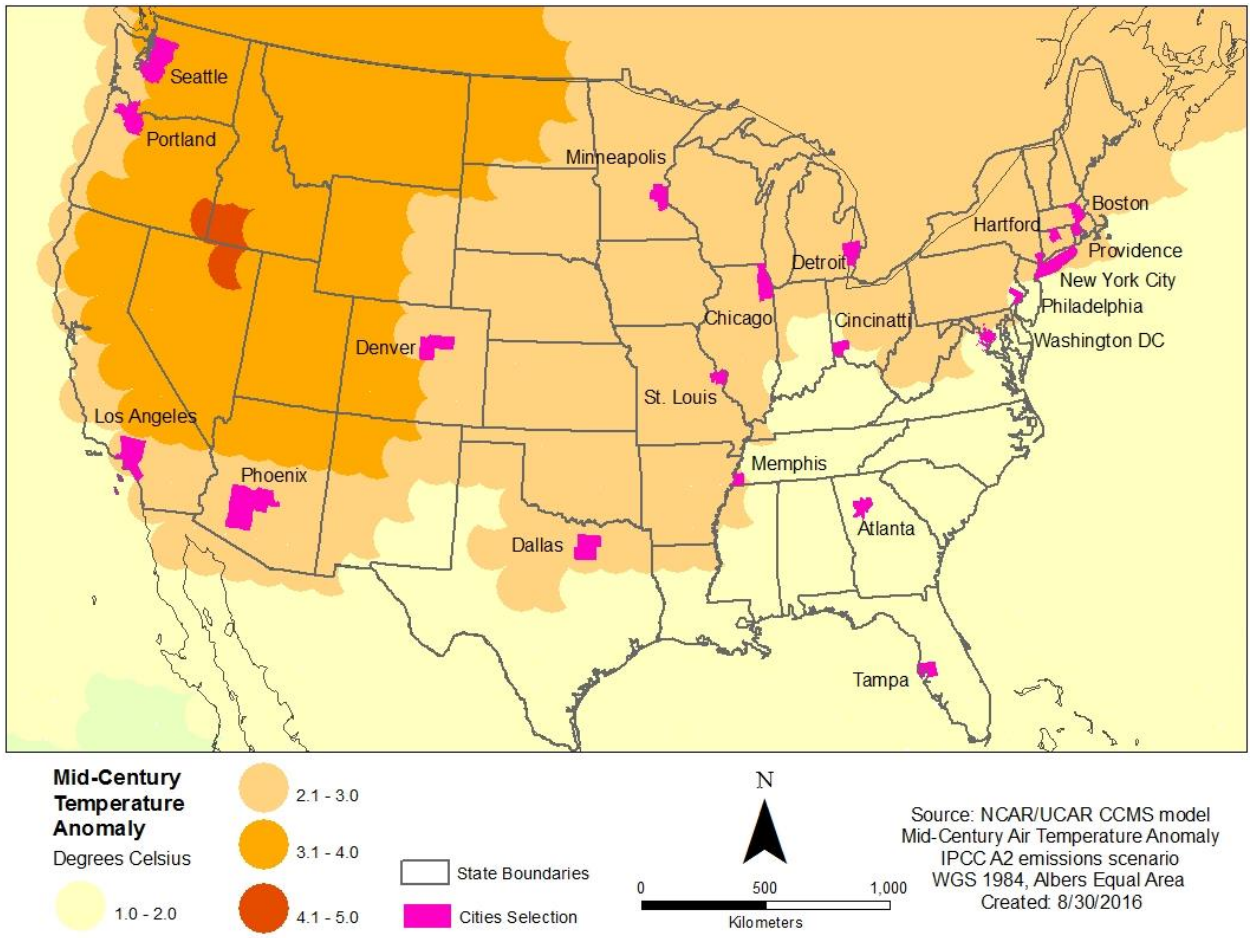

Figure 9. NCAR Community Climate System Model (CCMS) of Midcentury (2040-2059) air temperature anomalies for summer months (June-August).

The basic unit of analysis in the study at level 1 are census tracts, as defined by the 2010 U.S. Decennial Census boundaries. While various methods of aggregating and disaggregating U.S. Census data have been proposed to represent residential neighborhoods, census tracts, with their population average of around 4,000 (U.S. Census Bureau 2013) are frequently used in urban heat studies to define general neighborhood boundaries (Smoyer 1998; Johnson et al. 2009b). In this study, 17,807 census tracts provide the basic data regarding heat exposure and demographic and economic condition within the selected MSAs. Census tracts with very low population counts, less than 500 residents, were removed from the analysis. The level 2 unit of analysis are MSAs in which each of the selected cities (n=20) are located.-

Variables

Dependent Variable: UHRI

A quantitative index of biophysical factors related to urban heat, referred to as the urban heat risk index (*UHRI*), was developed and used as the dependent variable for our statistical analysis (Mitchell and Chakraborty, 2015). The equation used in this analysis is:

$$UHRI = (LST + NDBI) - NDVI$$

Where LST is land surface temperature, NDBI is the normalized difference built-up index which assesses built structure density, and NDVI the normalized difference vegetation index, which is an indicator of vegetation abundance. Prior studies have indicated strong correlations between landscape factors of NDBI and NDVI and the UHI (Dousset and Gourmelon 2003; Chen et al. 2006). LST, in particular, has been used to delineate the spatial extent of the surface UHI (Voogt 2002; Voogt and Oke 2003). Additionally, LST has been shown in previous research to have a

positive statistical association with rates of heat-related morbidity and mortality (Johnson and Wilson 2009a; Johnson et al. 2009b; Hondula et al. 2012). We used the equal weighting approach because there was no logical reason to assume that one of these factors contributes differentially to urban heat exposure. The values of LST, NDBI, and NDVI for each pixel in the study areas were derived using LANDSAT satellite Thematic Mapper (TM) 5 remotely sensed imagery. All images were captured on nearly cloud-free or "clear-sky" days during the summer of 2010 (May to September) to maintain temporal continuity with census demographic data. If multiple images qualified as "clear-sky", the image taken on the day with the highest atmospheric temperature was selected. Processing utilized the mono-window algorithm, which is based on the thermal radiance transfer equation, was used in the extraction of temperature values (Qin et al. 2001; Pu et al. 2006). LST, NDBI, and NDVI values were then averaged for the land portion of each census tract, excluding areas or water from calculations of temperature, structural density, and vegetation. The values of these biophysical indicators were then standardized using their z-scores before calculation of the *UHRI* scores for each tract.

Independent Variables – Level 1 Census Tract

Environmental justice studies conducted in the U.S. commonly rely on the decennial U.S. Census or more frequent surveys like the American Community Survey (ACS) to obtain information on the socio-demographic characteristics of residential populations. The 2010 U.S. Census provides a comprehensive and widely used set of demographic and socioeconomic indicators, as well as housing-related attributes. A review of prior public health studies (Basu and Ostro 2008; Johnson et al. 2009b; Reid et al. 2009; Uejio et al. 2011) show a wide variety of U.S. Census derived variables of age, race and ethnicity, gender, income level, education level, and

housing status that have been used as indicators of susceptibility to urban heat. The present study uses a control variable of population density, demographic variables related to race and ethnicity, and three variables related to socioeconomic status: median household income, the proportion of home owner-occupancy, and proportion of high school graduates at the census tract level (Table 10).

Table 10. Dependent and Level 1 variables at the census tract level. Level 2 variables at MSA level.

Variable Name	Data Source	Dates
Dependent Variable:		
Land Surface Temperature (LST)	LANDSAT 5, TM sensor, 120 meter resolution	UHRI for each MSA processed from same date
Normalized Difference Vegetation Index (NDVI)	LANDSAT 5, TM sensor, 30 meter resolution	imagery for all three values in summer 2010
Normalized Difference Built-up Index (NDBI)	LANDSAT 5, TM sensor, 30 meter resolution	
Independent Variables:	**Level 1**	
Non-Hispanic Black %	U.S. Census	2010
Non-Hispanic Asian %	U.S. Census	2010
Hispanic %	U.S. Census	2010
Owner-occupied homes %	U.S. Census	2010
Median household income $	2013 5-year ACS estimates	2009-2013
High School graduate %	2013 5-year ACS estimates	2009-2013
Population density mile^2	U.S. Census	2010
Independent Variables:	**Level 2**	
Dissimilarity index (*ID*)	U.S. Census	2010
Exposure Index (*xPx*)	U.S. Census	2010
Clustering (*SP*)	U.S. Census	2010
Centralization (*ACE*)	U.S. Census	2010
Concentration (*Delta*)	U.S. Census	2010

Independent Variables: Level 2 - MSA

Segregation here refers to the common understanding of the term in the United States as the racial or ethnic separation of groups from the majority White population (Holloway et al. 2012). Segregation and the inequalities which often result are a primary focus of the social sciences and an area of concern for advocates of racial, economic, and environmental justice. The study of patterns of residential segregation is necessarily spatial, since it involves analysis of the distribution of people within communities. Social scientists utilize several different indices to measure the level of segregation in areas. The most widely used measures of racial and ethnic segregation were classified by Massey and Denton (1989) and concern five dimensions of residential distribution across areas: evenness, exposure, clustering, concentration, and centralization. These measures capture many facets of segregation: evenness, the distribution of groups relative to each other; exposure, the possibility of interaction between or level of isolation with/from other groups; clustering, the degree to which minority areas adjoin each other; concentration, the relative amount of space occupied by a group; and centralization, the closeness of one group to the urban center (US Census 2002). Many of these measures involve global calculations across a wide area, such as a city, county or MSA. They are valid measures of segregation across large areas, but with the exception of Wong's implementation of local indices of dissimilarity and isolation, they cannot identify tract level segregation for the purpose of targeted public policy application (Wong 2002).

All values were calculated from US Census 2010 population measurements at the MSA level utilizing Geo-Segregation Analyzer version 1.2 (Apparicio 2013). Each segregation index value was calculated by comparing Non-Hispanic Whites to each of the three minority groups: Non-Hispanic Black, Non-Hispanic Asian, and Hispanic respectively. The indices were selected

based on their use in the pioneering work of Massey and Denton (1989), their recommended use by Acevedo-Garcia et al. (2003), and their prior use in publications by the US Census Bureau (Census 2002). *Evenness* was measured utilizing the dissimilarity index, notated as *ID* (Duncan and Duncan 1955); *exposure* with the isolation index - *xPx* (Bell 1954); *concentration* with the *Delta* index (Hoover 1941; Duncan et al. 1961); *clustering* with the spatial proximity index – *SP* (White 1986); and *centralization* with the absolute centralization index - *ACE* (Massey and Denton 1989). Centralization was computed using census tracts within the ZIP code boundary containing the city hall or the municipal center as a proxy for the historical core of the major city of each MSA. Table 11 contains details of all independent variables at both levels of analysis.

Table 11. Descriptive statistics of level 1 demographic, and level 2 segregation variables.

Variables Tract-level (N=17,807)	**Mean**	**SD**	**Minimum**	**Maximum**
Population Density per Mile^2	4,943.80	7,955.22	0.18	196,409.21
Non-Hispanic Black %	18.52	27.17	0.00	99.34
Non-Hispanic Asian %	7.96	10.77	0.00	88.88
Hispanic %	21.20	23.78	0.00	99.00
Owner-occupied Homes %	57.23	26.13	0.00	100.00
Median Household Income $	64,341.72	32,629.22	0.00	250,000.00
High School Graduates %	83.88	15.07	0.00	100.00
UHRI	0.07	2.71	-8.11	7.06
Variables MSA-level (N=20)	**Mean**	**SD**	**Minimum**	**Maximum**
Dissimilarity index (*ID*)				
Non-Hispanic Black	0.63	0.11	0.44	0.81
Non-Hispanic Asian	0.40	0.06	0.33	0.52
Hispanic	0.50	0.11	0.29	0.65
Isolation Index (*xPx*)				
Non-Hispanic Black	0.40	0.23	0.08	0.75
Non-Hispanic Asian	0.13	0.08	0.05	0.31
Hispanic	0.35	0.19	0.04	0.70
Clustering (*SP*)				
Non-Hispanic Black	1.42	0.26	1.06	1.90
Non-Hispanic Asian	1.08	0.07	1.01	1.29
Hispanic	1.30	0.22	1.02	1.88
Concentration (*Delta*)				
Non-Hispanic Black	0.73	0.11	0.41	0.85
Non-Hispanic Asian	0.65	0.10	0.50	0.85
Hispanic	0.68	0.11	0.50	0.85
Centralization (*ACE*)				
Non-Hispanic Black	0.67	0.19	0.13	0.87
Non-Hispanic Asian	0.47	0.28	-0.24	0.86
Hispanic	0.56	0.22	0.04	0.87

Statistical Methods

A two-level multilevel model was selected for the analysis of the interaction of tract-level and MSA level data. Multilevel models (MLM) are the preferred method for the analysis of data that are nested at different levels of hierarchy because it is specifically designed to investigate the relationships both within and between hierarchically clustered data (Raudenbush and Bryk 1986). An essential problem with hierarchical data is that individuals within clusters are more likely to be exposed to similar conditions, making it more likely that individuals within the cluster will be more similar to one another. This violates the assumption of independence of observations central to ordinary least squares regression (OLS) methods. MLM accounts for this violation of independence, and has advantages over alternate methods which implement linear regression to aggregate means of lower-level data at a higher level, or disaggregate the means of higher level variables at a lower level (Luke 2004). The primary advantage is that MLM analyzes individual level and group-level clustering to account for the variance within and between groups simultaneously, properly partitioning variance at the different levels. Additionally, MLM relaxes the assumption of independence of observations, adjusting for the effects of the clustering of variables within groups. The algorithm utilized by MLM is specifically structured to handle hierarchical data, while OLS is not. This study utilized SPSS version 23 by IBM Analytics for data editing and sorting into tract level and MSA level datasets. After the data was structured, HLM version 7.01 by Scientific Software International was used for construction of the two-level model and analysis.

A two-phase approach was taken in creating the model. It is common to test for the necessity of MLM techniques by first viewing scatter-plots and the results of an unconstrained null model containing only the dependent variable (Luke 2004; Peugh 2010). The results of the

null model are then used to calculate the interclass correlation coefficient (ICC) to assess the amount of variability attributable at the MSA level. If the variability at the highest level is considerable, the independent variables are introduced during a second phase of analysis.

As part of the first step lines of regression were computed and compared for the 20 MSAs with the slopes and intercepts of the socioeconomic and demographic variables. Visual inspection showed similar slope and direction for the socioeconomic variables, however, the demographic variables show distinct positive and negative relationships. Figures 10a-g display the slopes for the dependent variable, UHRI and the level 1 variables. (The results of spatial autoregressive modelling of the same data and contained in the appendix confirm this). This indicates considerable variability for the demographic variables, but consistency for the socioeconomic ones.

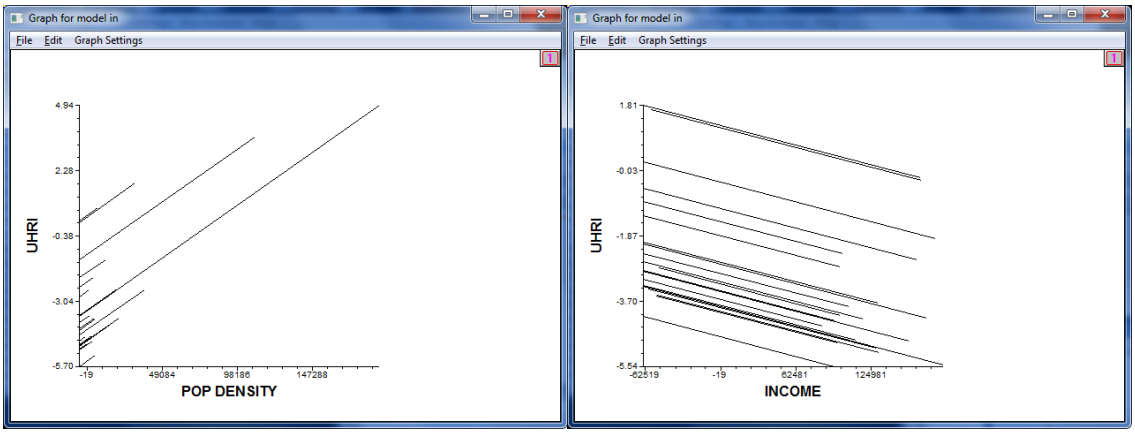

Figure 10 a-b. MSA level regression lines for the dependent variable UHRI and socioeconomic and demographic variables and: a – tract population density; b - median household income (Continued on next page).

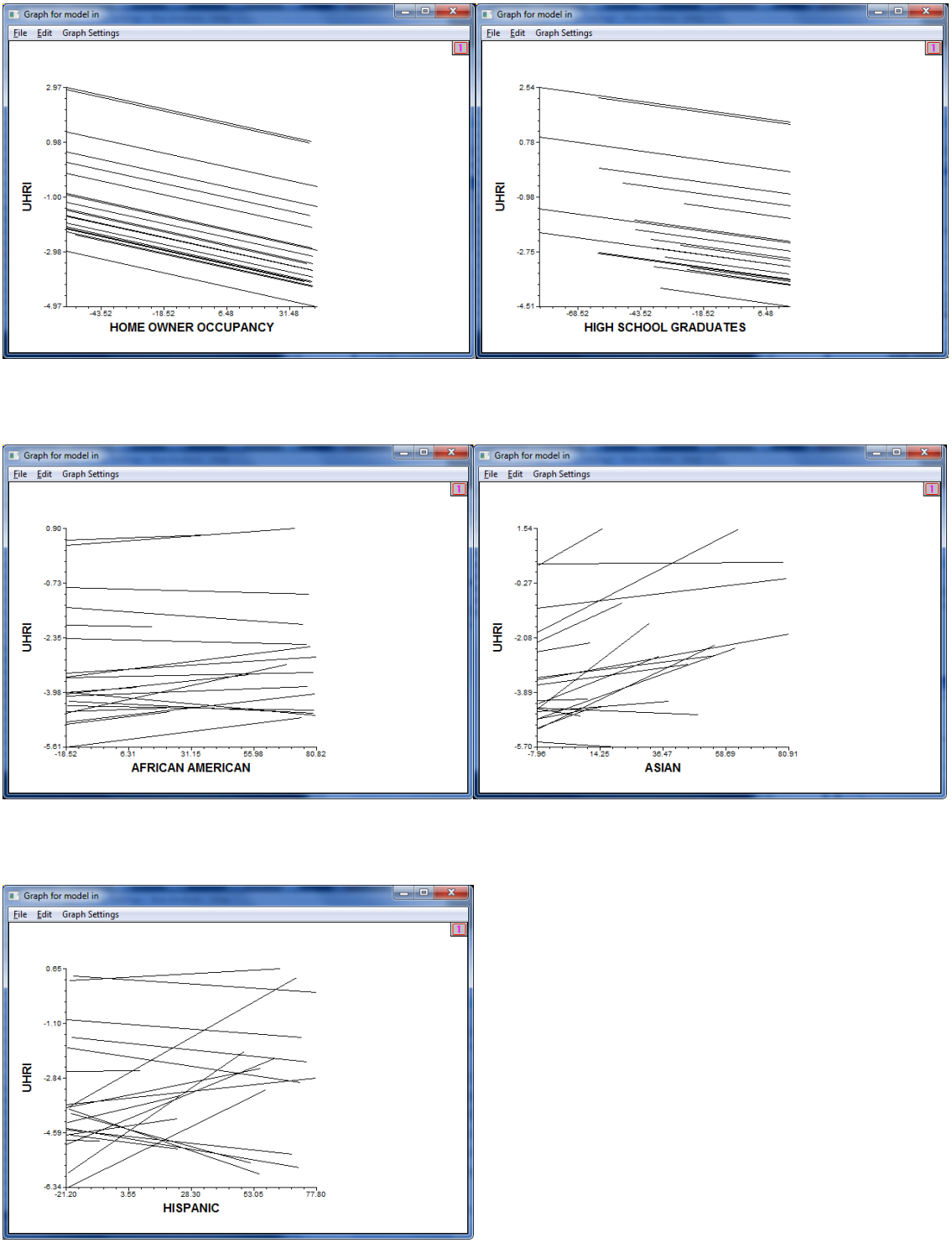

Figure 10 c-g. MSA level regression lines for the dependent variable UHRI and socioeconomic and demographic variables and: c- percentage home ownership occupancy; d – percentage high school graduates; e- percentage Non-Hispanic Black; f- percentage Non-Hispanic Asian; g – percentage Hispanic of any race.

After visual inspection, the next step in constructing a model involved running an unconditional, one-way random effects analysis of variance (ANOVA), or null-model. This model establishes the proportion of variance attributable at the MSA level. The equation for the null model is:

$$\text{Level 1: } UHRI_{ij} = \beta_{0j} + r_{ij}$$

$$\text{Level 2: } \beta_{0j} = \mu_{0j}$$

Where $UHRI_{ij}$ is the UHRI for a particular census tract within an MSA. The fixed effect is indicated by β_{0j} - the grand mean across all tracts, and error is split between into two parts – the variability between MSAs as μ_{0j}, and the variability between census tracts within each MSA, $r_{ij.}$ The estimated variance at level 2 of the model is 2.744 and 3.571 at level 1, both figures of which are used to calculate the interclass correlation coefficient (ICC) which measures the proportion of the variation in UHRI which occurs across the different MSAs. The ICC is calculated using the equation:

$$ICC = \frac{\tau 00}{(\tau 00 + \sigma 2)}$$

In the case of this model, the ICC is calculated as 3.571/ (3.571+2.744) = 0.565, meaning that MSAs account for 56.5% of the variability of the UHRI among tracts. This indicates that a high proportion of the variance is accounted for at the MSA level, suggesting considerable clustering. This is not a problem since MLM allows for correlated error structures at different levels.

This first phase of analysis provides several justifications for building a model containing the independent variables. First, from a theoretical standpoint a multi-level approach is appropriate because of the nested structure of the variables: tracts contained within MSAs with

data at both levels that are unsuitable for aggregation or disaggregation. Second, there is sufficient evidence from our graphs (Figure 10a-g) that the slope and intercept of the line of fit for the UHRI and demographic variables varies at the MSA level. Third, the high value of the ICC indicates considerable variance at the MSA level. All of these indicators signify the appropriateness of MLM as a statistical method, allowing the analysis to move to its second phase: model building.

Multilevel Model Construction

The construction of a model in MLM should follow directly from the research question, and the hypothesized relationship of the variables to the dependent variable and to each other (Peugh 2010). In this study, the first hypothesis—*Within metropolitan areas, higher levels of urban heat as measured by an urban heat risk index (UHRI) are associated with larger proportions of racial and ethnic minorities and with lower socioeconomic status of neighborhoods*—considers relationships at the census tract level. This relationship of socioeconomic and demographic variables as predictors of increased exposure to urban heat is encompassed at level 1. The second hypothesis—*Between metropolitan areas, greater levels of racial and ethnic segregation within a metropolitan area is associated with higher exposure to urban heat as measured by the UHRI*—concerns both the census tract and MSA levels. This relationship of segregation both to the demographic variables, and directly to urban heat exposure is considered at levels 1 and 2. These interrelationships between the UHRI and level 1 and level 2 variables are depicted in Figure 11. Here the level of exposure to the UHRI—elevated heat at the tract level—is hypothesized as having a direct relationship with the demographic and socioeconomic composition of the tract, and the segregated structure of the MSA. A control variable for tract level population density is also added at level 1.

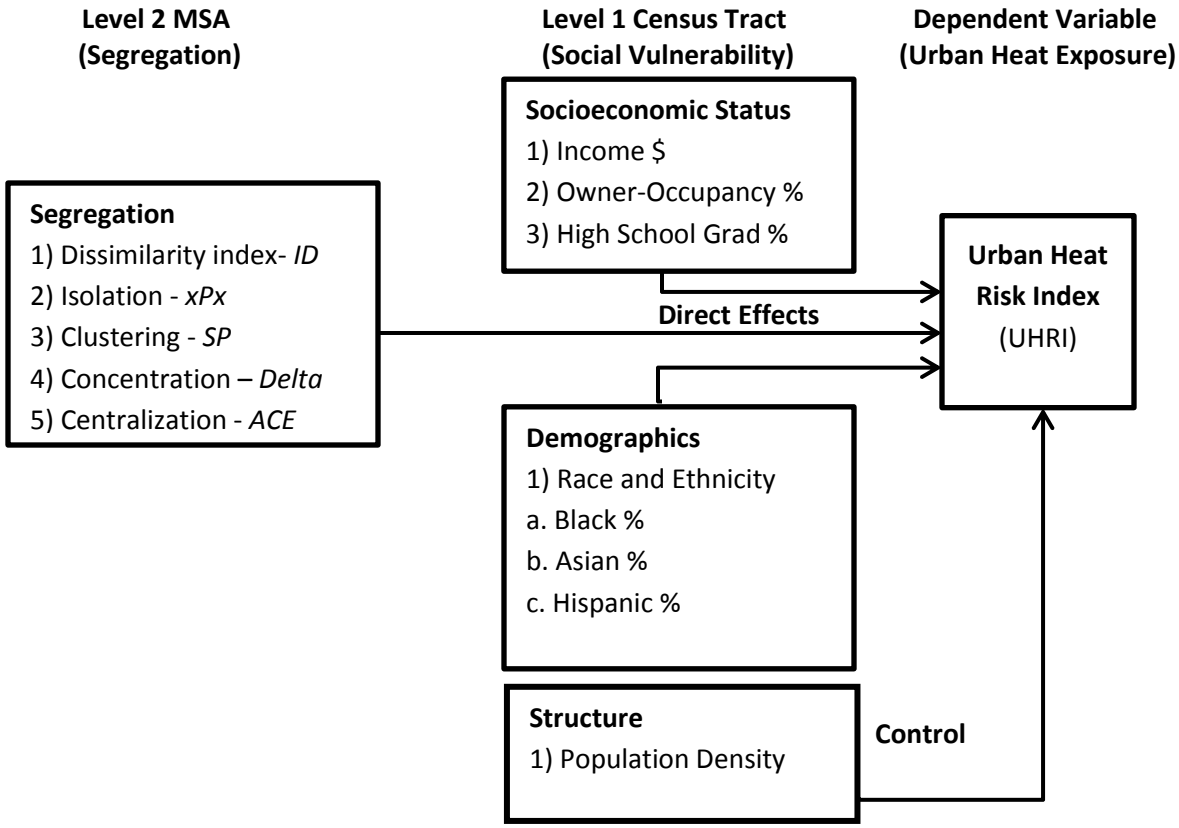

Figure 11. Structure of the multilevel model with hypothesized relationships.

Because the different level 2 indices of segregation can only compare two groups - Non-Hispanic Whites to each of the three minority groups- the different demographic classifications of race and ethnicity are considered as separate cases of the multilevel model.. This results in the race and ethnicity variables being divided into three cases, and the model adjusted and run or each case. For instance, one model will solely utilize the proportion of Blacks per tract at level 1 as the variable for race and ethnicity, keeping all other level 1 variables the same. At level 2 of this "Black" model case the segregation indices will be calculated only for the proportion of Non-Hispanic Blacks in contrast to Non-Hispanic Whites in that MSA. Table 12 lists the

variables used in each model case: Non-Hispanic Black percentage, Non-Hispanic Asian percentage, and Hispanic of any race percentage.

Table 12: Arrangement of variables in the three cases of the model.

	Linking Variable	Level 2 Independent Segregation *N=20*	Level 1 Dependent	Level 1 Independent *N=17,807*				
Case 1	MSA	Non-Hispanic Black 5-variables	UHRI tract level	Non-Hispanic Black %	Pop. Density ppKm^2	Median Household Income $	Home Owner-Occupancy %	Education: High School Graduates %
Case 2	MSA	Non-Hispanic Asian 4-variables	UHRI tract level	Non-Hispanic Asian %	Pop. Density ppKm^2	Median Household Income $	Home Owner-Occupancy %	Education: High School Graduates %
Case 3	MSA	Hispanic 5-variables	UHRI tract level	Hispanic %	Pop. Density ppKm^2	Median Household Income $	Home Owner-Occupancy %	Education: High School Graduates %

Centering Decisions

In MLM, the decision whether or not and how to center (i.e., rescale) the predictor variables so that their distributions of values center upon zero is critical to the results (Enders and Tofighi 2007). The choice of centering alters the interpretation of the intercept, thereby changing how the results of the model are interpreted. If the variables are uncentered and left as raw metrics it complicates the interpretation of the regression results when the variables are non-ratio and therefore lack a meaningful zero value. Centering the level 1 variables on the group mean-within the MSA clusters provides an unbiased estimate of the within group effects (Peugh 2010). Alternately, grand-mean centering expresses the predictors at level 1 as deviations from the mean value for all MSAs. Grand-mean centering results in slope estimates which combine level 1 and level 2 relationships, within MSA and between MSA variation, into an inseparable and

ambiguous mix. Grand-mean centering, consequently, is best suited for the analysis of level 2 relationships, while group mean centering is suited for the analysis of level 1, or level 1 and level 2 interactions. In the case of the present research question and hypotheses, which arise principally out of the relationship of the level 2 variables relating segregation to the level 1 predictors, group mean centering was utilized. The resulting multilevel UHRI exposure equation implements group mean centering at level 1 and grand-mean centering at level 2 where non-ratio index values indicative of segregation are used. It accounts for level 1 and level 2 variables as fixed effects, while a tract level random intercept allows for differences in the regression coefficient value, or magnitude of the differences in the relationship between the UHRI and predictor variables across tracts. Additionally, group mean centering of the level 1 variables reduces correlations with those at level 2 to zero, reducing multicollinearity as a problem in the model estimations (Raudenbush 2004). Collinearity of the level 1 variables was assessed by regressing them against UHRI to calculate the variance inflation factor (VIF), which was below 2.5 in all cases, within tolerances. For the level 2 variables, there was significant correlation between the dissimilarity index and the indices indicative of clustering in the case of Non-Hispanic Asians, isolation in the case of Non-Hispanic Blacks, and both clustering and isolation in the case of Hispanics. In all cases the VIF was below 3.7, indicating that collinearity was within tolerances.

Results

Multi-level modeling (MLM) was utilized in a statistical analysis of census tracts nested within metropolitan statistical areas (MSAs) of 20 cities of the U. S. An urban heat risk index

(UHRI) was the dependent variable while socioeconomic and demographic predictor variables at the tract level, or level 1 and predictor variables related to segregation at the MSA, or level 2 were used in creating the model. The model was created to test the relationship of factors indicative of segregation with demography, therefore cases were created using variables for Non-Hispanic Black, Non-Hispanic Asian, and Hispanic race and ethnicity at level 1, with their indicators of segregation relative to Non-Hispanic Whites at level 2. The results are summarized in Table 13.

Table 13: Multilevel modeling analysis results.

	NULL MODEL	LEVEL 1 MODEL			LEVEL 2 MODEL			COMBINED MODEL		
		ASIAN	BLACK	HISPANIC	ASIAN	BLACK	HISPANIC	ASIAN	BLACK	HISPANIC
FIXED EFFECTS										
Intercept	-0.968**	-0.97**	-0.97**	-0.97**				-20.63	-5.70	0.27
LEVEL 1 VARIABLES *N*=17807										
Population Density		4.3E-5***	4.4E-5***	4.3E-5***				4.3E-5***	4.4E-5***	4.4E-5***
Race/Ethnicity %		0.01***	1.7E-3***	-1.5-E3*				0.01***	1.7E-3***	-1.4-E3*
Owner-Occupied %		-0.02***	-0.02***	-0.02***				-0.02***	-0.02***	-0.02***
Med HH Income $		-1.0E-5***	-9.0E-6***	-9.0E-6***				-1.0E-5***	-9.0E-6***	-9.0E-6***
HS Graduates %		-0.01***	-0.01***	-0.01***				-0.012***	-0.01***	-0.01***
LEVEL 2 VARIABLES *N=20*										
Intercept					-20.63	-5.70	0.27			
Dissimilarity Index					9.44	15.51**	13.74*	9.44	15.51**	13.82*
Clustering (*SP*)					7.80	-2.37	-7.77**	7.79	-2.37	-7.79**
Isolation Index (*xPx*)					0.02	-5.55	4.53	0.03	-5.55*	4.55
Concentration (*D*)					13.44**	2.28	-3.14	13.44**	2.28	-3.16
Centralization (*ACE*)					-2.67	-1.73	4.60	-2.67	-1.73	4.60
RANDOM EFFECTS										
Sigma-Squared (r)	2.74	1.82	1.83	1.83	2.74	2.74	2.74	1.82	1.83	1.83
Tau (u0)	3.57	3.57	3.57	3.57	2.55	2.88	2.27	2.55	2.89	2.29
VARIANCE COMPONENTS										
Deviance	68641.62	61380.09	61477.95	61487.13	68602.79	68609.42	68606.09	61344.95	61449.45	61455.45
Log Likelihood	-34320.81	-30690.04	-30738.98	-30743.57	-34301.40	-34304.71	-34303.50	-30672.47	-30724.72	-30727.72
Chi-Squared	36034.48***	55822.94***	55521.56***	55489.69***	10686.46***	17177.93***	11524.59***	13839.09***	25831.84***	17557.74***
AIC	34324.81	30694.04	30742.98	30747.57	34305.40	34308.71	34307.50	30679.17	30728.72	30731.72
ICC	0.57									
Parameters	2	2	2	2	2	2	2	2	2	2

**p<.10; **p<.05; ***p<.01*

The first stage of model construction involved calculation of the interclass correlation coefficient (ICC) of an unconstrained or null model without predictor variables. This model had an ICC value of 0.565, indicative of a high amount of variability at the MSA level. Predictor variables were added in the construction of a level 1 and level 2 model, after which model fit was assessed. The addition of the predictor variables improved model fit at each stage as measured by the reduction in deviance. The null model had a deviance of 68,641.62 which is reduced to 61,350.33, 61,449.44, and 61,455.44 in models for the Asian, Black, and Hispanic cases, respectively. Similar improvements are noted in reduction of the Akaike Information Criterion (AIC), indicating model fit. Additionally, all of the model cases were significant in a *chi-squared* test for differences of the deviances. These results indicate good fit of the combined model with improved explanatory power of the predictors in accounting for variance compared with the null model or the separate level 1 or level 2 models.

Since the combined model displayed the best fit, analysis of the results for the individual predictor variables in the three cases is justified. At level 1, the control variable for population density is significantly and positively related with higher values of UHRI. The likely explanation of this are the higher values of temperature (LST), greater structural density (NDBI), and lower vegetation (NDVI) in areas with denser residential populations. Turning to the variables indicating socioeconomic status, there are consistent highly significant and negative associations for all of these variables with the UHRI. Greater tract level median household income, larger percentages of home owner-occupancy, and higher percentages of high school graduates are all associated with smaller UHRI values, indicating lower exposure to urban heat. This is consistent with the scatterplots, and also with a separate spatial autoregressive model (SAR, see appendix) run for each MSA with the same level 1 dataset. The different variables indicating minority race

and ethnicity are all significant in their association with the UHRI, but with differences in direction of the slope. The slope of the line for MSAs in the Black and Asian model cases are significantly and positively associated with increasing UHRI value. This indicated greater exposure for higher percentages of these two groups. Surprisingly, the slope in the Hispanic case is negative and the association is at a lower level of significance, $p < .10$. The level 1 results indicate that the association with higher urban heat levels and the socioeconomic variables are consistent at the tract level across MSAs. There was some inconsistency in the demographic variables, especially in tracts with greater percentages of Hispanic residents.

The next step of the analysis considered the association of the segregation related variables at level 2 with UHRI at level 1 in the three cases. Predictor variables at level 2 consisted of the five dimensions of segregation identified by Massey and Denton (1989), including evenness or *ID* for the dissimilarity index, isolation or *xPx*, concentration or *Delta*, clustering or *SP*, and finally centralization or *ACE*. The dissimilarity index at the MSA level is significantly and positively associated with the UHRI in the Black and Hispanic cases. This indicates that the increased unevenness of the population distribution for the Non-Hispanic Black and Hispanic populations in relation to Non-Hispanic Whites is associated with greater exposure to urban heat when measured between the MSAs. In the case of concentration, the Asian case was significantly and positively associated with the UHRI. So the greater the concentration level of Non-Hispanic Asians, the higher the exposure to urban heat. For the isolation variable, the Black case showed a significant and negative association with the UHRI, indicating that lower levels of isolation are associated with greater urban heat exposure. Finally, clustering is negatively and significantly associated with UHRI for the Hispanic case, meaning that lower

levels of Hispanic clustering are associated with higher UHRI levels. Centralization was not significantly associated with the UHRI at the MSA level in any of the cases.

Overall, each model presents different associations for the demographic variables and the UHRI. In the Black case, there are highly significant positive associations across tracts within the MSAs. Review of the descriptive statistics for level 2 in Table 3 shows that the Non-Hispanic Black variable has the highest segregation measures of any demographic group. When the indicators of segregation at the MSA level are entered into the Black model case, uneven distribution of the Black population is a significant factor in increased urban heat exposure. However, isolation appears to be a protective factor in the Black case, since lower isolation was associated with greater urban heat exposure. The segregation indicator for concentration, the relative amount of space occupied by the demographic group, is significant and positive for Asians. At level 1, viewing the lines of regression for the Non-Hispanic Asian percentage variable and the UHRI reveals pronounced slopes with a less ambiguous pattern than for the Non-Hispanic Black percentage variable. There is a significant, positive relationship with a higher coefficient of the Non-Hispanic Asian percentage variable and the UHRI. Finally, in the Hispanic case, the negative association of the demographic variable with urban heat is surprising. The dissimilarity index was significant and positive, indicating that evenness in the distribution of the Hispanic community relative to Whites increases exposure. However, the index for clustering was significant and negative, so tracts with higher percentages of Hispanics that are more tightly clustered may be a protective factor in urban heat exposure.

Discussion

The original research question focuses on investigating whether: (a) minority and/or lower socioeconomic status neighborhoods have greater exposure to urban heat in urban areas, and (b) segregation at the MSA level a significant factor in increased minority exposure? These questions focus on concerns about socioeconomic and racial/ethnic status and their interplay in the inequitable exposure to hazards. Our study expands prior environmental justice research by demonstrating that the socially and technically constructed urban environment presents differential exposure to neighborhoods to produce a landscape of thermal inequity. This landscape manifests itself technologically through the built urban structure of buildings, roads, and factories with their thermal capacity to store and emit heat, one aspect of urban microclimates. The second technologically based contributor in the formation of this landscape are the processes of industrial production which emit greenhouse gases, causing an increasing temperature baseline and rising number of summer temperature anomalies attendant to global climate change. Socially, the landscape of thermal inequity arises from settlement patterns subject to segregation and economic inequality which establish the urban ecology of each city. The combinations of these technological and social factors contribute to a landscape which defines the level of heat exposure for individuals. Our hypotheses address the social dimension of this landscape by examining socioeconomic and minority status and whether segregation is also associated with greater urban heat exposure.

Regarding the first hypothesis, the results of this study suggest that neighborhoods of lower socioeconomic status have greater exposure to urban heat. There are consistent associations for census tracts with higher levels of the UHRI and lower income, home ownership, and education levels across MSAs. This is borne out by examination of the lines of

regression for the 20 cities in this study, and by the significant associations between variables for the multi-level models. Results for the demographic indicators, however, differ for the racial and ethnic groups. Viewing the lines of regression for the 20 cities reveals ambiguous relationships across the three variables representing the percentage of Non-Hispanic Blacks, Non-Hispanic Asians and Hispanics. While significant positive associations exist in the Asian and Black model cases, the Hispanic model case is significant and negative. This finding corresponds with Jesdale et al.'s national study (2013) which used a multigroup dissimilarity index to account for segregation and found a high probability of exposure to heat-related land cover for areas with high percentages of Non-Hispanic Blacks and Asians, but a weaker probability of exposure in Hispanic areas. Blacks and Asians had a 52% and 32% higher probability than Whites of living in conditions with greater exposure to heat-risk related land cover while the probability for Hispanics was 21%. These results indicate that the portion of the first hypothesis relating to lower socioeconomic status and inequitable exposure to urban heat is validated under the study's model. However, the association of urban heat with race and ethnicity is more complex.

The second hypothesis in this study was tested to determine whether residential segregation of minority racial and ethnic groups from Non-Hispanic Whites could account for some of the observed variance between MSAs. The multi-dimensional aspect of residential segregation was accounted for by using five indicators, allowing a more nuanced examination of its spatial manifestation in cities. Greater levels of segregation in at least one of the five indicators were associated with greater levels of exposure for each demographic group: the dissimilarity index indicative of evenness of distribution relative to Whites in the Black and Hispanic model cases, and the *Delta* index of concentration in the Asian model case. However, in the Hispanic model case, greater clustering was significant and negative, while in the Black

model case isolation was significant and negative in the relationship with increasing urban heat indicated by the UHRI. These results arise from the complex and historically contingent urban ecology of different demographic groups. Because the residential settlement of specific demographic groups differ from city to city, generalizations are more difficult to make. For instance, associations between the centralization of minority populations and their exposure to urban heat depend on the history of minority settlement within the MSA. Bolin et al. (2013) use the example of Hispanic settlement in Phoenix and contrast it with other cities, like Los Angeles, in order to emphasize how the social forces which shape neighborhoods are connected with land use and land cover patterns and greater exposure to urban heat. Grineski et al. (2013) discuss the impact of changing economic, social, and environmental conditions shape neighborhoods to produce inequitable exposure to heat in Ciudad Juárez. Similar social contingencies make generalizations about the exposure of Black neighborhoods in the "inner city" dependent on which city is being studied. Urban revitalization and gentrification have changed the neighborhood structure of many socioeconomically dynamic post-industrial cities in a process described by Ehrenhalt (2012) as "demographic inversion." In these instances, the urban core has become a desirable location for predominantly educated, affluent, and White young urbanites desiring the amenities available in downtown locations. Gentrification displaces minorities and urban poor in central cities, who seek affordable housing alternatives in the inner ring suburbs where the housing stock developed in the 1950's is now declining in condition and value. These shifts are likely to reduce minority exposure to urban heat. Despite this, general associations of the dissimilarity index between the MSAs in this study indicate that this aspect of segregation is significant in both Non-Hispanic Black and Hispanic exposure. Consequently, caution is needed when generalizing segregation and demographic associations between higher exposure to urban

heat and minority status. The socioeconomic disparities, measured by income, home ownership, and lower levels of education are consistently significant predictors of greater heat exposure.

Conclusion

The application of multilevel modeling in this study provides insight into the interaction of a social phenomenon – segregation and its involvement in neighborhood level environmental exposure to urban heat. From an environmental justice perspective, this underscores how structural social factors are intertwined and function with the built structure of urban areas to present different levels of environmental exposure. Both of these factors of structure, social and built, contribute in creating the landscape of urban areas, resulting in patterns of thermal exposure to different groups depending on where they live within residential areas. In the case of thermal exposure, in which the urban heat island and an increasing temperature baseline interact, the source of the hazard is not a specific toxic source, but rather the urban structure and the processes of industrial production themselves. Bullard has said "Because of the complexity of the climate change crisis, we cannot continue to plan (climate mitigation and adaptation) for it using the tools of the past….we cannot assume that a uniform plan can work for all in terms of ensuring social justice." (Bullard 2016). In the case of thermal inequity, where the material arrangement and density of cities themselves, and not a specific point source of environmental exposure is present, the redesign of urban structures and addition of vegetation to lower the thermal impact on neighborhoods is an issue. Utilizing tools like multilevel modelling enable environmental justice researchers to better understand the underlying social dynamics of environmental exposure so that communities most at risk are identified and attention focused on

more targeted, effective social policy, and urban design. While the material arrangement of cities can be altered using a variety of strategies, residential segregation is the broader and more complex issue in this problem. The persisting social justice issue of racially and ethnically segregated residential patterns and their intertwining with lower socioeconomic status continues to define the life possibilities and environmental exposures of people.

CHAPTER FIVE:

CONCLUSION

An increasing global temperature baseline and the projected expansion in number of extreme heating days has engaged the attention of natural hazards researchers on the public health implications of heat waves. Because of their high population density and the continued pace of urbanization, much of the public health impact of heat waves falls on urban areas, both in developed and less-developed nations. The high risk to urbanized populations focuses attention on urban heat as a topic relevant to urban climatology, natural hazards, and climate justice. Uneven and inequitable exposure of populations in cities is the result of both the variable intensity of urban heat and the social structure of cities. Urban morphologies cause variations in urban heat leading to differing biophysical vulnerability. The varying urban ecologies of cities create differences in social vulnerability. The combination of the biophysical dimension of vulnerability and social vulnerability can be understood using Cutter's theory of hazards-of-place as a theoretical framework. This dissertation shows how the differential exposure to urban heat by socially vulnerable groups leads to inequity of exposure. This inequity is a problem of distributive injustice which is evident in the major U.S. cities examined in this study.

This dissertation has addressed the need for a comprehensive and systematic analysis of the thermal pattern of major U.S. cities using a critical geography perspective. By extending the research conducted by Morello-Frosch (2002; 2006; 2013), Harlan (2006; 2013), Jenerette (2011), Jesdale (2006; 2013), and other scholars working on the issue of urban heat risk and

climate change it contributes to natural hazards research and the emerging fields of climate justice and vulnerability studies. It expands upon GIS methods established by prior environmental justice and public health studies conducted at the metropolitan scale (Grineski et al. 2012; Johnson et al. 2012; Collins et al. 2013) to examine many of the most populous and structurally dense U.S. metropolitan areas. These areas are at high risk of increased extreme heating days - places of elevated biophysical vulnerability, but also have different settlement patterns and place-based differences creating varying social vulnerability. The term "landscape of thermal inequity" describes the interaction of a physical and social structure, shaped by the human activities which create our cities. Like other environmental justice issues, the most abstracted byproduct of modern life—risk, falls disproportionately on those who are least able to cope with or mitigate its effects. Conscious consideration of this landscape, its environmental effects and impact on human well-being, is necessary to establish the need for and possibility of its physical and social restructuring along more equitable lines**.**

Contribution of each article

The first article, in chapter 2, expands on established methodologies for the examination of the association of variables related to social vulnerability and exposure to elevated LST. In the Pinellas County study area census tracts with larger proportions of socially disadvantaged people and with higher proportions of some minorities were associated with higher temperature. This is due to the ability of economically affluent people to choose residences in neighborhoods with greater access to amenities, like waterfront locations and parks, with lower structural density thus lessening their exposure to higher LST. The second article, in chapter 3, implements a composite

dependent variable, the UHRI, provides greater context to urban heat than simply using LST. By studying the three largest cities in the U.S. the influence of urban ecologies with diverse racial and ethnic populations yielded different statistical associations, while socioeconomic disadvantage retained its consistent association with urban heat exposure as observed in the Pinellas County study. In the third article, chapter 4, a large-scale study of 20 cities at both tract and MSA levels consistently showed that neighborhoods with lower socioeconomic status are likely to experience elevated urban heat levels. A statistical model which tested five variables associated with segregation allowed for a multidimensional examination of this important social process, and the association of urban heat with racial and ethnic differences of U.S. cities. Overall, the models showed significant and positive associations for the proportion of Black and Asian residents and exposure to increased UHRI, but significantly negative associations for the proportion of Hispanic residents. The study's findings also suggest that the indicators of segregation, especially the dissimilarity index indicative of minority and non-Hispanic White residential unevenness, were significantly associated with increased exposure to urban heat.

The three articles make three methodological and theoretical contributions to the emerging climate justice literature. First, by conducting cross-sectional studies which retain consistent aggregation at the census tract level, allowing for generalizations about urban heat in U.S. cities. Second, the studies are consistent in their findings which relate lower socioeconomic status of census tracts with higher levels of LST and the UHRI. A variety of statistical techniques that include bivariate correlations, ordinary least squares regression, spatial autoregressive models, and multilevel modeling all yielded results that indicate the association of increased urban heat and lower socioeconomic status, suggesting that distributive inequities exist across urban areas of the U.S. Third, while the statistical results for minority groups were less

consistent, they nevertheless indicate that significant associations exist depending on the specific urban ecology of the city. Additionally, segregation is a significant contributor in the association of race and ethnicity and exposure with higher levels of urban heat as measured by the UHRI.

Limitations and Further Research

Among the empirical limitations of this dissertation is the absence of data related to health outcomes for areas with elevated urban heat. The scope of this research did not extend to the use of public health data which could relate specific urban heat patterns to morbidity and mortality rates. While the premise was not empirically tested, there are indications in the literature that health outcomes are related to variations in urban heat and factors of social vulnerability. Studies by Smoyer (1998) in St. Louis and by Harlan et al. (2016) in Phoenix noted the association of higher urban heat and socioeconomic disadvantage and increased rates of mortality. Another issue arises from regional variation in climate and urban structure. This dissertation did not address regional differences in exposure to urban heat, a topic which is of interest considering the regional impacts of a higher temperature baseline and the projected increase in days of extreme heat conditions. A separate spatial regression analysis (SAR) of the twenty cities may indicate regional differences between the south and the rest of the country. For instance, four of the five southern MSAs failed to indicate significant associations between the UHRI and median household income (Appendix H). Regional racial and ethnic differences were not within the scope of this dissertation and should be explored.

Theoretically this work is related to that of Jenerette et al. (2011) and that of Morello-Frosch and Lopez (2006) and their exploration of "riskscapes" specific to particular urban areas.

It expands the riskscape hypothesis within the framework of geography and environmental justice – proposing that the social and physical landscape establishes the level of risk for different neighborhoods. Because the scope of this work is limited to cities of the U.S., its specific findings are unique within that particular social and urban context. In the U.S., like elsewhere, urban patterns reflect the social and technological currents of specific historical eras. Residential segregation was imposed through widespread exclusionary zoning, real estate steering and redlining (Jackson 1980). These practices established the inequity in residential settlement patterns which persists to this day. Many of the cities selected as study areas underwent considerable suburbanization during the post-war period. The expansion of transportation networks into areas surrounding cities increasing the availability of cheap land leading to sprawling subdivisions, distant from the previously established urban core (Cohen 2004). The era of suburbanization was also characterized by the large-scale abandonment of central cities by White middle-class families termed "White-flight." In the present era, many downtowns are undergoing gentrification, and a demographic inversion which is the converse of suburbanization (Ehrenhalt 2012). The downtowns of economically prosperous cities are being structurally and socially transformed by this process. While these patterns may be specific to U.S. cities, by using the hazards-of-place model as a theoretical construct, the same mode of analysis using the UHRI to represent biophysical vulnerability and different variables for social vulnerability could be applied in different urban contexts. Additionally, the term *landscape of thermal inequity* and its critical geography perspective could be generally applied to the issue of urban heat and distributive environmental justice since it encompasses varying social and urban contexts.

In summary, these studies have explored inequities of exposure to urban heat within a climate justice framework. The literature, up to this point, has largely consisted of separate fields of research: urban climatology, natural hazards, and public health. These present different understandings of an issue which demands broad perspective, especially to recognize social factors in the structuring of urban ecologies. This involves addressing the history of different communities in cities in order to understand the structure of their landscapes: social and built. Factors like residential segregation have been embedded into the urban structure through a variety of policies, yet this has been inadequately developed as an explanation for present distributional inequities in the exposure to hazards related to climate change. A climate justice approach offers a coherent framework for the broad recognition of these issues, an essential step toward developing new policy solutions.

REFERENCES

Acevedo-Garcia, D., Lochner, K.A., Osypuk, T.L. and Subramanian, S.V. 2003. Future directions in residential segregation and health research: a multilevel approach. *American Journal of Public Health,* 93(2), 215-221.

Agrawala, S., T. Ota, A.U. Ahmed, J. Smith, and M. van Aalst. 2003. *Development and climate change in Bangladesh: focus on coastal flooding and the Sundarbans*. France: OECOD.

Aniello, C., K. Morgan, A. Busbey, and L. Newland. 1995. Mapping micro-urban heat islands using LANDSAT TM and a GIS. *Computers and Geosciences,* 21 (8): 965-969.

Anselin, L. 2005. *Exploring Spatial Data with GeoDa: A Workbook*. Spatial Analysis Laboratory, Department of Geography: University of Illinois, Urbana-Champaign. *Center for Spatially Integrated Social Science*.

Anselin, L., and A.K. Bera. 1998. Spatial dependence in linear regression models with an introduction to spatial econometrics. In *Handbook of Applied Economic Statistics,* Ed. Ullah, A., New York, NY: Marcel Dekker.

Anselin, L., Y. Kho, and I. Syabri. 2005. GeoDa: An introduction to spatial data analysis. *Geographical Analysis,* 38 (1): 5-22.

Apparicio, P., J.C. Martori, A.L. Pearson, L. Fournier, and D. Apparicio. 2014. An open-source software for calculating indices of urban residential segregation. *Social Science and Computer Review*, 32(1): 117-128.

Barnett, J., and J. Campbell. 2010. *Climate Change and Small Island States: Power, Knowledge, and the South Pacific*. London: Earthscan.

Basu, R., and J.M. Samet. 2002. Relation between elevated ambient temperature and mortality: A review of the epidemiologic evidence. *Epidemiologic Reviews*, 24 (2): 190-202.

Basu, R., W.Y. Feng, and B.D. Ostro. 2008. Characterizing temperature and mortality in nine California Counties. *Epidemiology*, 19 (1): 138–45.

Basu, R., and B.D. Ostro. 2008. A multicounty analysis identifying the populations vulnerable to mortality associated with high ambient temperature in California. *American Journal of Epidemiology*, *168*(6), 632-637.

Bell, W. 1954. A probability model for the measurement of ecological segregation. *Social Forces*, 32(4), 357-364.

Bolin, B., Barreto, J. D., Hegmon, M., Meierotto, L., and York, A. 2013. Double exposure in the Sunbelt: the sociospatial distribution of vulnerability in Phoenix, Arizona. In *Urbanization and Sustainability*. Netherlands: Springer. 159-178.

Boone, C. G., G.L. Buckley, J.M. Grove, and C. Sister. 2009. Parks and people : an environmental justice inquiry in Baltimore, Maryland. *Annals of the Association of American Geographers*, 99 (4): 767–787.

Browning, C. R., D. Wallace, S.L. Feinberg, and K.A. Cagney. 2006. Neighborhood social processes, physical conditions, and disaster-related mortality: the case of the 1995 Chicago heat wave. *American Sociological Review, 71*(4), 661-678.

Brulle, R. J., and D.N. Pellow. 2006. Environmental justice: human health and environmental inequalities. *Annual Review Public Health, 27*, 103-124.

Buechley RW, J. Van Bruggen, L.E. Truppi. 1972. Heat island = death island? *Environmental Research*, 5(1) 85-92.

Bullard, R. 2000. *Dumping in Dixie: Race, Class, and Environmental Quality*. Boulder, Colo: Westview Press.

Bullard, R. D. 2003. Confronting environmental racism in the 21st Century. *Race, Poverty and the Environment, 10*(1), 49-52.

Bullard, R., D., Gardezi, M., Chennault, C., and Dankbar, H. 2016. Climate change and environmental justice: A conversation with Dr. Robert Bullard. *Journal of Critical Thought and Praxis, 5*(2), 3.

Bullard, R. D., Mohai, P., Saha, R., and Wright, B. 2008. Toxic wastes and race at twenty: why race still matters after all of these years. *Environmental Law, 38*, 371.

Byrne, J., A. C., Portanger, C., Lo, A., Matthews, T., Baker, D., and Davison, A. 2016. Could urban greening mitigate suburban thermal inequity?: the role of residents' dispositions and household practices. *Environmental Research Letters, 11*(9), 095014.

Center for Disease Control and Prevention. 2012. Extreme Heat. Web http://emergency.cdc.gov/disasters/extremeheat/heat_guide.asp (last accessed 18 April 2017)

Chakraborty, J. 2011. Revisiting Tobler's First Law of Geography: spatial regression models for assessing environmental justice and health risk disparities. In *Geospatial Analysis of Environmental Health*. ed. Maantay, J. A., New York: Springer.

Chakraborty J., Maantay J.A., and Brender J.D. 2011. Disproportionate proximity to environmental health hazards: methods, models, and measurement. *American Journal of Public Health,* 101 (S1): S27-S36.

Chakraborty J, Collins T W, Grineski S E, Montgomery M C, Hernandez M. 2014. Comparing disproportionate exposure to acute and chronic pollution risks: a case study in Houston Texas. *Risk Analysis,* 34(11) 2005-2020.

Chen Xiao-Ling, Hong-Mei Zhao, Ping-Xiang Li, and Zhi-Yong Yin. 2003. Remote sensing image-based analysis of the relationship between urban heat island and land use/cover changes. *Remote Sensing of Environment,* 104 (2) 133-146.

Chow W., Chuang W.C., and Gober P. 2012. Vulnerability to extreme heat in metropolitan Phoenix: spatial, temporal, and demographic dimensions. *The Professional Geographer*, 64 (2) 286-302.

Christidis, N., Jones, G.S., and Stott, P.A. 2015. Dramatically increasing chances of extremely hot summers since the 2003 European heatwave. *Nature Climate Change,* 5(1) 93-104.

Clarke J.F. 1972. Some effects of the urban structure on heat mortality. *Environmental Research,* 5 (1) 93-104.

Cliff, A., and Ord, J. K. 1981. *Spatial Processes: Models and Applications*. London: Pion

Cohen, L. 2003. *A Consumers' Republic*: *The Politics of Mass Consumption in Postwar America.* New York: Knopf

Collins C.A., 1999. Racism and health: segregation and causes of death amenable to medical intervention in major U.S. cities. *Annuals of the New York Academy of the Sciences,* 896(1), 396-398

Collins, T.W., Grineski, S.E., Ford, P., Aldouri, R., Aguilar, M.D.L.R., Velázquez-Angulo, G. and Lu, D. 2013. Mapping vulnerability to climate change-related hazards: children at risk in a US-Mexico border metropolis. *Population and Environment*, *34*(3), 313-337.

Cooper, R.S., Kennelly, J.F., Durazo-Arvizu, R., Oh, H.J., Kaplan, G., and Lynch, J. 2001. Relationship between premature mortality and socioeconomic factors in Black and White populations of U.S. metropolitan areas. *Public Health Reports,* 116(5), 464-473.

Curriero, F.C., Heiner, K.S., Samet, J.M., Zeger, S.L., Strug, L., and Patz, J.A. 2002. Temperature and mortality in 11 cities of the eastern United States. *American Journal of Epidemiology*, 155(1): 80-87.

Cutter, S. L., Boruff, B. J., and Shirley, W. L. 2003. Social vulnerability to environmental hazards. *Social Science Quarterly*, *84*(2), 242-261.

Cutter, S.L., Emrich, C.T., Webb, J.J., and Morath, D. 2009. Social vulnerability to climate variability hazards: a review of the literature. *Final Report to Oxfam America.*

Cutter, S. L., and Finch, C. 2008. Temporal and spatial changes in social vulnerability to natural hazards. *Proceedings of the National Academy of Sciences*, *105*(7), 2301-2306.

Cutter, S. L., Mitchell, J. T., and Scott, M. S. 1997. Handbook for conducting a GIS-based hazards assessment at the county level. *University of South Carolina, Columbia, SC*.

Dixon, P.G., Brommer, D.M., Hedquist, B.C., Kalkstein, A.J., Goodrich, G.B., Walter, J.C., and Cerveny, R.S. 2005. Heat mortality versus cold mortality. *Bulletin of the American Meteorological Society*, 86 (7): 937-943.

Donoghue, J.M., Graham, M.A., Jentzen, J.M., Lifschultz, B.D., Luke, J.L., and Mirchandani, H.G. 1997. Criteria for the diagnosis of heat-related death: National Association of Medical Examiners: position paper. *The American Journal of Forensic Medicine and Pathology,* 18 (1): 11-14.

Dousset B., and Gourmelon F. 2003. Satellite multi-sensor data analysis of urban surface temperatures and landcover. *ISPRS Journal of Photogrammetry and Remote Sensing*, 58 (1) 43-54.

Dousset B., Gourmelon F, Laaidi K., Zeghnoun A., Giraudet E., Bretin P., Mauri E., and Vandentorren S. 2011. Satellite monitoring of summer heat waves in the Paris metropolitan area. *International Journal of Climatology*, 31(2) 313-323.

Downey, L. 2007. US metropolitan-area variation in environmental inequality outcomes. *Urban Studies,* 44(5-6), 953-977.

Downey, L., and Hawkins, B. 2008. Race, income, and environmental inequality in the United States. *Sociological Perspectives*, *51*(4), 759-781.

Duncan, O. D., and Duncan, B. 1955. A methodological analysis of segregation indexes. *American Sociological Review*, *20*(2), 210-217.

Duncan, O. D., Cuzzort, R. P., and Duncan, B. 1961. Statistical geography: problems in analyzing areal data. *Statistical Geography: Problems in Analyzing Areal Data.*

Ehrenhalt, A., 2012. *The Great Inversion and the Future of the American City.* Vintage.

Elliot M. R., Wang Y., Lowe, R. A., Kleindorfer P. R. 2004. Environmental justice: frequency and severity of US chemical industry accidents and the socioeconomic status of surrounding communities. *Journal of Epidemiology and Community Health* 58 (1) 24-30.

Ellis, F.P., and Nelson, F. 1978. Mortality in the elderly in a heat wave in New York City. August 1975, *Environmental Research.* 15 (3): 504-512.
Enders, C. K., and Tofighi, D. 2007. Centering predictor variables in cross-sectional multilevel models: a new look at an old issue. *Psychological Methods*, *12*(2), 121.
Florida Department of Health. 2011. Descriptive analysis of heat-related illness treated in Florida hospitals and emergency departments. October, 2011.
Fouillet A., Rey G., Laurent F., Pavillon G., Bellec S., Guihenneuc-Jouyaux C., and Hémon D. 2006. Excess mortality related to the August 2003 heat wave in France. *International archives of occupational and environmental health*, 80 (1) 16-24.
Gaffen, D., and Ross, R. 1998. Increased summertime heat stress in the US. *Nature*, 396 (6711): 529–530.
Galster, G., and Cutsinger, J. 2007. Racial settlement and metropolitan land-use patterns: does sprawl abet Black-White segregation?. *Urban Geography*, *28*(6), 516-553.
Gilbert, A., and Chakraborty, J. 2011. Using geographically weighted regression for environmental justice analysis: cumulative cancer risks from air toxics in Florida. *Social Science Research*, 40 (1): 273–286.
Golden, J.S. 2004. The built environmental induced urban heat island effect in rapidly urbanizing arid regions-a sustainable urban engineering complexity. *Environmental Sciences, I* (4): 321-349.
Grimmond, S. 2007. Urbanization and global environmental change: local effects of urban warming. *The Geographical Journal*, 173 (1): 83-88.
Grineski, S.E., Collins, T.W., Ford, P., Fitzgerald, R., Aldouri, R., Velásquez-Angulo, G., and Lu, D. 2012. Climate change and environmental injustice in a bi-national context. *Applied Geography,* 33, 25-35.
Grineski S., Collins T., McDonald Y., Aldouri R., Aboargob F., Eldeb A., Romo Aguilar L., and Velázquez-Angulo G. 2013. Double exposure and the climate gap: changing demographics and exposure to extreme heat in Ciudad Juárez, Mexico. *Local Environment* 20 (2) 180-201.
Hales, S., Edwards, S. J., and Kovats, R. S. 2003. Impacts on health of climate extremes. *Climate Change and Health: Risks and Responses.* Geneva: World Health Organization.
Harlan, S. L., Brazel, A. J., Prashad, L., Stefanov, W. L., and Larsen, L. 2006. Neighborhood microclimates and vulnerability to heat stress. *Social Science and Medicine,* 63 (11): 2847–63.
Harlan, S. L., Declet-Barreto, J.H., Stefanov, W.L., and Petitti, D.B. 2013. Neighborhood effects on heat deaths: social and environmental predictors of vulnerability in Maricopa County, Arizona." *Environmental Health Perspectives (Online)* 121, (2):197.
Hart, K.D., Kunitz, S.J., Sell, R.R., and Mukamel, D.B. 1998. Metropolitan governance, residential segregation, and mortality among African Americans. *American Journal of Public Health*, 88(3), 434-438.
Hattis, D., Ogneva-Himmelberger, Y., and Ratick, S. 2012. The spatial variability of heat-related mortality in Massachusetts. *Applied Geography,* 33: 45-52.
Hayhoe, K., Sheridan, S., Kalkstein, L., and Greene, S. 2010. Climate change, heat waves, and mortality projections for Chicago. *Journal of Great Lakes Research*, 36: 65–73.
Heynen, N., Perkins, H.A., and Roy, P. 2006. The political ecology of uneven urban green space: the impact of political economy on race and ethnicity in producing environmental inequality in Milwaukee. *Urban Affairs Review*, 42 (1): 3–25.

Hollander, J. 2011. *Sunburnt Cities:The Great Recession, Depopulation, and Urban Planning in the American Sunbelt*. London New York: Routledge.

Holloway, S. R., Wright, R., and Ellis, M. 2012. The racially fragmented city? Neighborhood racial segregation and diversity jointly considered. *The Professional Geographer*, *64*(1), 63-82.

Hondula, D.M., Davis, R.E., Leisten, M.J., Saha, M.V., Veazey, L.M., and Wegner, C.R. 2012. Fine-scale spatial variability of heat related mortality in Philadelphia County, USA, from 1983-2008: a case-series analysis. *Environmental Health*, 11 (1): 1-11.

Hoover, E. M. 1941. Interstate redistribution of population, 1850–1940. *The Journal of Economic History*, *1*(02), 199-205.

Huang, C., Barnett, A. G., Wang, X., Vaneckova, P., FitzGerald, G., and Tong, S. 2011. Projecting future heat-related mortality under climate change scenarios: a systematic review. *Environmental Health Perspectives*, *119*(12), 1681.

Huang, G., Zhou, W., and Cadenasso, M. L. 2011. Is everyone hot in the city? Spatial pattern of land surface temperatures, land cover and neighborhood socioeconomic characteristics in Baltimore, MD. *Journal of environmental management*, *92*(7), 1753-1759.

Illinois Department of Public Health. 1997. Heat-Related Mortality in Chicago, Illinois, July 1995. Web http://www.idph.state.il.us/cancer/pdf/HEAT.PDF (last accessed 18 April 2017)

Imhoff M.L., Zhang P., and Bounoua L. 2010. Remote sensing of the urban heat island effect across biomes in the continental USA. *Remote Sensing of Environment* 114 (3) 504-513.

Intergovernmental Panel on Climate Change. 2007. *Climate Change 2007*: *The Physical Science Basis. Contribution of Working Group I to the Fourth Assessment Report of the Intergovernmental Panel on Climate Change.* eds. Solomon, S., Qin, D., Manning, M., Chen, Z., Marquis, K.B., Averyt, M., Tignor, M., Miller, H.L. New York: Cambridge University Press

Jackson, K. T. 1980. Race, ethnicity, and real estate appraisal: The home owners loan corporation and the federal housing administration. *Journal of Urban History*, *6*(4), 419-452.

Jenerette G D, Harlan SL, Stefanov WL, and Martin CA 2011. Ecosystem services and urban heat riskscape moderation: water, green spaces, and social inequality in Phoenix, USA. *Ecological Applications* 21 (7) 2637-2651.

Jenerette, G. D., Harlan, S. L., Buyantuev, A., Stefanov, W. L., Declet-Barreto, J., Ruddell, B. L., ... and Li, X. 2016. Micro-scale urban surface temperatures are related to land-cover features and residential heat related health impacts in Phoenix, AZ USA. *Landscape Ecology*, *31*(4), 745-760.

Jesdale, B.M., Morello-Frosch, R., and Cushing, L. 2013. The racial/ethnic distribution of heat risk-related land cover in relation to residential segregation. *Environmental Health Perspectives*, 121(7), 811.

Johnson, D.P., and Wilson, J.S. 2009a. The socio-spatial dynamics of extreme urban heat events: The case of heat-related deaths in Philadelphia. *Applied Geography*, *29*(3), 419-434.

Johnson, D.P., Wilson, J.S., Luber, G.C. 2009b. Socioeconomic indicators of heat-related health risk supplemented with remotely sensed data. *Int'l Journal of Health Geographics*, *8*(1), 57.

Johnson, D.P., Stanforth, A., Lulla, V., and Luber, G. 2012. Developing an applied extreme heat vulnerability index utilizing socioeconomic and environmental data. *Applied Geography,* 35 (1): 23-31.

Kalkstein, L. S. 1991. A new approach to evaluate the impact of climate on human mortality. *Environmental Health Perspectives*, *96*, 145.

Kalkstein, L., and Davis, R. E. 1989. Weather and human mortality: an evaluation of demographic and interregional responses in the United States. *Annals of the Association of American Geographers,* 79 (1): 44-64.

Kalkstein, L.S., and Greene, J.S. 1997. An evaluation of climate/mortality relationships in large U.S. cities and the possible impacts of climate change. *Environmental Health Perspectives,* 105 (1): 84.

Kissling, W.D., and Carl, G. 2008. Spatial autocorrelation and the selection of simultaneous autoregressive models. *Global Ecology and Biogeography,* 17 (1): 59-71.

Klinenberg, E. 1999. Denaturalizing disaster: A social autopsy of the 1995 Chicago heat wave. *Theory and Society* 28 (2) 239-295.

----------. 2001. Dying alone: The social production of urban isolation. *Ethnography,* 2 (4): 501-531.

----------. 2002. *Heat Wave: A Social Autopsy of Disaster in Chicago.* Chicago: University of Chicago Press

Kramer, M.R. and Hogue, C.R. 2008. Place matters: variation in the Black/White very preterm birth rate across U.S. metropolitan areas, 2002-2004. *Public Health Reports,* 123(5), 576-585.

Landry, S. M., and Chakraborty, J. 2009. Street trees and equity: evaluating the spatial distribution of an urban amenity. *Environment and Planning A*, 41 (11): 2651–2670.

Lopez, R. 2002. Segregation and Black/White differences in exposure to air toxics in 1990. *Environmental Health Perspectives,* 110(Suppl 2), 289-295.

Lu D., and Weng Q. 2006. Use of impervious surface in urban land-use classification. *Remote Sensing of Environment* 102 (1) 146-160.

Luber, G., and McGeehin, M. 2008. Climate change and extreme heat events. *American Journal of Preventive Medicine*, 35 (5): 429–35.

Luke, D.A. 2004. *Multilevel Modeling*, Series: Quantitative Applications in the Social Sciences (Volume 143) Sage Publications

Massey, D. S., and Denton, N. A. 1989. Hypersegregation in US metropolitan areas: Black and Hispanic segregation along five dimensions. *Demography*, *26*(3), 373-391.

Massey, D. S., and Tannen, J. 2015. A research note on trends in Black hypersegregation. *Demography*, *52*(3), 1025-1034.

McCarthy, M. P., Best, M. J., and Betts, R. A. 2010. Climate change in cities due to global warming and urban effects. *Geophysical Research Letters*, 37 (9).

McGeehin, M. A, and Mirabelli, M. 2001. The potential impacts of climate variability and change on temperature-related morbidity and mortality in the United States. *Environmental Health Perspectives,* 109 (Suppl 2): 185–9.

Medina-Ramón, M., and Schwartz, J. 2007. Temperature, temperature extremes, and mortality: A study of acclimatization and effect modification in 50 United States cities. *Occupational and Environmental Medicine*, 64 (12): 827-833.

Meehl, G. A, and Tebaldi, C. 2004. More intense, more frequent, and longer lasting heat waves in the 21st century. *Science,* 305 (5686): 994–7.

Melillo, J. M., Richmond, T. T., and Yohe, G. 2014. Climate change impacts in the United States. *Third National Climate Assessment*.

Mendez M. A. 2015. Assessing local plans for public health co-benefits in environmental justice communities. *Local Environment: The International Journal of Justice and Sustainability.* 20 (on-line)

Mishra V., Ganguly A. R., Nijssen B., and Lettenmaier D. P. 2015. Changes in observed climate extremes in global urban areas. *Environmental Research Letters* 10 (2) 024005.

Mitchell, B. C., and Chakraborty, J. 2014. Urban heat and climate justice: a landscape of thermal inequity in Pinellas County, Florida. *Geographical Review*, *104*(4), 459-480.

Mitchell, B. C., and Chakraborty, J. 2015. Landscapes of thermal inequity: disproportionate exposure to urban heat in the three largest US cities. *Environmental Research Letters*, *10*(11), 115005.

Mohai, P., Pellow, D., and Roberts, J. T. 2009. Environmental justice. *Annual Review of Environment and Resources*, *34*, 405-430.

Morello-Frosch, R., Pastor Jr., M., Porras, C., and Sadd, J. 2002. Environmental justice and regional inequality in southern California: implications for future research. *Environmental Health Perspectives*, 110(Suppl 2), 149-154.

Morello-Frosch, R. and Jesdale, B.M. 2006. Separate and unequal: residential segregation and estimated cancer risks associated with ambient air toxics in US metropolitan areas. *Environmental Health Perspectives.*114(3), 386-393.

Morello-Frosch, R., and Lopez, R. 2006. The riskscape and the color line: examining the role of segregation in environmental health disparities. *Environmental research*, *102*(2), 181-196.

Mueller, B., Zhang, X., and Zwiers, F. W. 2016. Historically hottest summers projected to be the norm for more than half of the world's population within 20 years. *Environmental Research Letters*, *11*(4), 044011.

NASA Land Processes Distributed Active Archive Center (LP DAAC). MODIS. USGS/Earth Resources Observation and Science (EROS) Center, Sioux Falls, South Dakota. 2001.

National Center for Atmospheric Research, Community Earth System Model (NCAR/UCAR, CESM) 2014 Web http://www.cesm.ucar.edu/models/ (last accessed 18 April 2017)

National Oceanic and Atmospheric Administration's National Data Buoy Center. 2010. Web http://www.ndbc.noaa.gov/station_page.php?station=cwbf1 (last accessed 18 April 2017)

National Weather Service 2013 Natural hazards statistics. Web http://www.nws.noaa.gov/om/hazstats.shtml (last accessed 18 April 2017)

O'Neill, M. S. 2003. Air conditioning and heat-related health effects. *Applied Environmental Science and Public Health*. 1, 9-12.

Oke T. R. 1992. *Boundary Layer Climates: 2nd edition*. London, New York: Routledge

O'Neill, M. S., Zanobetti, A., and Schwartz, J. 2003. Modifiers of the temperature and mortality association in seven US cities. *American Journal of Epidemiology*, *157*(12), 1074-1082.

Osypuk, T.L. and Acevedo-Garcia, D. 2008. Are racial disparities in preterm birth rates larger in hypersegregated areas? *American Journal of Epidemiology*. 167(11), 1295-1304

Peugh, J.L. 2010. A practical guide to multilevel modeling. *Journal of School Psychology*, *48*(1), 85-112.

Peel, M. C., Finlayson, B. L., and McMahon, T. A. 2007. Updated world map of the Köppen-Geiger climate classification, *Hydrology and Earth System Science*, 11, 1633-1644.

Poumadere, M., Mays, C., Le Mer, S., and Blong, R. 2005. The 2003 heat wave in France: dangerous climate change here and now. *Risk analysis*, *25*(6), 1483-1494.
Price, J. C. 1977. Thermal inertia mapping: a new view of the earth. *Journal of Geophysical Research*, *82*(18), 2582-2590.
Pu R., Gong P., Michishita .R, and Sasagawa T. 2006. Assessment of multi-resolution and multi-sensor data for urban surface temperature retrieval. *Remote Sensing of Environment* 104 (2) 211–225.
Pulido, L. 2000. Rethinking environmental racism: White privilege and urban development in Southern California. *Annals of the Association of American Geographers*, 90 (1): 12-40.
Qin, Z., Karnieli, A., and Berliner, P. 2001. A mono-window algorithm for retrieving land surface temperature from LANDSAT TM data and its application to the Israel-Egypt border region. *International Journal of Remote Sensing*, 22 (18): 3719–3746.
Raudenbush, S.W. and Bryk, A.S. 1986. A hierarchical model for studying school effects. *Sociology of Education*, 59 (1) 1-17.
Raudenbush, S. W. 2004. *HLM 6: Hierarchical linear and nonlinear modeling*. Scientific Software International.
Reardon, S. F., and O'Sullivan, D. 2004. Measures of spatial segregation. *Sociological Methodology*, *34*(1), 121-162.
Reid, C. E., O'Neill, M. S., Gronlund, C. J., Brines, S. J., Brown, D. G., Diez-Roux, A. V., and Schwartz, J. 2009. Mapping community determinants of heat vulnerability. *Environmental Health Perspectives*, *117*(11), 1730.
Robine J.M., Chueng S.L.K., Le Roy S,. Van Oyen H., Griffiths C., Michel J.P., and Herrmann F.R. 2008. Death toll exceeded 70,000 in Europe during the summer of 2003 *Comptes rendus biologies* 331 (2) 171-178.
Semenza J. C., Rubin C. H., Falter K. H., Selanikio J. D., Flanders W. D., Howe H. L., and Wilhelm J. L. 1996. Heat-related deaths during the July 1995 heat wave in Chicago. *The New England Journal of Medicine* 335 (2) 84–90.
Shaposhnikov D., Revich B., Bellander .T, Bedada G. B., Bottai M., Kharkova T., ... and Pershagen G. 2014. Mortality related to air pollution with the Moscow heat wave and wildfire of 2010 *Epidemiology (Cambridge, Mass.)* 25 (3) 359.
Sheridan, S. C., Kalkstein, A. J., and Kalkstein, L. S. 2008. Trends in heat-related mortality in the United States, 1975–2004. *Natural Hazards*, 50 (1): 145–160.
Shonkoff, S.B., Morello-Frosch, R., Pastor, R., and Sadd, J. 2011. The climate gap: environmental health and equity implications of climate change and mitigation policies in California - A Review of the Literature, *Climatic Change*, 109 (1): 485-503.
Smoyer, K.E. 1998. Putting risk in its place: methodological considerations for investigating extreme event health risk *Social Science and Medicine* 47 (11) 1809-24.
Stewart, I. D. 2010. A systematic review and scientific critique of methodology in modern urban heat island literature. *International Journal of Climatology*. 31(2), 200-217.
Stone, B., Hess, J. J., and Frumkin, H. 2010. Urban form and extreme heat events: are sprawling cities more vulnerable to climate change than compact cities? *Environmental Health Perspectives*, 118 (10): 1425–8.
Talen, E., and Anselin, L. 1998. Assessing spatial equity: an evaluation of measures of accessibility to public playgrounds. *Environment and Planning A*, 30: 595-614.
Uejio, C. K., Wilhelmi, O. V., Golden, J. S., Mills, D. M., Gulino, S. P., and Samenow, J. P. 2011. Intra-urban societal vulnerability to extreme heat: the role of heat exposure and the

built environment, socioeconomics, and neighborhood stability. *Health and Place*, *17*(2), 498-507.
UNDESA. 2002. *World Population Aging 1950-2050.* United Nations Department ot Economic and Social Affairs Population Division. New York
---------- 2011. *World Urbanization Prospects, the 2011 Revision.* United Nations Department ot Economic and Social Affairs Population Division. New York
United States Census Bureau. 2002. "Racial and Ethnic Residential Segregation in the United States: 1980-2000" Web https://www.census.gov/hhes/www/housing/resseg/pdf/app_b.pdf (last accessed 18 April 2017)
----------. 2013. "Finding Data from My Community" Web https://www2.census.gov/geo/pdfs/education/brochures/MyCommunity.pdf (last accessed 18 April 2017)
----------. 2015. Summary File *2009 – 2014 American Community Survey*. U.S. Census Bureau's American Community Survey Office 2014 Web http://ftp2.census.gov/ (last accessed 18 April 2017)
----------. 2010. *2010 Census*. Web http://www.census.gov/2010census/data/. (last accessed 18 April 2017)
United States Department of Health and Human Services. 2010. Agency for Healthcare Research and Quality - Index of Racial and Economic Separation. Web https://archive.ahrq.gov/research/findings/nhqrdr/nhdr10/nhdr10.pdf (last accessed 18 April 2017)
United States Environmental Protection Agency. 2014. Web https://www3.epa.gov/climatechange/pdfs/climateindicators-full-2014.pdf (last accessed 18 April 2017)
United States Geological Survey. *EarthExplorer* LANDSAT 5 TM. Web https://landsat.usgs.gov/landsat-data-access (last accessed 18 April 2017)
Vanos, J.K. 2015. Children's health and vulnerability in outdoor microclimates: a comprehensive review. *Environment International*, 76, 1-15.
Voogt, J.A., 2000. Urban heat island, T. Munn (Ed.), *Encyclopedia of global Environmental Change*, Vol. 3, Wiley, Chichester pp. 660–666.
Voogt, J. A. and Oke, T.R. 2003. Thermal remote sensing of urban climates. *Remote Sensing of Environment*, 86 (3): 370–384.
Walker, G. 2012. *Environmental Justice: Concepts, Evidence, and Politics*. London and New York: Routledge.
White, K., and Borrell, L.N. 2011. Racial/ethnic residential segregation: framing the context of health risk and health disparities. *Health and Place*, 17(2), 438-448.
White, M. J. 1986. Segregation and diversity measures in population distribution. *Population Index*, 198-221.
Whitman, S., Good, G., Edmund, R., Benbow, N., Shou, W., and Mou, S. 1997. Public health briefs: Mortality in Chicago attributed to the July 1995 heat wave. *American Journal of public Health*, 87 (9): 1515–1518.
Wolf, T., and McGregor, G. 2013. The development of a heat wave vulnerability index for London, United Kingdom. *Weather and Climate Extremes*, *1*, 59-68.
Wong, D. W. 2002. Modeling local segregation: a spatial interaction approach. *Geographical and Environmental Modelling*, *6*(1), 81-97.

Zanobetti, A., and Schwartz, J. 2008. Temperature and mortality in nine US cities. *Epidemiology*, 19 (4): 563-570.

Zha Y., Gao J., and Ni S. 2003. Use of normalized difference built-up index in automatically mapping urban areas from TM imagery. *International Journal of Remote Sensing* 24 (3) 583-594.

APPENDICES

Appendix A:

Workflow for processing LANDSAT thermal imagery for Pinellas County study using the mono-window algorithm.

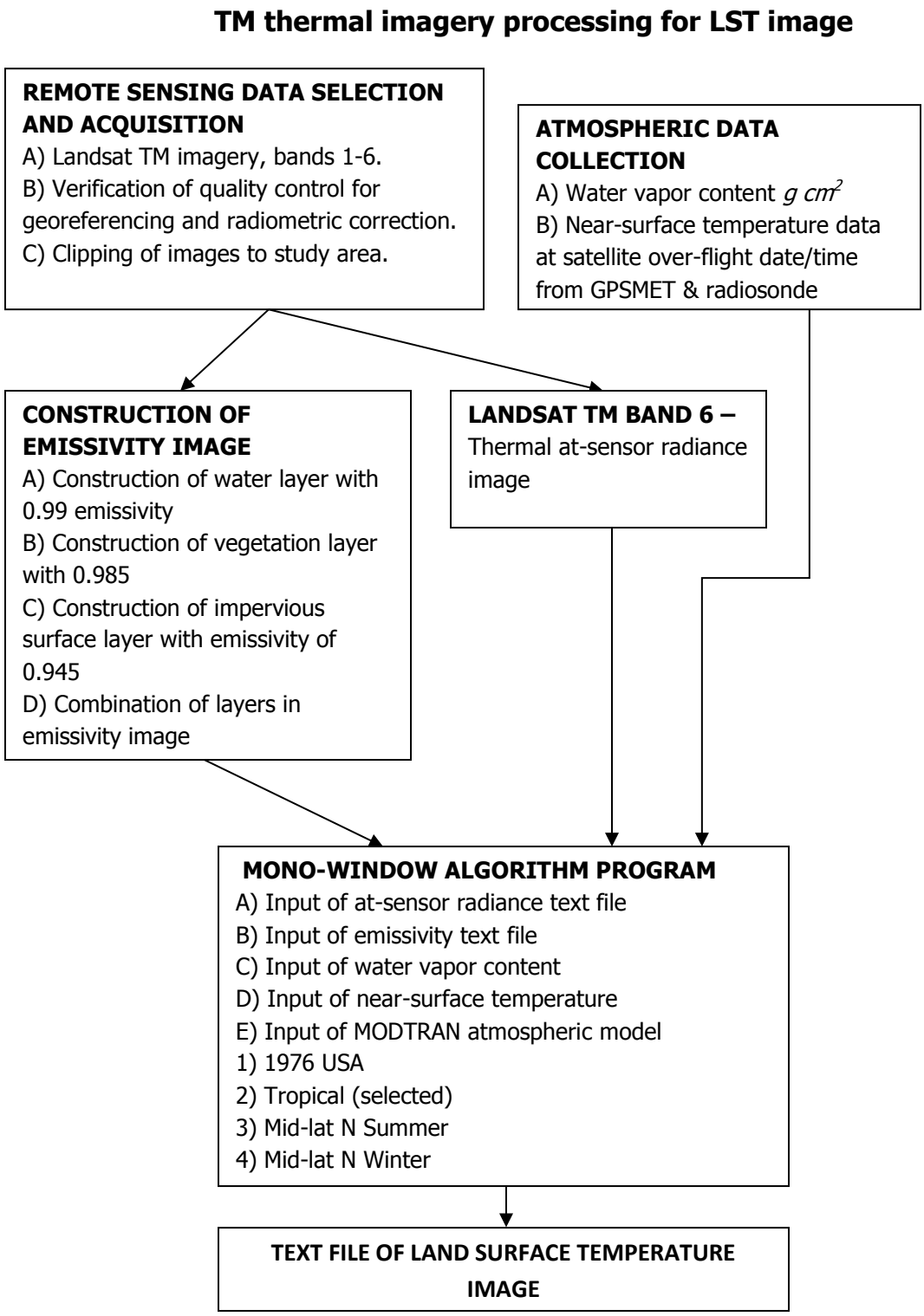

Appendix B:

Moran's I and Spatial Weights: Chicago, Los Angeles, New York City, and Pinellas County. Output of GeoDa ver. 1.6.7.9

Chicago ordinary least squares regression results with variables standardized. ZBio_Risk is UHRI. Significant Moran's I indicating spatial autocorrelation effects of model. Scatterplot of results after 8500 meter spatial weights matrix using spatial error method.

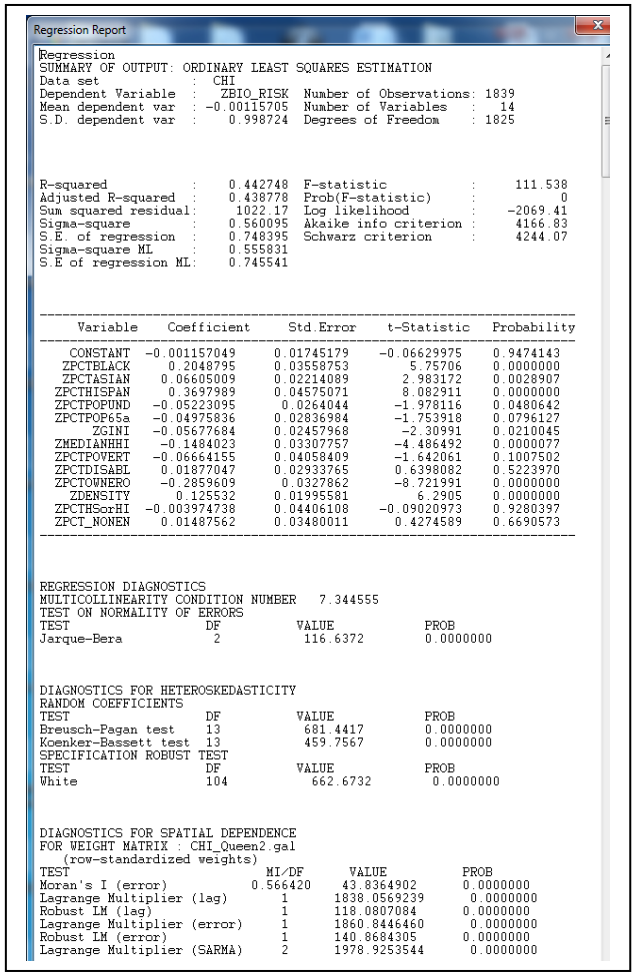

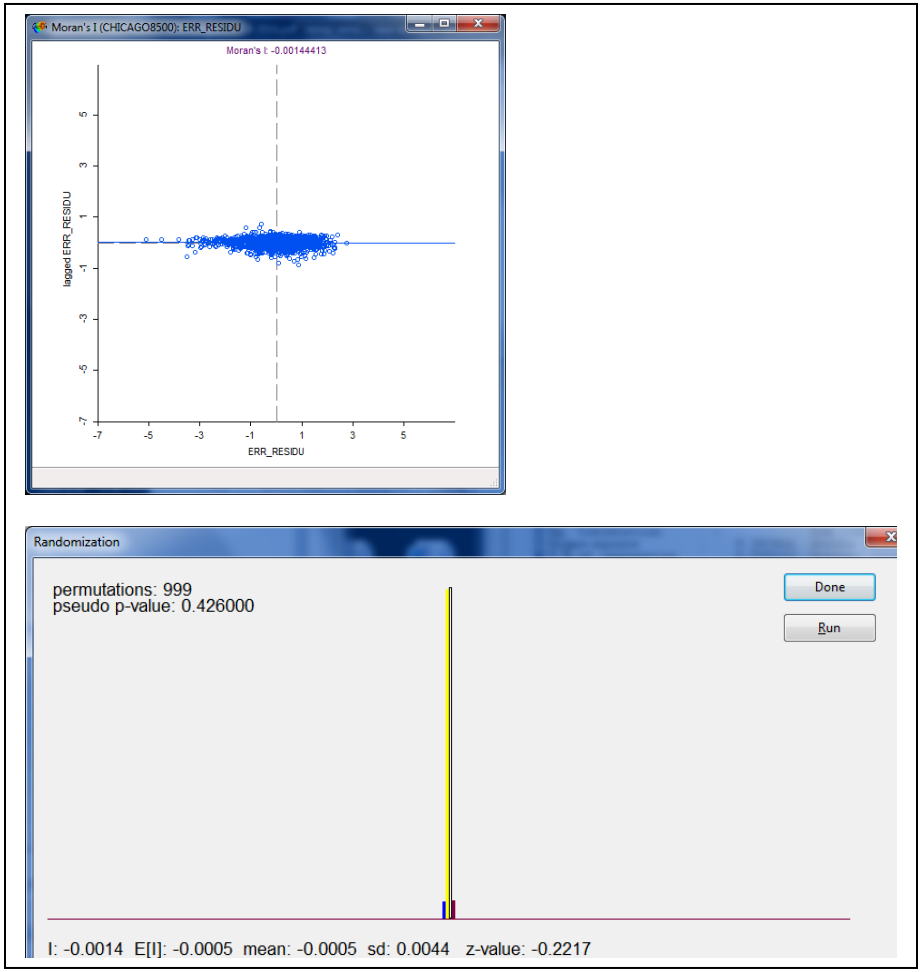

Los Angeles ordinary least squares regression results with variables standardized. ZBio_Risk is UHRI. Significant Moran's I indicating spatial autocorrelation effects of model. Scatterplot of results after 7400 meter spatial weights matrix using spatial error method.

Regression Report

```
Regression
SUMMARY OF OUTPUT: ORDINARY LEAST SQUARES ESTIMATION
Data set            :  LA_JOIN
Dependent Variable  :    ZBIORISK  Number of Observations: 2927
Mean dependent var  :7.17458e-009  Number of Variables   :   14
S.D. dependent var  :     0.99829  Degrees of Freedom    : 2913

R-squared           :    0.490659  F-statistic           :  215.858
Adjusted R-squared  :    0.488386  Prob(F-statistic)     :       0
Sum squared residual:     1485.75  Log likelihood        : -3160.89
Sigma-square        :    0.510041  Akaike info criterion :  6349.79
S.E. of regression  :    0.714171  Schwarz criterion     :  6433.53
Sigma-square ML     :    0.507601
S.E of regression ML:    0.712461

------------------------------------------------------------------------
     Variable     Coefficient      Std.Error    t-Statistic    Probability
------------------------------------------------------------------------
    CONSTANT  5.755941e-009      0.01320052   4.36039e-007     1.0000000
  ZPCTPOPUND    -0.1079904      0.02184802       -4.9428     0.0000008
  ZPCTPOP65a    -0.1744239      0.01951587      -8.937538     0.0000000
   ZPCTBLACK     0.1320323      0.01582063       8.345575     0.0000000
   ZPCTASIAN    0.03657198      0.01778859       2.055924     0.0398795
  ZPCTHISPAN     0.1834475      0.02974273       6.167808     0.0000000
  ZPCTDISABL    0.07679589      0.01659377       4.627995     0.0000039
  ZPCTHSGRAD    0.01736856      0.01755504      0.9893776     0.3225530
  ZPCT_NONEN     0.1519349       0.0247903       6.128806     0.0000000
  ZPCTPOVERT    0.06104741      0.02387422       2.557043     0.0106070
  ZMEDIANHHI    -0.3055737      0.02662722      -11.47599     0.0000000
  ZPCTOWNERO   -0.05670411      0.02446215      -2.318035     0.0205166
        ZGINI    -0.1581697      0.01614019      -9.799739     0.0000000
    ZDENSITY    -0.0644686      0.01930634      -3.339245     0.0008506
------------------------------------------------------------------------

REGRESSION DIAGNOSTICS
MULTICOLLINEARITY CONDITION NUMBER    6.767605
TEST ON NORMALITY OF ERRORS
TEST                    DF          VALUE            PROB
Jarque-Bera              2          842.9951         0.0000000

DIAGNOSTICS FOR HETEROSKEDASTICITY
RANDOM COEFFICIENTS
TEST                    DF          VALUE            PROB
Breusch-Pagan test      13          496.1784         0.0000000
Koenker-Bassett test    13          215.4759         0.0000000
SPECIFICATION ROBUST TEST
TEST                    DF          VALUE            PROB
White                   104           830.7169         0.0000000

DIAGNOSTICS FOR SPATIAL DEPENDENCE
FOR WEIGHT MATRIX : LA_QUEEN.gal
   (row-standardized weights)
TEST                           MI/DF       VALUE           PROB
Moran's I (error)           0.381638      N/A             N/A
Lagrange Multiplier (lag)          1      1281.9442257      0.0000000
Robust LM (lag)                    1       79.8067283       0.0000000
Lagrange Multiplier (error)        1      1332.3252889      0.0000000
Robust LM (error)                  1       130.1877916      0.0000000
Lagrange Multiplier (SARMA)        2      1412.1320172      0.0000000
```

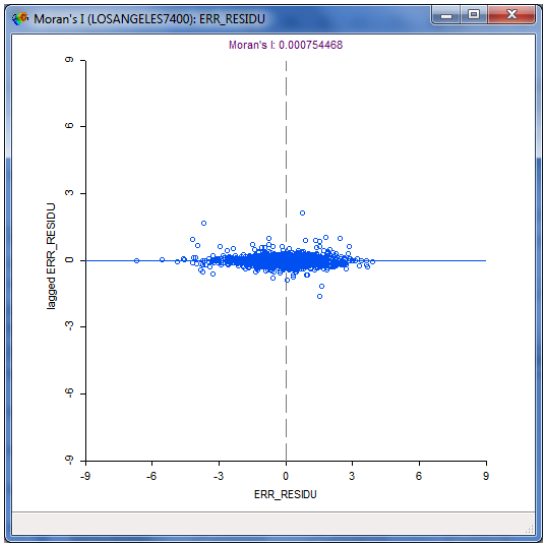

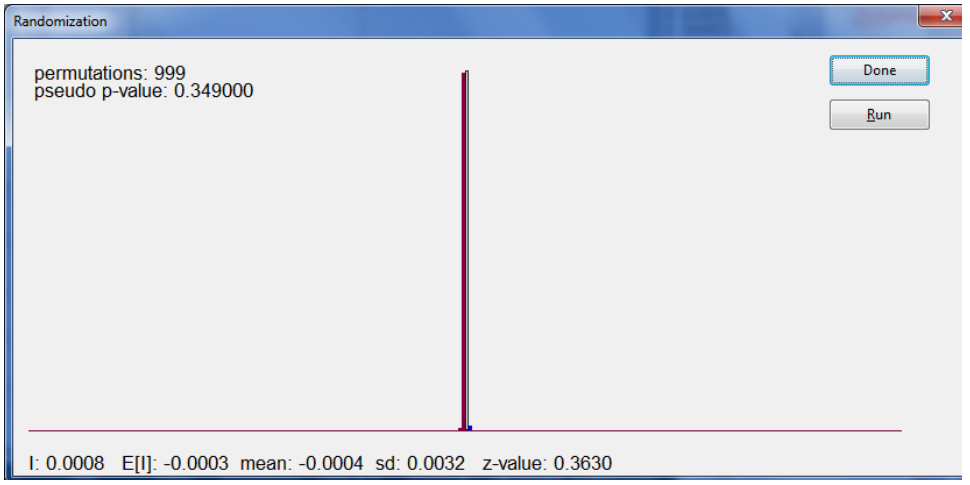

New York City ordinary least squares regression results, with variables standardized. ZBio_Risk is UHRI. Significant Moran's I indicating spatial autocorrelation of model. Scatterplot of results after 7300 meter spatial weights matrix using spatial error method.

Regression Report

```
SUMMARY OF OUTPUT: ORDINARY LEAST SQUARES ESTIMATION
Data set            :   NYC
Dependent Variable  :    ZBIORISK  Number of Observations: 3095
Mean dependent var  : 0.000175729  Number of Variables   :   13
S.D. dependent var  :    0.999952  Degrees of Freedom    : 3082

R-squared           :    0.558963  F-statistic           :  325.506
Adjusted R-squared  :    0.557246  Prob(F-statistic)     :       0
Sum squared residual:     1364.88  Log likelihood        : -3124.64
Sigma-square        :    0.442855  Akaike info criterion :  6275.28
S.E. of regression  :    0.665473  Schwarz criterion     :  6353.77
Sigma-square ML     :    0.440995
S.E of regression ML:    0.664074

------------------------------------------------------------------------
    Variable   Coefficient       Std.Error     t-Statistic   Probability
------------------------------------------------------------------------
    CONSTANT  3.578724e-005      0.01196191    0.002991766     1.00000
    ZDENSITY      0.1668477      0.01670898      9.985513     0.00000
         V32    0.007061131      0.01469747     0.4804318     0.63101
         V33     -0.1208501      0.01703318      -7.09498     0.00000
      ZBLACK      0.1050121      0.01585709      6.622406     0.00000
      ZASIAN      0.1182354      0.0160683       7.358302     0.00000
   ZHISPANIC    -0.08953992      0.0176446      -5.074637     0.00000
  ZOWNER_OCC     -0.3894614      0.02282193     -17.06523     0.00000
     ZINCOME     -0.1526411      0.02033751     -7.505396     0.00000
       ZGINI    -0.08104739      0.01385543     -5.849502     0.00000
      ZHS_EDU      0.1509411      0.01354761      11.14153     0.00000
    ZNON_ENG      0.123315       0.01918368      6.42812      0.00000
   ZDISABLED    -0.01388924      0.01555159     -0.8931076     0.37187
------------------------------------------------------------------------

REGRESSION DIAGNOSTICS
MULTICOLLINEARITY CONDITION NUMBER   4.523296
TEST ON NORMALITY OF ERRORS
TEST                     DF          VALUE            PROB
Jarque-Bera               2          278.1010         0.00000

DIAGNOSTICS FOR HETEROSKEDASTICITY
RANDOM COEFFICIENTS
TEST                     DF          VALUE            PROB
Breusch-Pagan test       12          435.5128         0.00000
Koenker-Bassett test     12          294.5572         0.00000

DIAGNOSTICS FOR SPATIAL DEPENDENCE
FOR WEIGHT MATRIX : NYC73k.gwt
   (row-standardized weights)
TEST                          MI/DF        VALUE           PROB
Moran's I (error)             0.1496        50.0373        0.00000
Lagrange Multiplier (lag)          1       1206.1172        0.00000
Robust LM (lag)                    1        349.5008        0.00000
Lagrange Multiplier (error)        1       2357.7759        0.00000
Robust LM (error)                  1       1501.1595        0.00000
Lagrange Multiplier (SARMA)        2       2707.2767        0.00000
========================== END OF REPORT ==============================
```

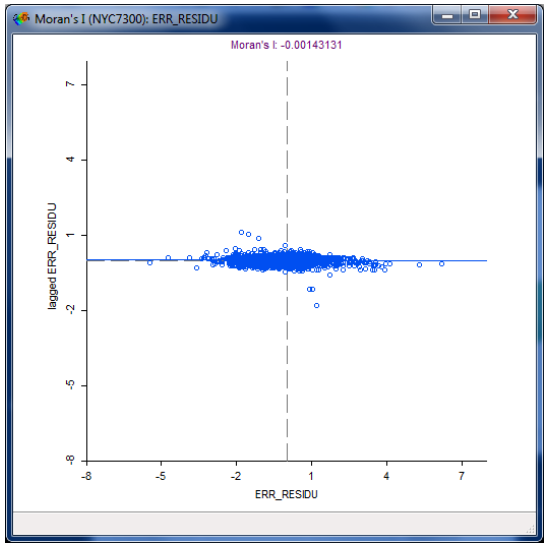

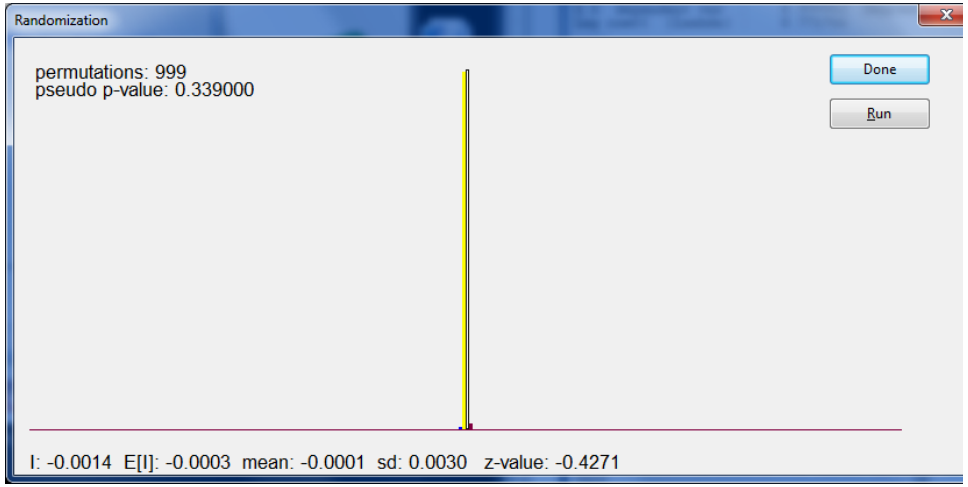

Pinellas County ordinary least squares regression results, with variables standardized. ZMean_1 is LST. Significant Moran's I indicating spatial autocorrelation. Scatterplot of results after 2400 meter spatial weights matrix using spatial error method.

Regression Report

```
SUMMARY OF OUTPUT: ORDINARY LEAST SQUARES ESTIMATION
Data set            :   GEODAFinal
Dependent Variable  :      ZMEAN_1  Number of Observations:   244
Mean dependent var  :2.11802e-017  Number of Variables   :     9
S.D. dependent var  :     0.997949  Degrees of Freedom    :   235

R-squared           :     0.254995  F-statistic           :      10.0543
Adjusted R-squared  :     0.229633  Prob(F-statistic)     :4.83855e-012
Sum squared residual:      181.036  Log likelihood        :     -309.807
Sigma-square        :     0.770367  Akaike info criterion :      637.615
S.E. of regression  :     0.877705  Schwarz criterion     :      669.089
Sigma-square ML     :     0.741952
S.E of regression ML:     0.861366

------------------------------------------------------------------------
    Variable   Coefficient      Std.Error    t-Statistic   Probability
------------------------------------------------------------------------
    CONSTANT  -8.399888e-008     0.05618933  -1.494926e-006     1.00000
  ZPOP_DENSI     0.3343989     0.06083218       5.497072     0.00000
  ZBELOW_POV     0.2276069     0.08345886       2.727175     0.00687
    ZUNDER_5    -0.01200357        0.11885     -0.1009976     0.91965
    ZOVER_65     0.08598726     0.09073833      0.9476399     0.34429
       ZBLACK    -0.04992815     0.09444954     -0.5286225     0.59757
      ZASIAN      0.1257547     0.06495708       1.935966     0.05407
   ZHISPANIC     0.03327267      0.0804599      0.413531     0.67959
  ZOWNER_OCC     -0.1262963     0.07509622      -1.681794     0.09394
------------------------------------------------------------------------

REGRESSION DIAGNOSTICS
MULTICOLLINEARITY CONDITION NUMBER   4.774680
TEST ON NORMALITY OF ERRORS
TEST                   DF           VALUE             PROB
Jarque-Bera             2            2.6901          0.26052

DIAGNOSTICS FOR HETEROSKEDASTICITY
RANDOM COEFFICIENTS
TEST                   DF           VALUE             PROB
Breusch-Pagan test      8            30.6825          0.00016
Koenker-Bassett test    8            26.8582          0.00075

DIAGNOSTICS FOR SPATIAL DEPENDENCE
FOR WEIGHT MATRIX : se2400.gwt
   (row-standardized weights)
TEST                           MI/DF        VALUE           PROB
Moran's I (error)              0.3171        8.0232         0.00000
Lagrange Multiplier (lag)           1         44.6702         0.00000
Robust LM (lag)                     1          0.2210         0.63831
Lagrange Multiplier (error)         1         55.3889         0.00000
Robust LM (error)                   1         10.9397         0.00094
Lagrange Multiplier (SARMA)         2         55.6099         0.00000
========================= END OF REPORT =============================
```

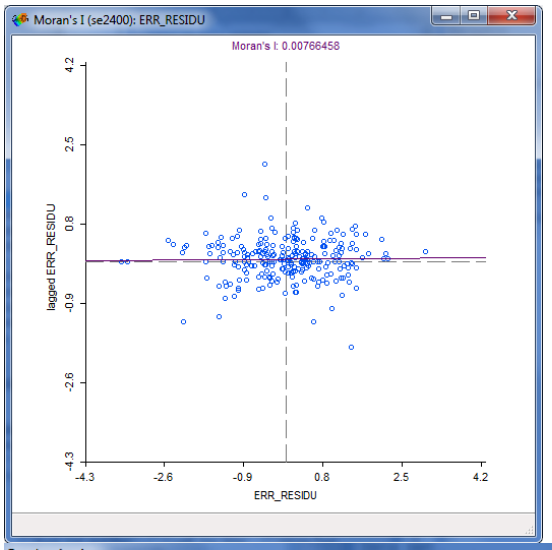

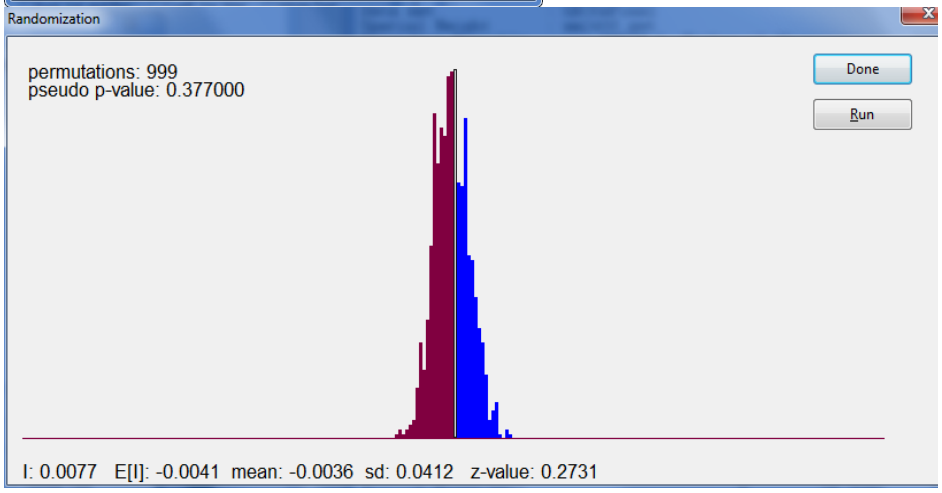

Appendix C:

Table of Climate Data

Climate Data and Population 2010 with Predicted Increase in Heating Days by 2050

MSA	STATE	REGION	CLIMATE TYPE	KOPPEN CLASS	HEATING DAYS-CURRENT*	INCREASE IN HEATING DAYS BY 2050*	NEW TOTAL HEATING DAYS	MSA SIZE (millions)
Atlanta	GA	South	Humid Subtropical	Cfa	5	43	48	5.4
Boston	MA	Northeast	Humid Continental	Dfa	11	40	51	4.6
Chicago	IL	Midwest	Humid Continental	Dfa	5	13	18	9.5
Cincinnati	OH	Midwest	Humid Continental	Dfa	4	18	22	2.1
Dallas	TX	South	Humid Subtropical	Cfa	11	11	22	6.5
Denver	CO	West	Semiarid Steppe	Bsk	9	79	88	2.6
Detroit	MI	Midwest	Humid Continental	Dfa	9	6	15	4.3
Hartford	CT	Northeast	Humid Continental	Dfa	6	25	31	1.2
Los Angeles	CA	West	Mediterranean	Csa	1	59	60	12.9
Memphis	TN	South	Humid Subtropical	Cfa	9	9	18	1.3
Minneapolis	MN	Midwest	Humid Continental	Dfb	8	15	23	3.3
New York	NY	Northeast	Humid Continental	Dfa	11	44	55	19
Philadelphia	PA	Northeast	Humid Continental	Dfa	6	48	54	5.9
Phoenix	AZ	West	Midlatitude Desert	Bwh	7	77	84	4.2
Portland	OR	West	Marine Westcoast	Cfb	4	38	42	2.3
Providence	RI	Northeast	Humid Continental	Dfa	7	31	38	1.6
Seattle	WA	West	Marine Westcoast	Cfb	2	52	54	3.5
St Louis	MO	Midwest	Humid Continental	Dfa	11	24	35	2.8
Tampa	FL	South	Humid Subtropical	Cfa	3	33	36	2.8
Washington	DC	South	Humid Subtropical	Cfa	16	37	53	5.7

***Source: Natural Resources Defense Council, May 2012 https://www.nrdc.org/sites/default/files/killer-summer-heat-report.pdf**

Appendix D:

Table of Atmospheric Data

Land Surface Temperature Processing Data for Mono-window Algorithm

CITY	DAY #	LANDSAT IMAGE DATE	TAO CELSIUS*	TEMP KELVIN*	WATER gm/c3*	WEATHER STATION*	CLOUDS?
Atlanta	211	7/30/2010	32.77	305.92	4.38	Peachtree City, GA	Yes
Boston	146	5/26/2010	33.27	306.42	3.13	Chatham, MA	No
Chicago	255	9/12/2010	23.88	297.03	1.59	Davenport, IA	No
Cincinnati	266	9/23/2010	31.66	304.81	3.74	Wilmington, OH	No
Dallas	171	6/20/2010	33.88	307.03	3.81	Ft. Worth, TX	No
Denver	197	7/16/2010	30.61	303.76	1.26	Denver, CO	No
Detroit	186	7/5/2010	31.66	304.81	3.31	White Lake, MI	Yes
Hartford	185	7/4/2010	32.77	305.92	2.15	Upton, NY	Yes
Los Angeles	269	9/26/2010	37.22	310.37	1.4	San Diego, CA	No
Memphis	255	9/12/2010	27	300.15	2.13	Nashville, TN	Yes
Minneapolis	139	5/19/2010	22.77	295.92	0.67	Chanhassen, MN	No
New York City	185	7/4/2010	33	306.15	2.15	Upton, NY	No
Philadelphia	240	8/28/2010	26.11	299.26	1.93	Upton, NY	No
Phoenix	225	8/13/2010	38.89	312.04	1.23	Flagstaff, AZ	No
Portland	224	8/12/2010	20.61	293.76	2.37	Salem, OR	No
Providence	146	5/26/2010	32.22	305.37	3.13	Chatham, MA	Yes
Seattle	208	7/27/2010	20.61	293.76	1.36	Quillayute, WA	Yes
St. Louis	198	7/17/2010	32.22	305.37	3.86	Springfield, MO	No
Tampa	197	7/16/2010	31	304.15	4.55	Ruskin, FL	Yes
Washington DC	263	9/20/2010	23.6	296.75	1.39	Sterling, VA	No

*Source: http://weather.uwyo.edu/upperair/naconf.html

Appendix E:

LANDSAT Overflight and Weather Data

LANDSAT Imagery and Weather Data

MSA	LANDSAT NUMBER	DATA	PATH	ROW	HIGH TEMP (Degrees C)	PRECIP	DAY OF YEAR
Atlanta	LT50190362010211EDC00	07/30/10	19	36	35.00	0	211
Boston/Providence	LT50120312010146EDC00	05/26/10	12	31	34.44	1.2	146
Chicago	LT50230312010255PAC01	09/10/10	23	31	31.67	1.55	255
Cincinnati	LT50200332010266GNC01	09/23/10	20	33	35.56	0	266
Dallas	LT50270372010171EDC00	06/20/10	27	37	37.78	0.79	171
Denver	LT50330332010197EDC00	07/16/10	33	33	35.00	0	197
Detroit	LT50200312010186GNC01	07/05/10	20	31	36.67	0	186
Hartford	LT50130312010185EDC00	07/04/10	13	31	35.00	0	185
Los Angeles	LT50410362010269EDC00	09/26/10	41	36	30.56	0	269
Los Angeles	LT50410372010269EDC00	09/26/10	41	37	30.56	0	269
Memphis	LT50230352010255PAC01	09/12/10	23	35	36.11	0	255
Minneapolis	LT50260292010139PAC01	05/19/10	26	29	26.11	0	139
New York City	LT50130322010185EDC00	07/04/10	13	32	38.33	0	185
Philadelphia	LT50140322010240EDC00	08/28/10	14	32	29.44	0	187
Phoenix	LT50370362010225PAC01	08/13/10	37	36	43.33	0	225
Portland	LT50460282010224EDC00	08/12/10	46	28	28.33	0	208
Seattle	LT50460272010208PAC01	07/27/10	46	27	35.00	0.18	208
St. Louis	LT50240332010198EDC00	07/17/10	24	33	35.56	0.14	198
Tampa	LT50170412010197EDC00	07/16/10	17	41	34.44	0.01	197
Washington D.C.	LT50150332010263EDC00	09/20/10	15	33	37.22	4.66	263

Appendix F:

Table of Calculated Segregation Indices Using Census 2010 Population Counts

Indices of Segregation for Twenty U.S. MSAs Contrasting Non-Hispanic White With Selected Minorities

	HISPANIC					ASIAN					BLACK				
MSA	ID	SP	ISOLAT-ION	DELTA	CENTRAL-ITY	ID	SP	ISOLAT-ION	DELTA	CENTRAL-ITY	ID	SP	ISOLAT-ION	DELTA	CENTRAL-ITY
BOSTON	0.55	1.31	0.25	0.74	0.68	0.38	1.07	0.16	0.62	0.57	0.61	1.57	0.33	0.77	0.77
HARTFORD	0.59	1.88	0.34	0.72	0.51	0.37	1.03	0.08	0.52	0.37	0.66	1.90	0.37	0.71	0.66
NEW YORK	0.65	1.41	0.47	0.71	0.54	0.52	1.18	0.31	0.72	0.53	0.81	1.18	0.31	0.72	0.53
PHILADELPHIA	0.62	1.62	0.64	0.74	0.67	0.44	1.10	0.14	0.58	0.49	0.75	1.67	0.64	0.79	0.73
PROVIDENCE	0.65	1.62	0.38	0.81	0.82	0.42	1.09	0.06	0.68	0.68	0.60	1.24	0.13	0.80	0.82
ATLANTA	0.52	1.25	0.28	0.50	0.11	0.40	1.07	0.14	0.50	-0.01	0.62	1.40	0.64	0.41	0.34
DALLAS	0.51	1.28	0.46	0.60	0.46	0.43	1.08	0.15	0.65	0.42	0.56	1.28	0.36	0.62	0.50
MEMPHIS	0.56	1.14	0.44	0.62	0.04	0.33	1.01	0.06	0.59	-0.24	0.69	1.34	0.75	0.60	0.13
TAMPA	0.42	1.18	0.30	0.50	0.42	0.33	1.02	0.05	0.54	0.37	0.56	1.34	0.37	0.64	0.49
WASHINGTON D.C.	0.48	1.17	0.27	0.62	0.44	0.33	1.06	0.18	0.56	0.15	0.67	1.45	0.61	0.61	0.57
CHICAGO	0.58	1.50	0.49	0.67	0.57	0.42	1.09	0.17	0.61	0.40	0.77	1.81	0.67	0.75	0.70
CINCINNATI	0.38	1.02	0.07	0.60	0.44	0.46	1.02	0.07	0.64	0.37	0.68	1.46	0.50	0.77	0.77
DETROIT	0.44	1.33	0.70	0.54	0.49	0.49	1.07	0.12	0.60	0.51	0.74	1.82	0.70	0.72	0.70
MINNEAPOLIS	0.43	1.17	0.13	0.66	0.65	0.41	1.14	0.13	0.64	0.61	0.51	1.27	0.21	0.72	0.75
ST LOUIS	0.29	1.03	0.04	0.57	0.41	0.39	1.03	0.06	0.61	0.39	0.73	1.65	0.65	0.75	0.78
DENVER	0.49	1.24	0.40	0.82	0.86	0.33	1.02	0.06	0.79	0.79	0.62	1.18	0.18	0.84	0.83
LOS ANGELES	0.62	1.38	0.63	0.73	0.61	0.49	1.29	0.31	0.71	0.53	0.68	1.65	0.28	0.77	0.71
PHOENIX	0.51	1.34	0.48	0.85	0.87	0.33	1.02	0.06	0.85	0.83	0.44	1.06	0.08	0.85	0.87
PORTLAND	0.34	1.05	0.18	0.80	0.76	0.36	1.04	0.11	0.82	0.83	0.45	1.07	0.08	0.84	0.87
SEATTLE	0.33	1.05	0.13	0.77	0.78	0.39	1.08	0.19	0.82	0.86	0.49	1.10	0.12	0.84	0.82

Appendix G:

Table of Bivariate Correlations UHRI with Level 1 Variables for Multilevel Modeling Study

Bivariate Correlations UHRI and Demographic and Socioeconomic Variables by MSA

MSA	BLACK	ASIAN	HISPANIC	OWNER OCCUPANCY	MEDIAN HOUSEHOLD INCOME	HIGH SCHOOL GRADUATES
ATLANTA	.247**	.015	.147**	-.607**	-.462**	-.287**
BOSTON	.232**	.266**	.501**	-.802**	-.607**	-.440**
CHICAGO	.227**	-.052*	.395**	-.638**	-.520**	-.462**
CINCINNATI	.226**	.045	.266**	-.482**	-.416**	-.429**
DALLAS	.015	.236**	.058*	-.368**	-.138**	-.015
DENVER	.251**	.134**	.221**	-.355**	-.249**	-.234**
DETROIT	.315**	-.041	.163**	-.497**	-.620**	-.491**
HARTFORD	.443**	-.025	.723**	-.823**	-.809**	-.726**
LOS ANGELES	.214**	-.101**	.536**	-.440**	-.615**	-.583**
MEMPHIS	.200**	.091	.003	-.486**	-.312**	-.170*
MINNEAPOLIS	.379**	.168**	.281**	-.499**	-.504**	-.406**
NEW YORK CITY	.106**	.071**	.312**	-.605**	-.438**	-.336**
PHILADELPHIA	.425**	.107**	.375**	-.512**	-.700**	-.624**
PHOENIX	.075*	-.138**	.192**	-.021	-.160**	-.252**
PORTLAND	.346**	.259**	.374**	-.572**	-.500**	-.326**
PROVIDENCE	.709**	.388*	.679**	-.780**	-.715**	-.667**
SEATTLE	.443**	.239**	.372**	-.679**	-.487**	-.306**
ST LOUIS	.323**	.076	.227**	-.677**	-.580**	-.497**
TAMPA	.219**	-.135**	-.016	-.318**	-.420**	-.216**
WASHINGTON DC	.234**	-.144**	.073*	-.638**	-.453**	-.253**

*$p<.05$; **$p<.01$

Appendix H:

Table of Spatial Autoregression Models for Twenty City Study

Results of Spatial Autoregression Model Calculated for Twenty U.S. MSAs Using Expanded Variable Set

REGION	NORTHEAST UHRI					SOUTH UHRI					MIDWEST UHRI					WEST UHRI				
DEPENDENT VARIABLE = UHRI	BOS	HAR	NYC	PHI	PRO	ATL	DAL	MEM	TPA	WAS DC	CHI	CIN	DET	MIN	SL	LA	DEN	PHX	PRT	SEAT
% age 5 and under	0.011	-0.096	-0.048***	0.046	-0.011	-0.211***	0.002	-0.276***	-0.166***	-0.108**	.089*	0.025	-.124*	-0.027	-0.015	- .089*	0.019	-0.076	-.161*	-.085*
% age 65 and over	-0.386**	0.044*	-0.134***	-0.051***	-0.039*	-0.058***	-0.048***-0	0.007	0.015*	-0.037**	-0.01	-.179*	-0.011	-.161*	-0.028	-.109*	-.176*	-.150*	-0.03	-.055**
% Non-Hispanic black	-0.018***	0.012*	-0.013	-0.006**	0.074***	0.010**	-0.004	0.007	0.018***	0.005	.084*	-0.069	-.058***	.158*	-.093***	.092*	0.036	.075**	0.032	0.007
% Non-Hispanic Asian	0.008	0.068*	0.031**	0.017	0.133***	0.047***	0.022**	0.093	0.064**	0.061***	.101*	.135**	.079*	.077**	.146*	.169*	.102*	0.048	.174*	-0.018
% Hispanic	0.001	0.030**	-0.111***	-0.007	-0.001	0.033***	-0.008	-0.016	0.017*	0.013	0.132	0.088	0.005	0.019	-0.035	.291*	.271***	.169***	.193*	0.053
% disabled	-0.018*	0.078**	0.014	0.069***	0.063**	0.015	0.003	0.034	0.014	0.071**	0.022	.203*	.119*	.144*	0.026	.047*	.131***	0.041	.085**	.129*
% high school education	0.000	0.043***	-0.007	-0.013**	0.014	-0.004	0.013	-0.004	-0.016*	0.071**	-0.016	-0.092	-0.011	.089*	-0.074	-.119*	0.037	-.206*	0.014	-.073**
% Non-English speaking	0.015	0.028	0.079***	0.015	0.007	-0.008	0.029**	0.106*	.135*	-0.011	.054*	0.025	.130*	0.015	-0.011	0.122	0.044	-.-016	-.065	-.052***
% owner-occupied homes	-0.039***	-0.043***	-0.269***	0.003	-0.034***	-0.033***	-0.034***	-0.039***	-0.022***	-0.031***	0.009	0.121	-.186*	-.245*	-.247*	-.211*	-0.170***	0.06	-.155*	-.338*
Median household income	-0.389***	-0.071***	-0.076***	-0.613***	-0.0491**	0.000	-.000	0.023	0.008	-0.281**	-.123*	-.170**	-.265*	-.246*	-.145**	-.256*	-.162***	--.359*	-.142*	-0.005
Gini coefficient	-0.706	-7.777***	-0.076***	0.714	-4.722*	0.594	-7.993***	0.515	-0.624	-1.963*	.114*	-0.033	-.117*	-.132*	-0.034	-.127*	-.118***	-.135*	-.141*	-.085*
Population density	0.389***	0.650***	0.496***	1.419**	0.658**	0.000	0.278	0.429**	0.558***	0.787***	.230*	0.048	.239*	-.300*	.228*	-.227*	-.269***	-.127*	.519*	.462*
Spatial error term (rho)	0.942***	0.331***	0.772***	0.951***	0.829***	0.737***	0.439***	1.019***	0.865***	0.943***	.960**	1.012***	1.003***	0.644***	0.966***	.906**	0.742***	0.974***	0.649***	0.955***
Pseudo-r-square	0.825	0.804	0.689	0.770	0.798	0.640	0.451	0.408	0.578	0.583	0.73	0.461	0.526	0.582	0.759	0.613	0.533	0.422	0.738	0.739
log likelihood	-1069.59	-427.05	-2605.91	-1373.84	-348.47	-1072.65	-2311.53	-414.68	-986.26	-2016.51	-1451.51	-369.47	-1210.69	-685.14	-292.77	-2775.93	-636.26	-1065.17	-351.3	-536.1
AIC	2165.2	880.09	5237.82	2773.68	722.95	2171.31	4649.06	855.37	1996.53	4059.01	2929.01	764.94	2447.39	1396.27	611.54	5577.86	1299.25	2154.03	728.6	1100.21
Weights distance	7500M	2800M	7300M	11900M	9800M	4200M	2000M	5000M	7500M	10500M	5500M	2500M	2500M	2700M	5500M	7200M	3500M	9600M	5200M	16000M
N	646	263	3095	792	214	628	1174	220	560	975	1838	335	1163	664	384	2927	587	916	459	718

**p<.05; **p<.01; ***p<.001*

Appendix I: Multilevel Model for UHRI and Demographic and Socioeconomic Variables in Twenty City Study

Level-1 Model

UHRI = B0 + B1*(Pop Density) + B2*(Race/Ethnicity) + B3*(Owner Occupancy) + B4*(Income) + B5*(HS Education) + **r**

Level-2 Model

B0 = G00 + G01*(ID) + G02*(SP) + G03*(xPx) + G04*(Delta) + G05*(ACE) + u0
B1 = G10
B2 = G20
B3 = G30
B4 = G40
B5 = G50

Mixed Model

UHRI = G00 + G01*(ID) + G02*(SP) + G03*(xPx) + G04*(Delta) + G05*(ACE) + G10*(Pop Density) + G20*(Race/Ethnicity) + G30*(Owner Occupancy) + G40*(Income) + G50*(HS Education) + u0+ r

Appendix J: UHRI Imagery and Demographic and Income Maps of Twenty U.S. Cities with NDVI, NDVI and LST scaled at the pixel level, and the UHRI, demographic and socioeconomic data at the census tract level.

Atlanta MSA NDVI, NDBI, and LST with UHRI

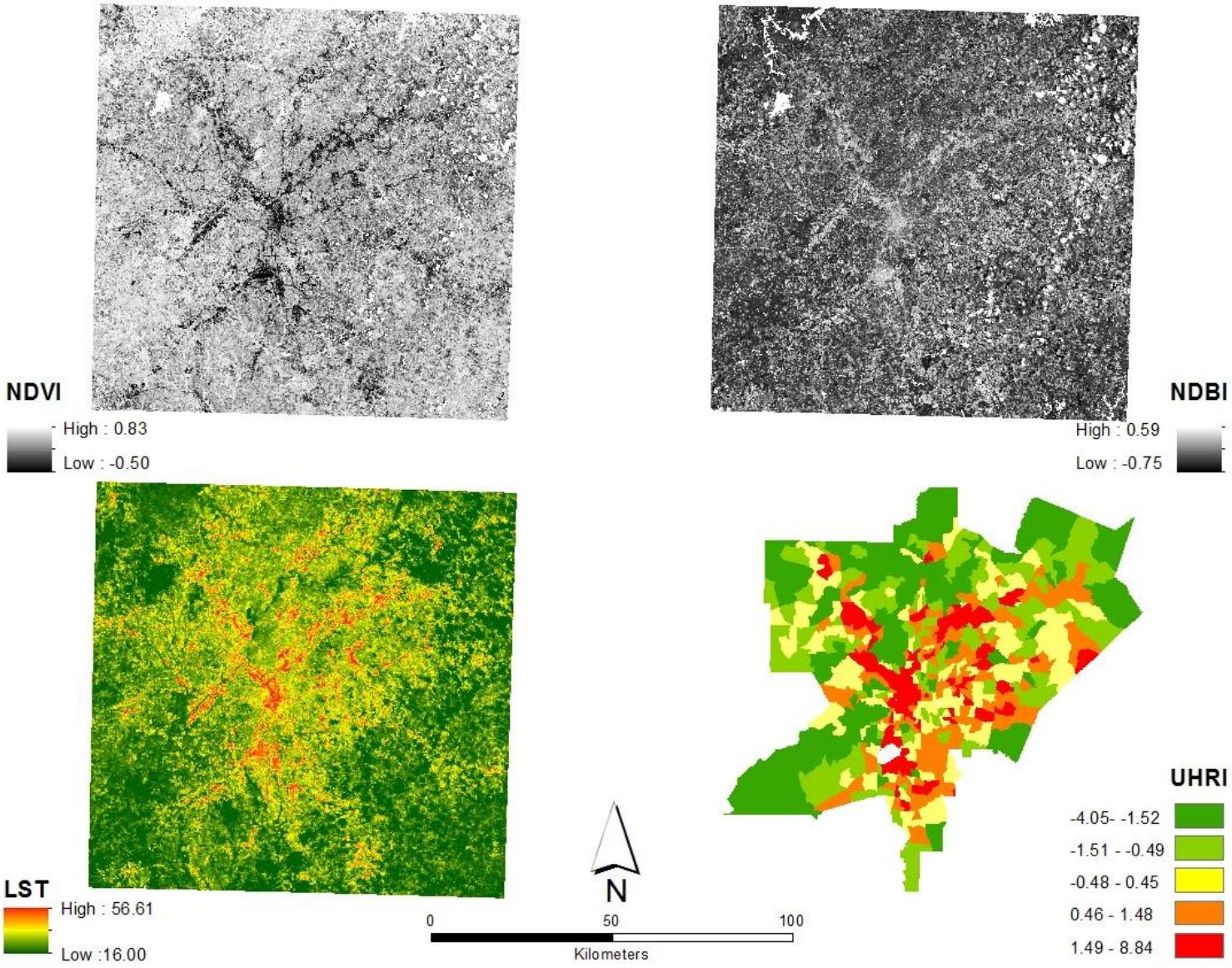

Atlanta MSA median household income by quintile; percentage Black, Hispanic, and Asian population by tract

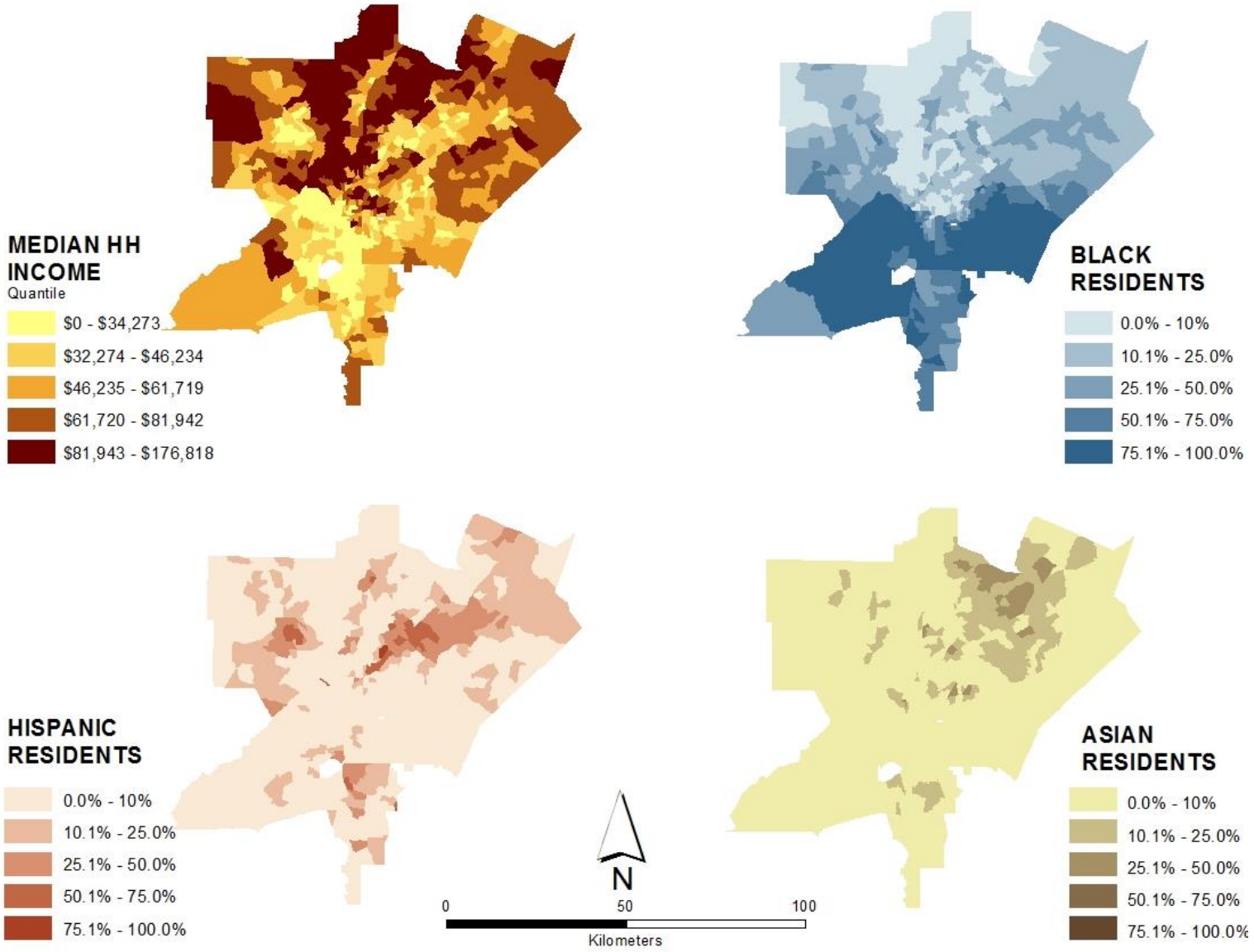

Boston MSA NDVI, NDBI, and LST with UHRI

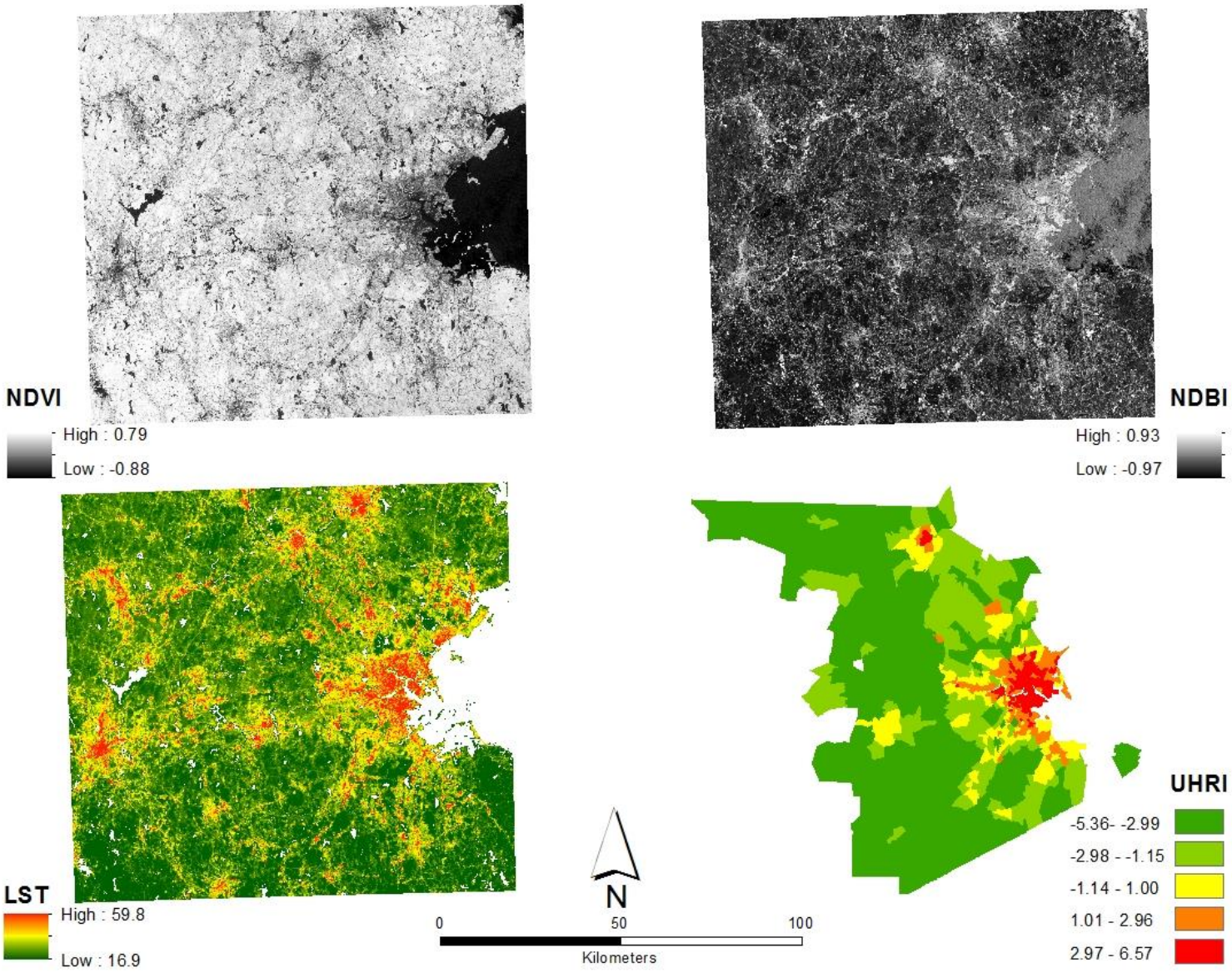

Boston MSA median household income by quintile; percentage Black, Hispanic, and Asian population by tract

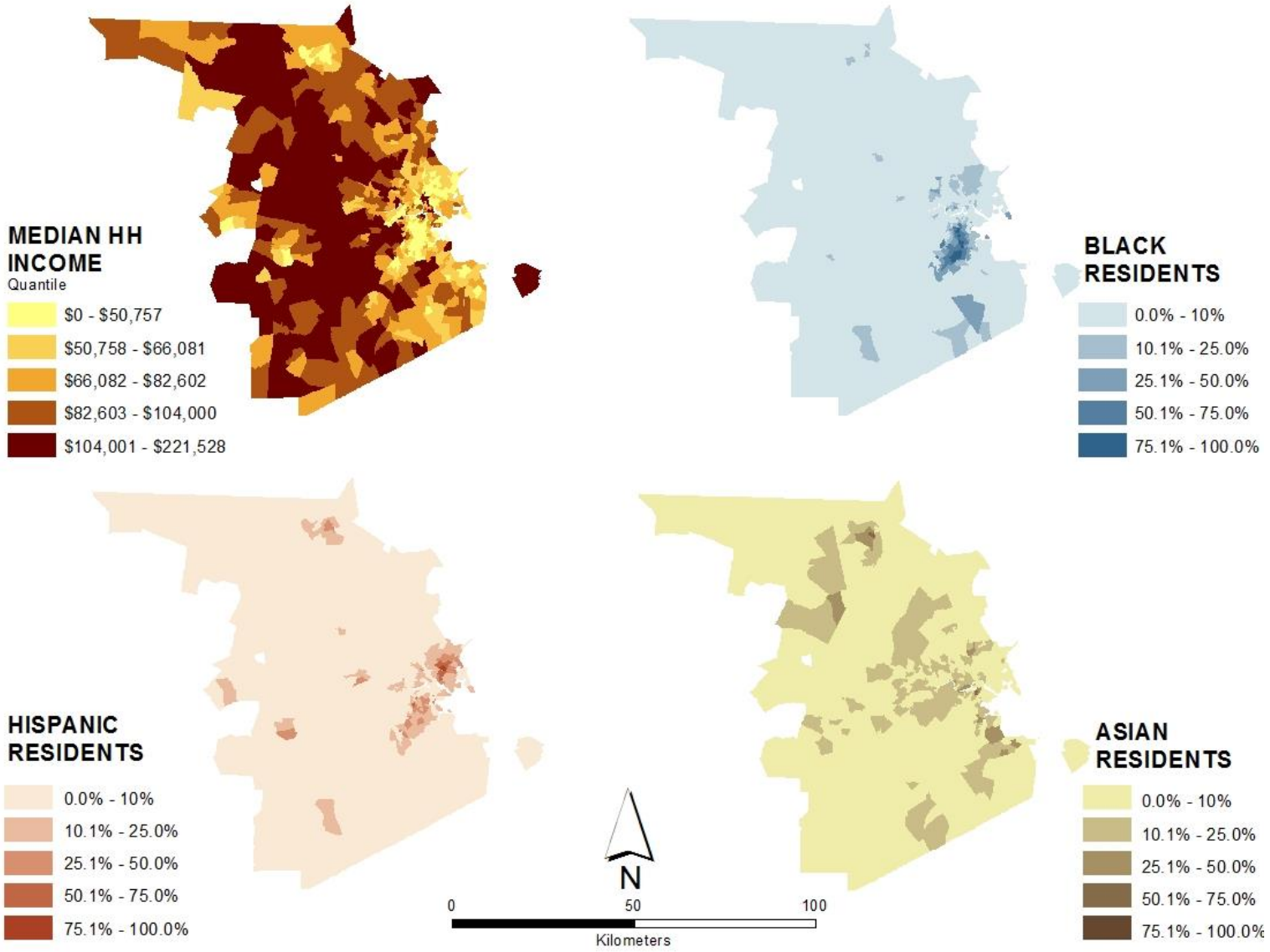

Chicago MSA NDVI, NDBI, and LST with UHRI

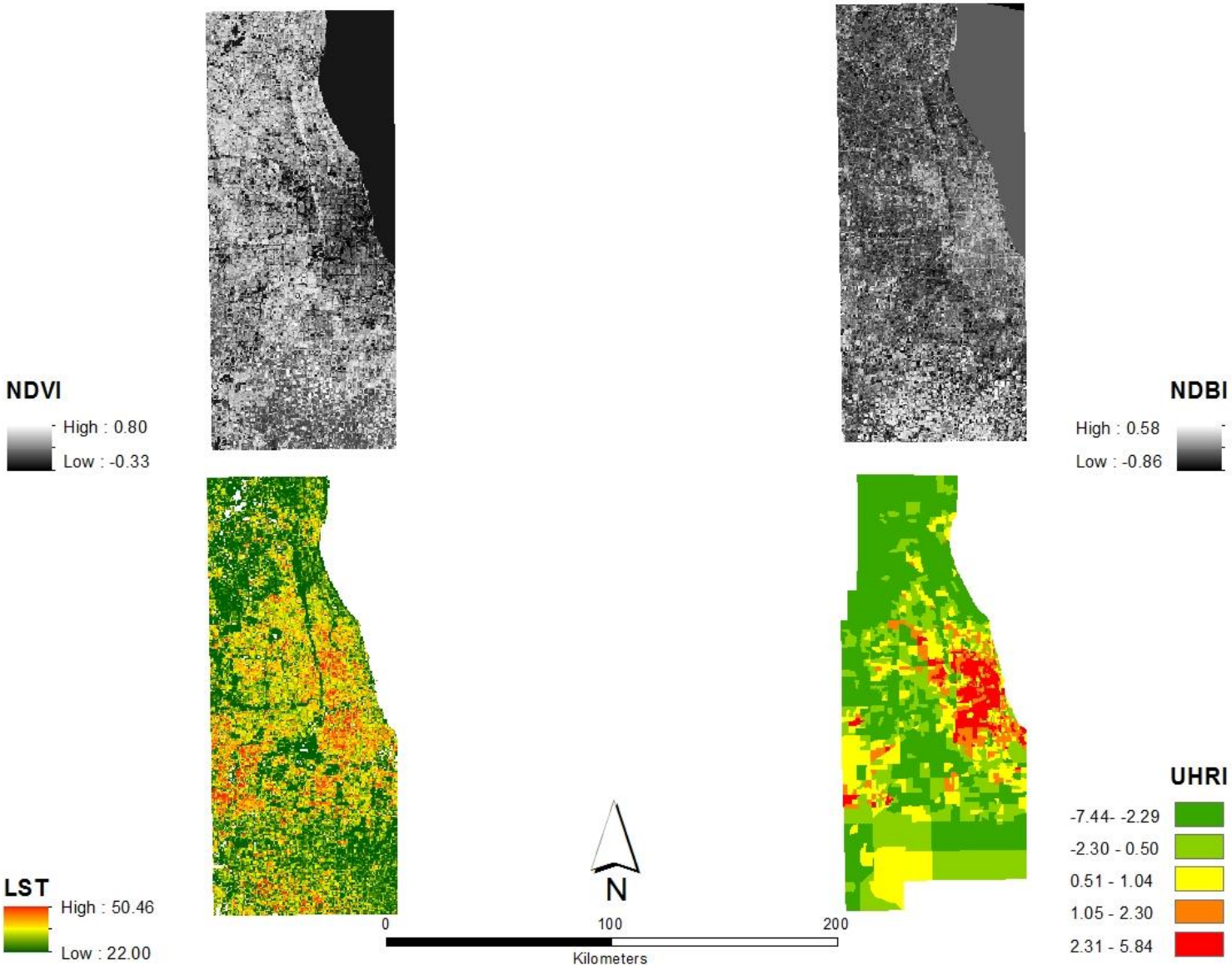

Chicago MSA median household income by quintile; percentage Black, Hispanic, and Asian population by tract

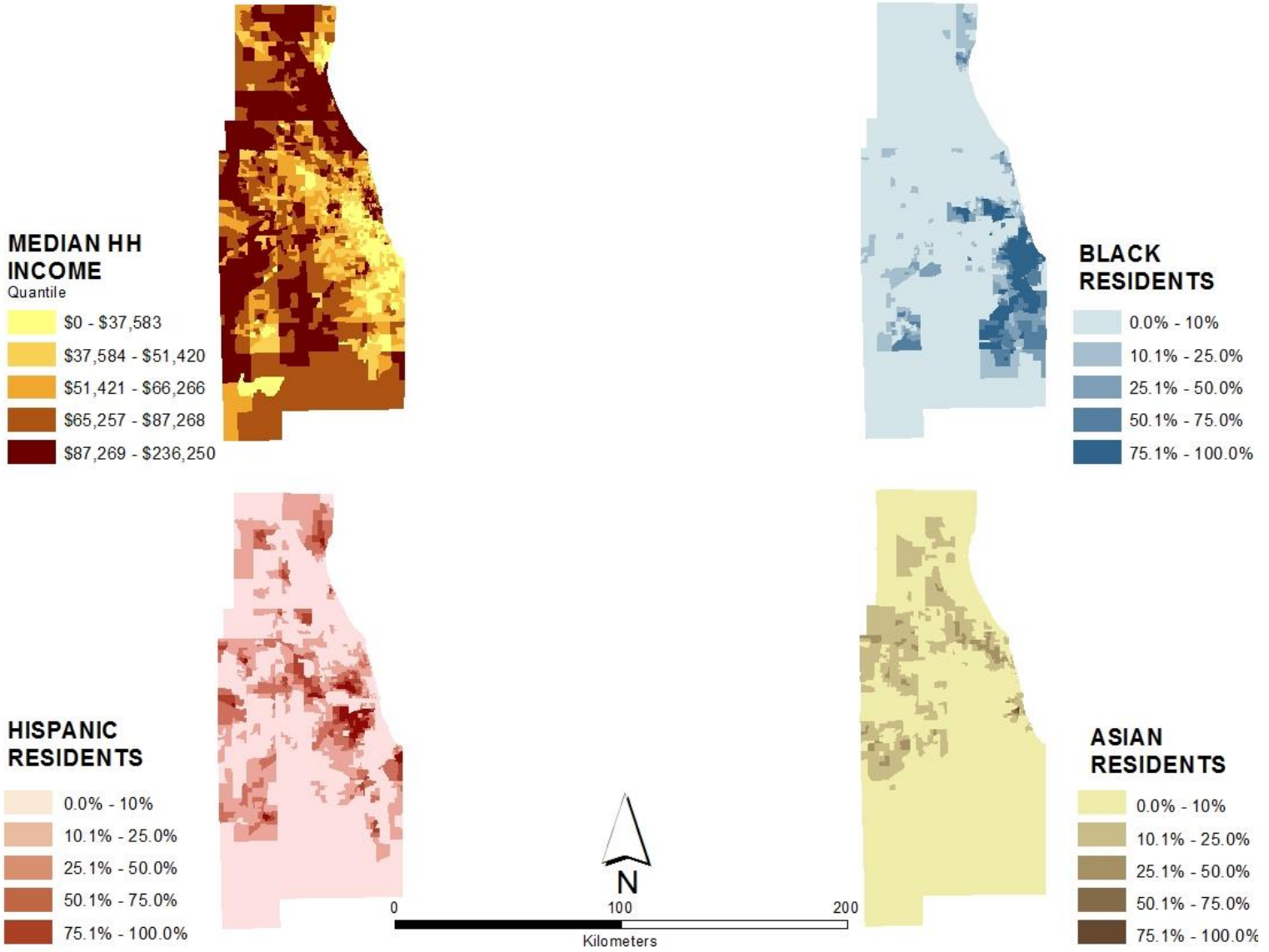

Cincinnati MSA NDVI, NDBI, and LST with UHRI

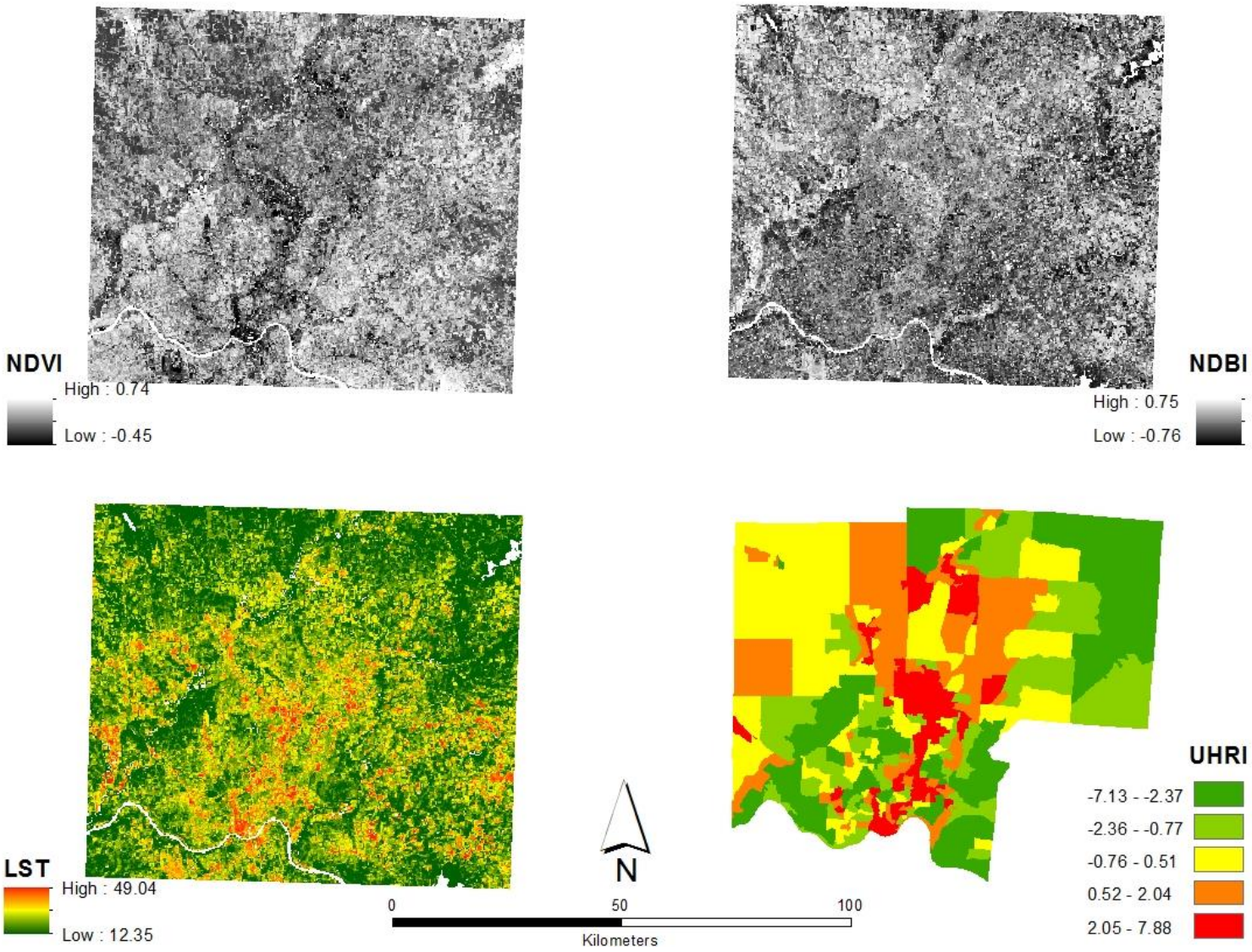

Cincinnati MSA median household income by quintile; percentage Black, Hispanic, and Asian population by tract

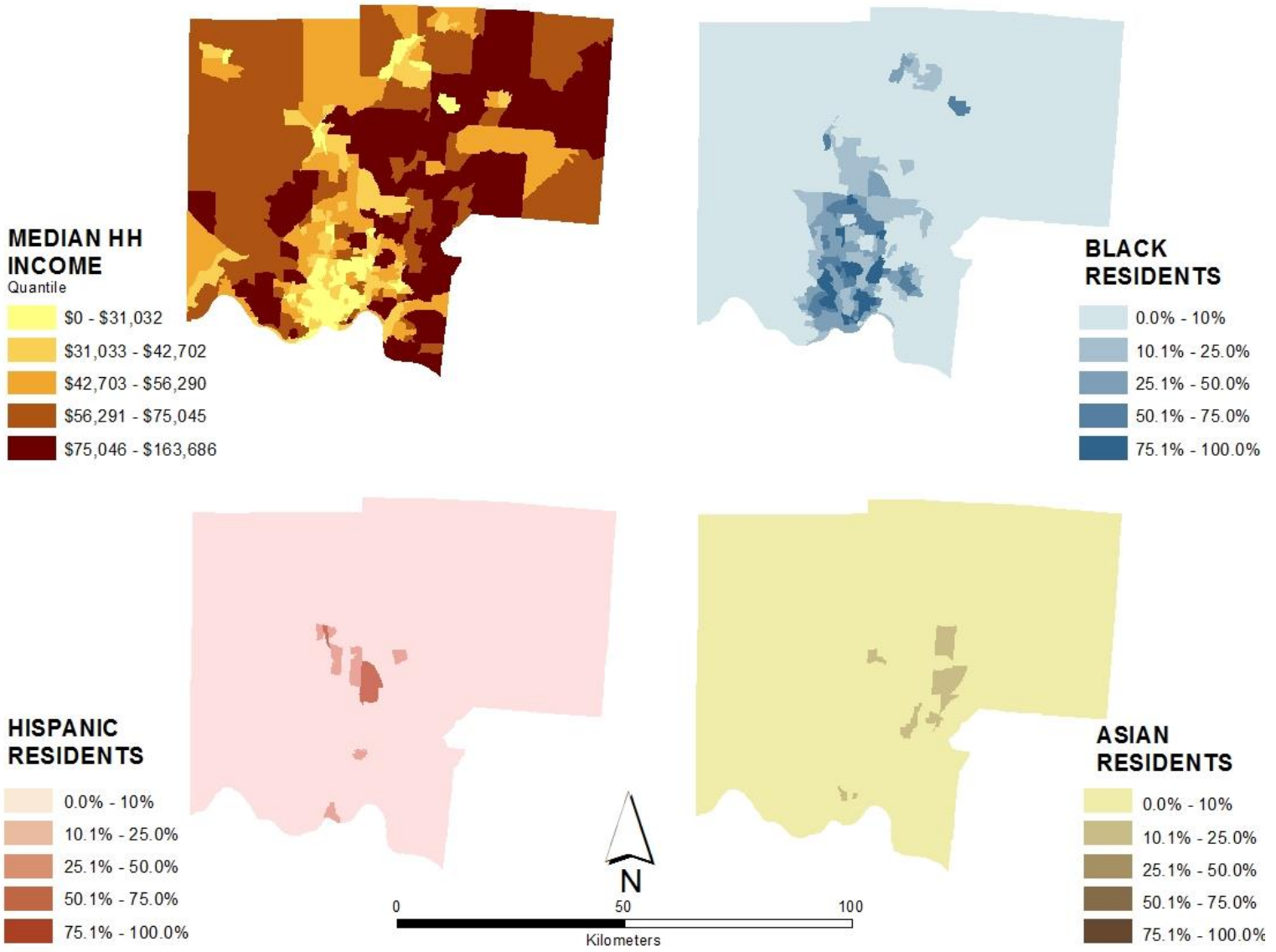

Dallas MSA NDVI, NDBI, and LST with UHRI

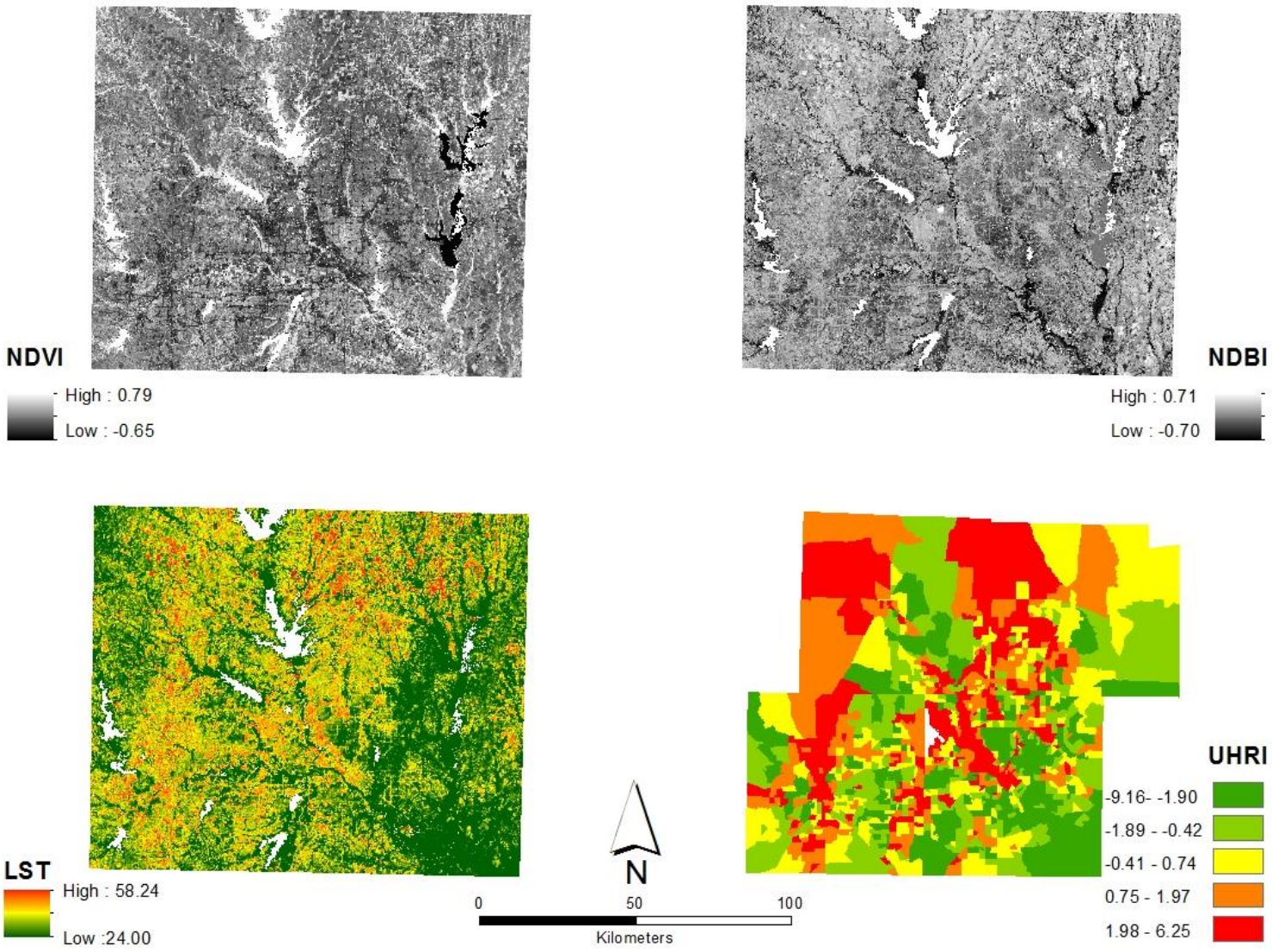

Dallas MSA median household income by quintile; percentage Black, Hispanic, and Asian population by tract

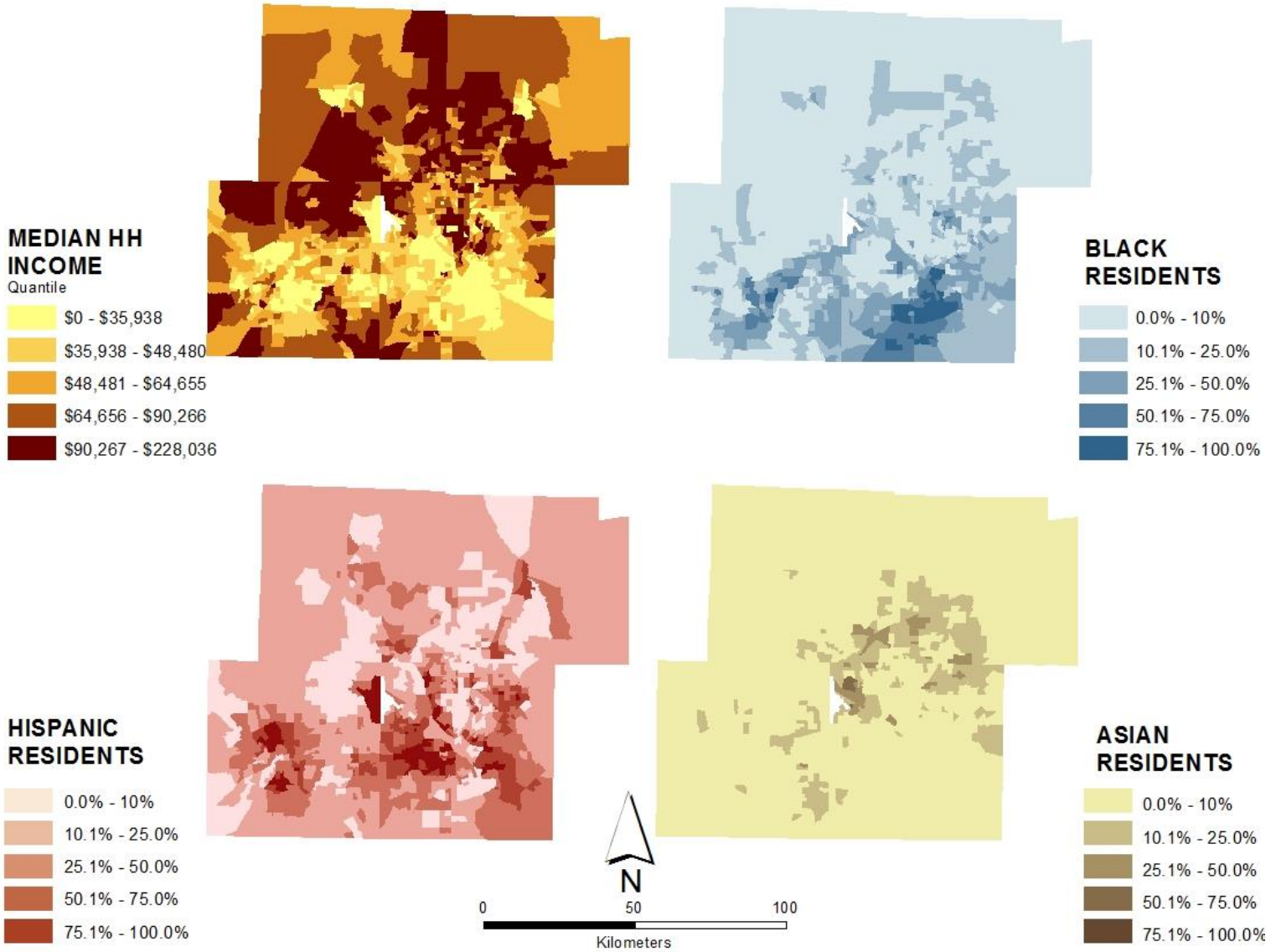

Denver MSA NDVI, NDBI, and LST with UHRI

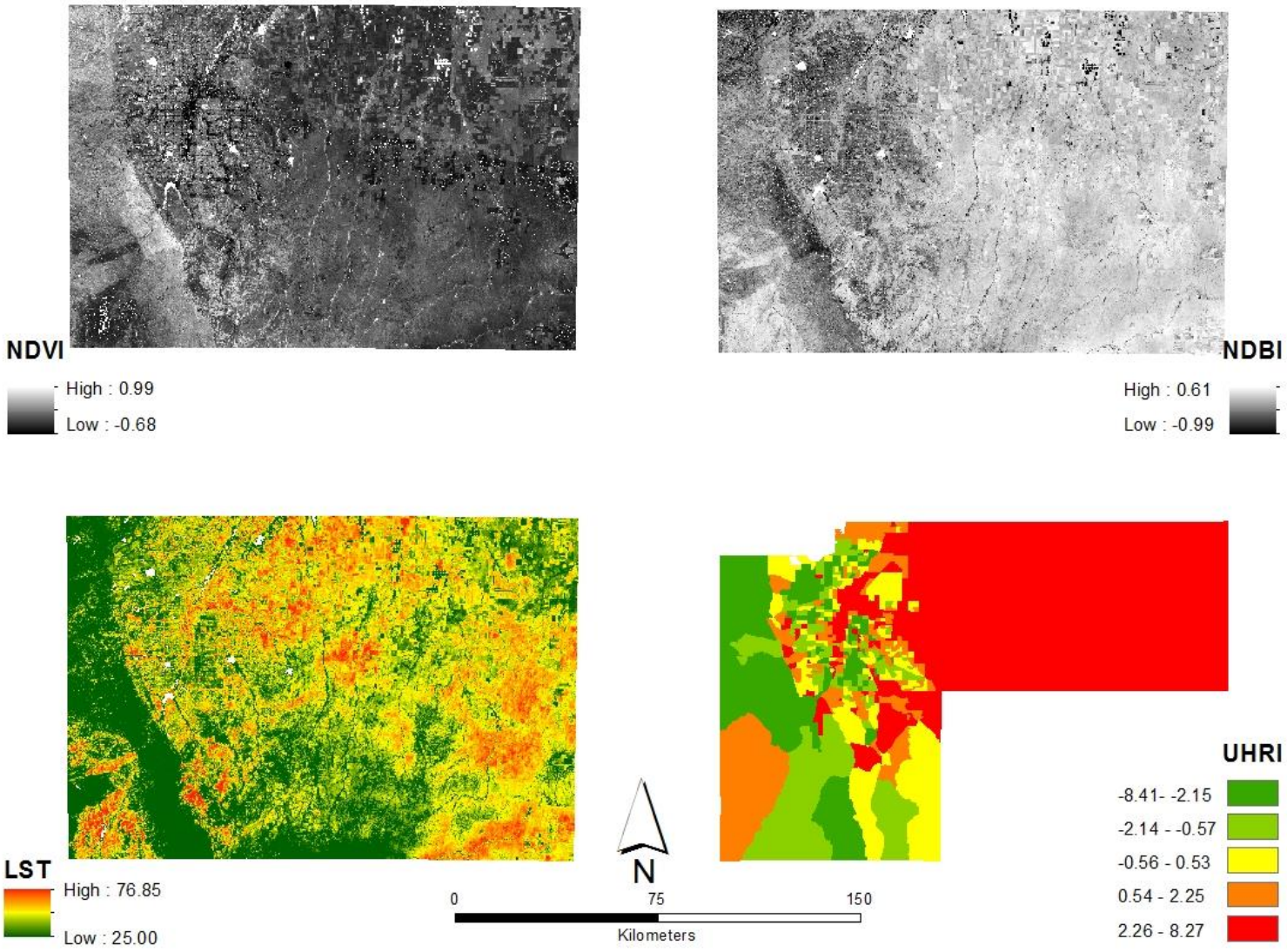

Denver MSA median household income by quintile; percentage Black, Hispanic, and Asian population by tract

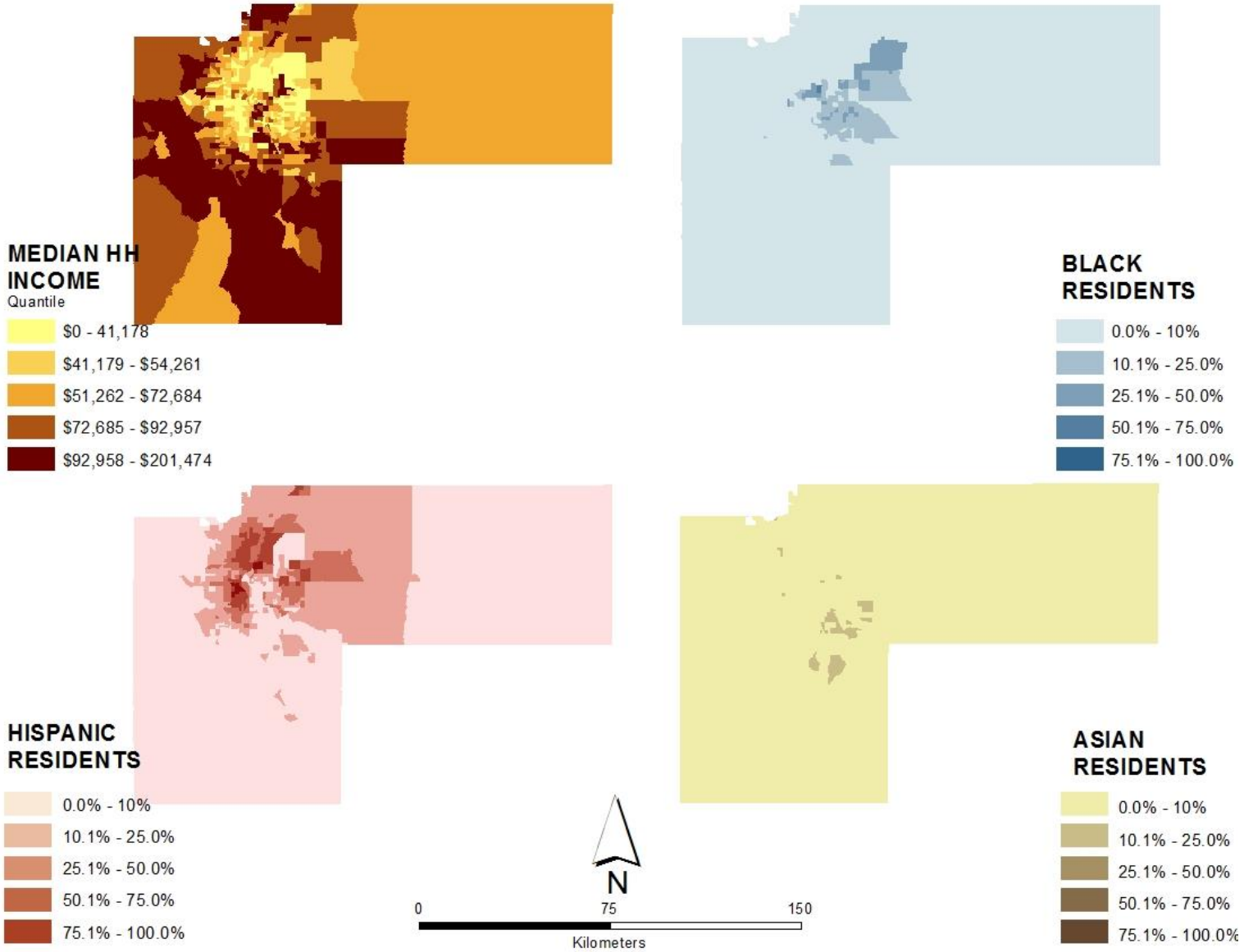

Detroit MSA NDVI, NDBI, and LST with UHRI

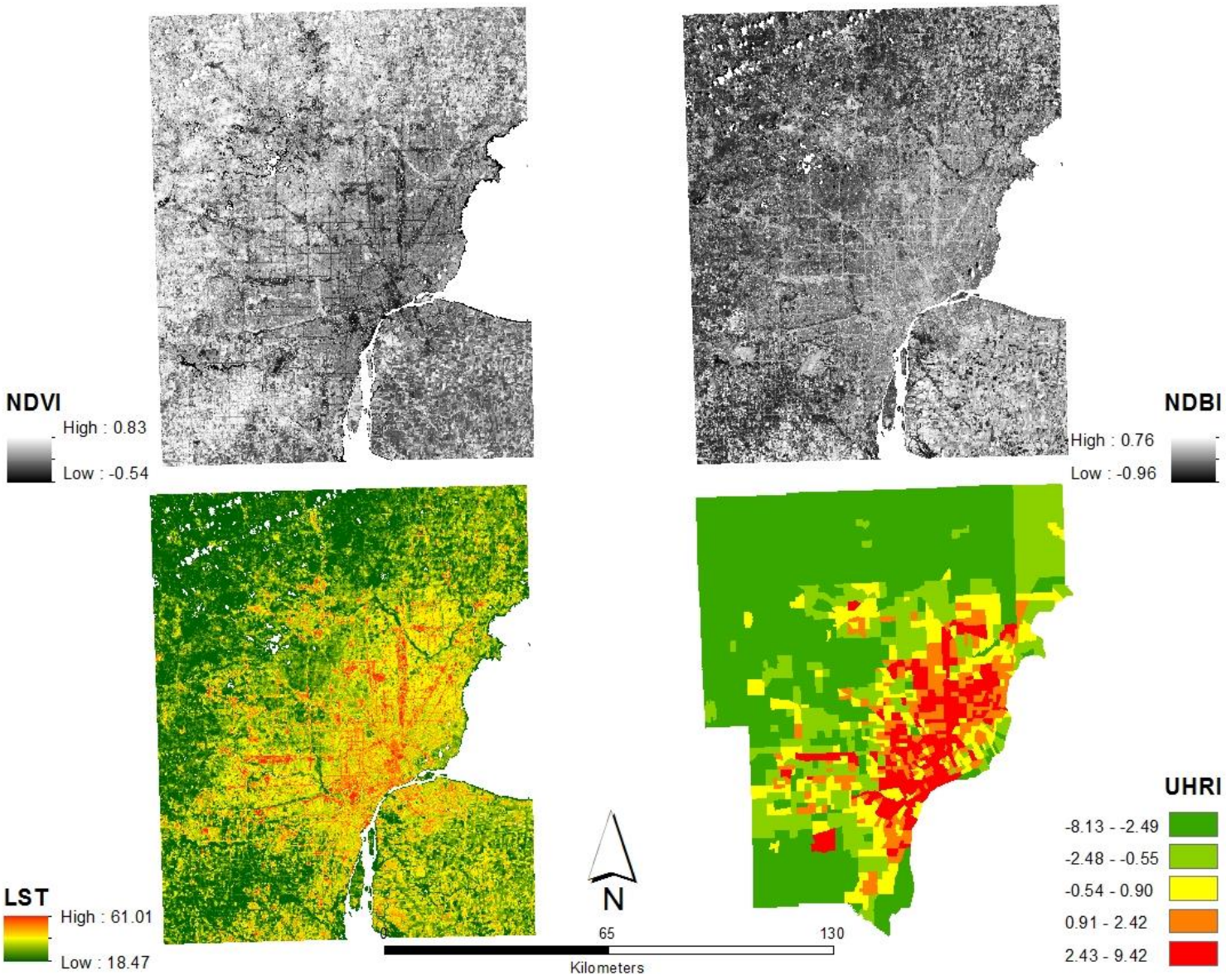

Detroit MSA median household income by quintile; percentage Black, Hispanic, and Asian population by tract

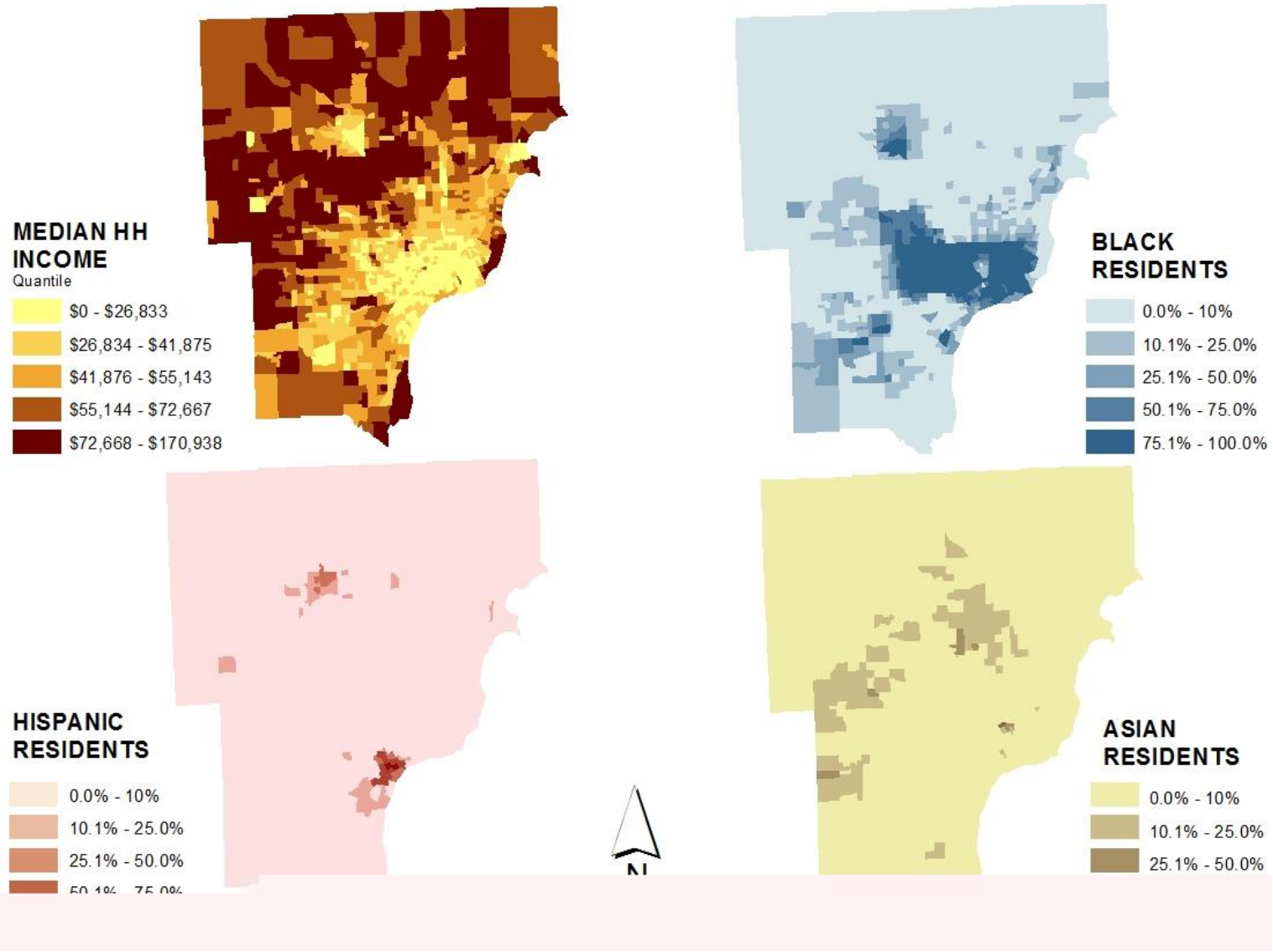

Hartford MSA NDVI, NDBI, and LST with UHRI

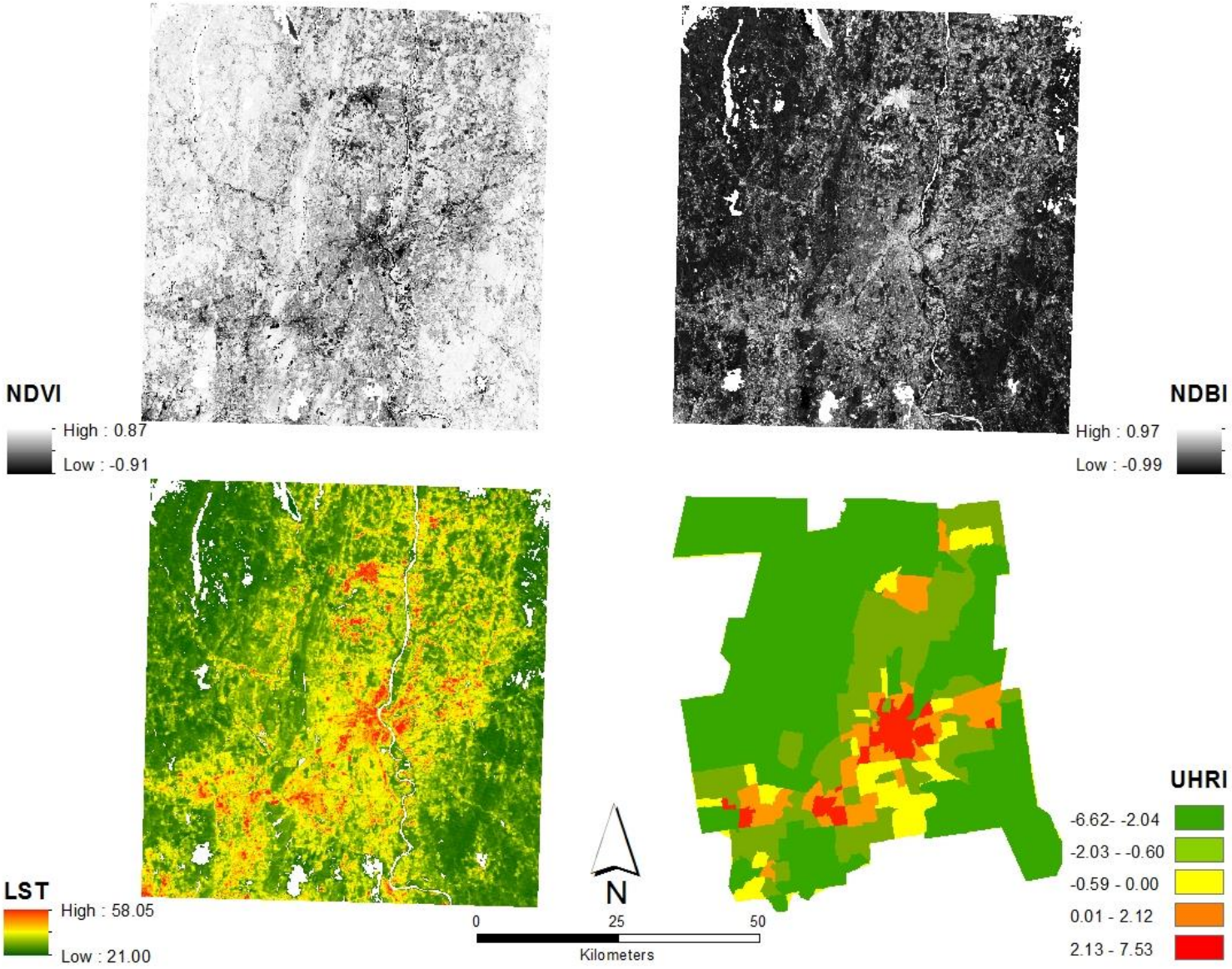

Hartford MSA median household income by quintile; percentage Black, Hispanic, and Asian population by tract

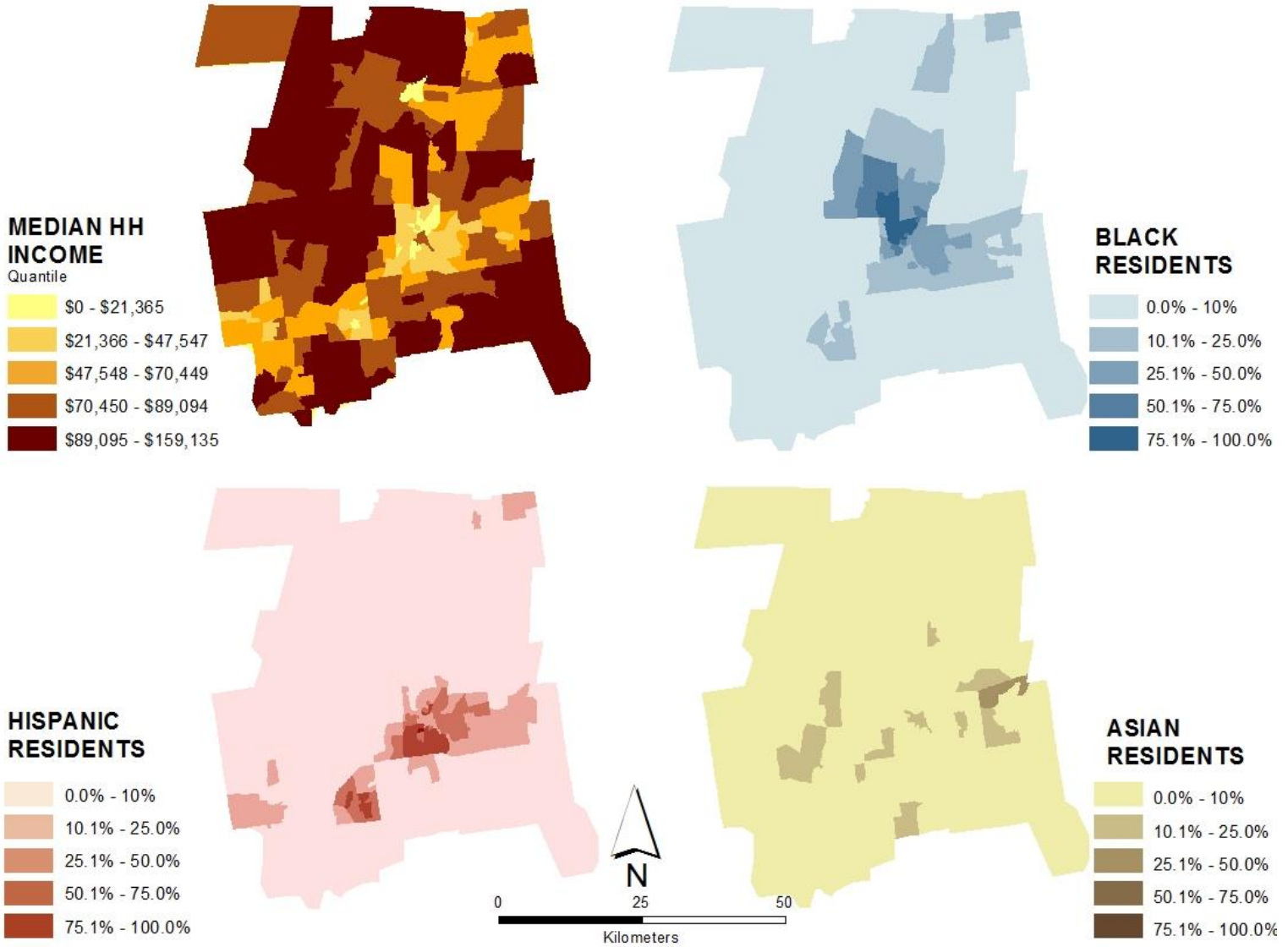

Los Angeles MSA NDVI, NDBI, and LST with UHRI

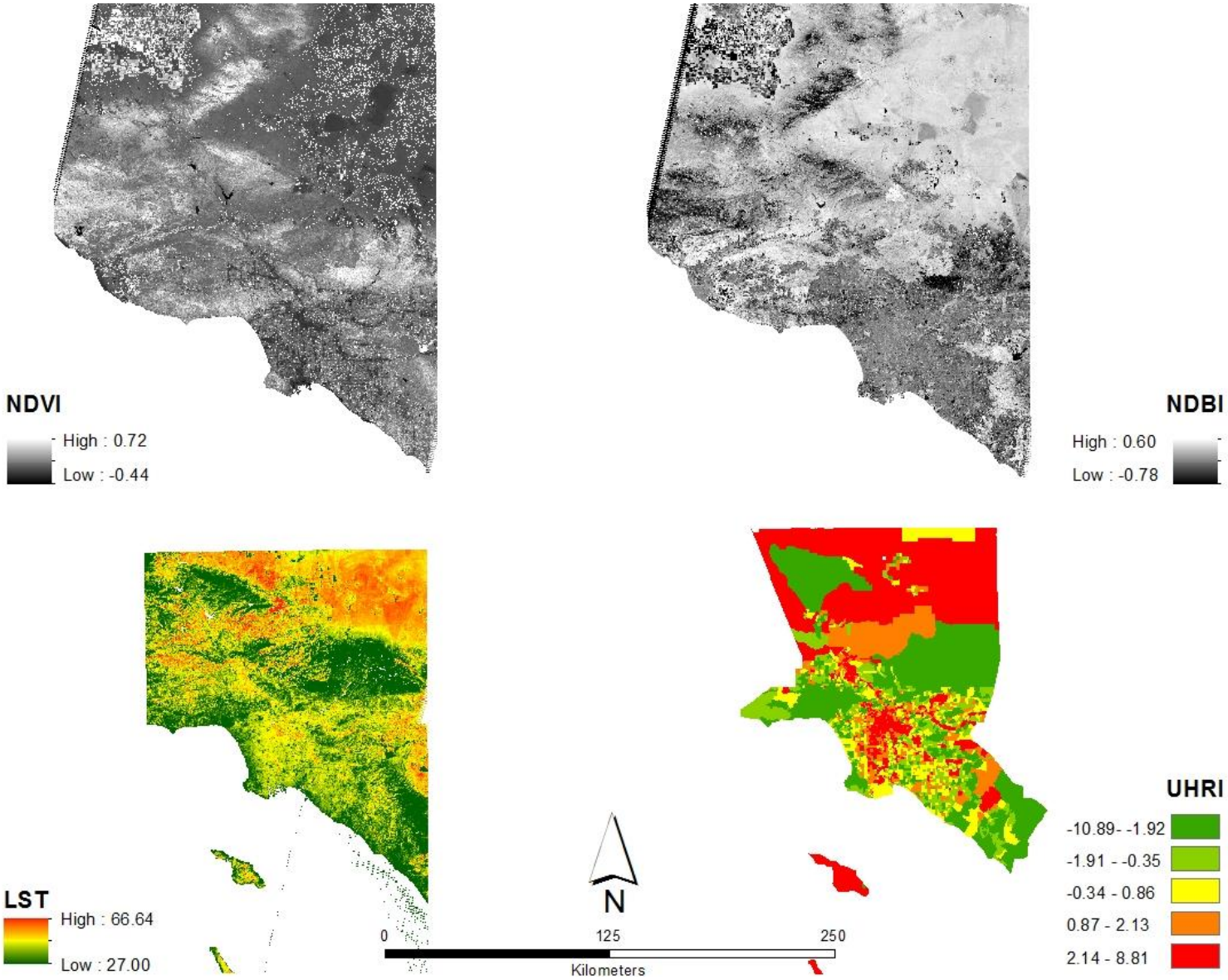

Los Angeles MSA median household income by quintile; percentage Black, Hispanic, and Asian population by tract

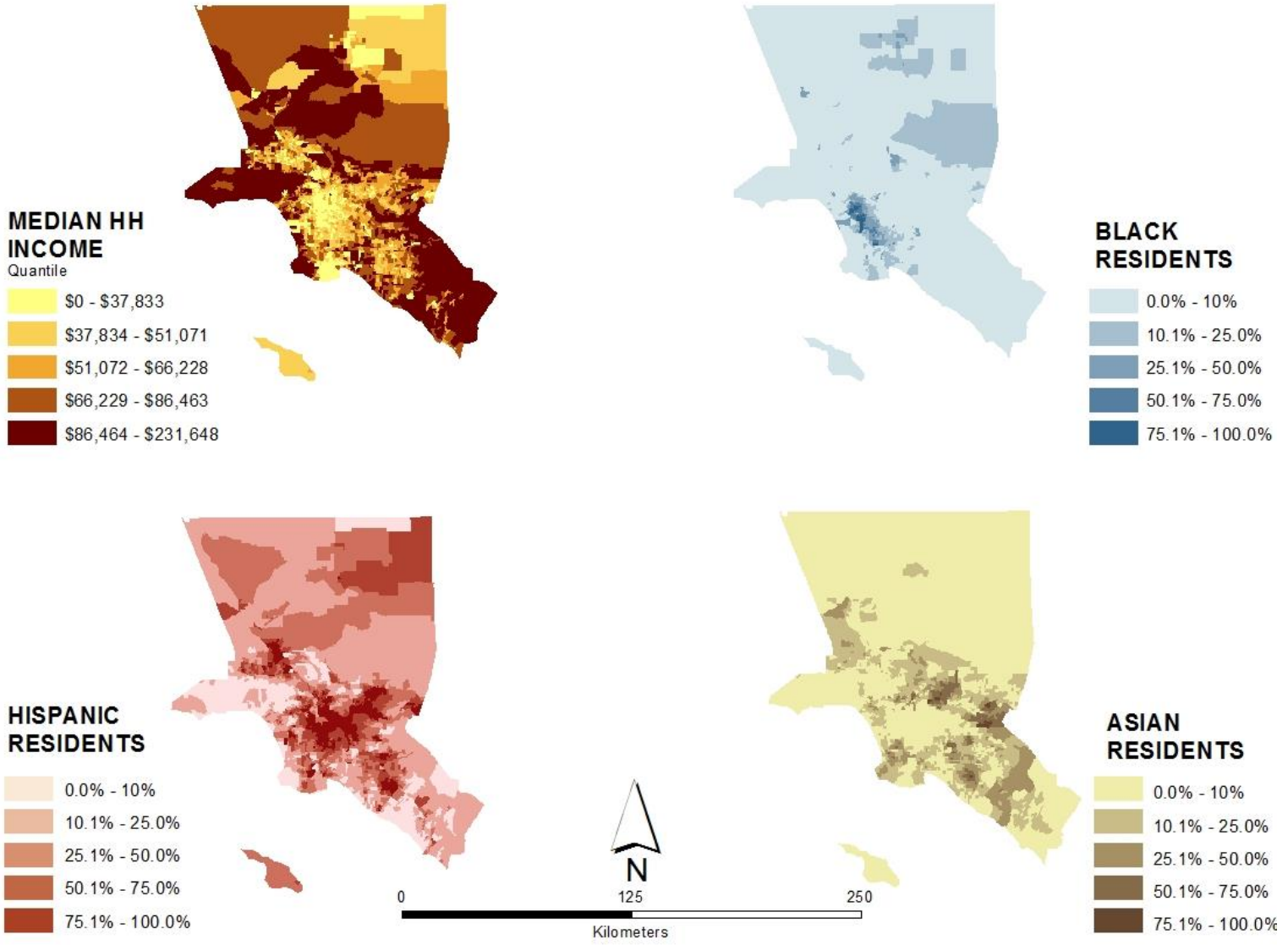

Memphis MSA NDVI, NDBI, and LST with UHRI

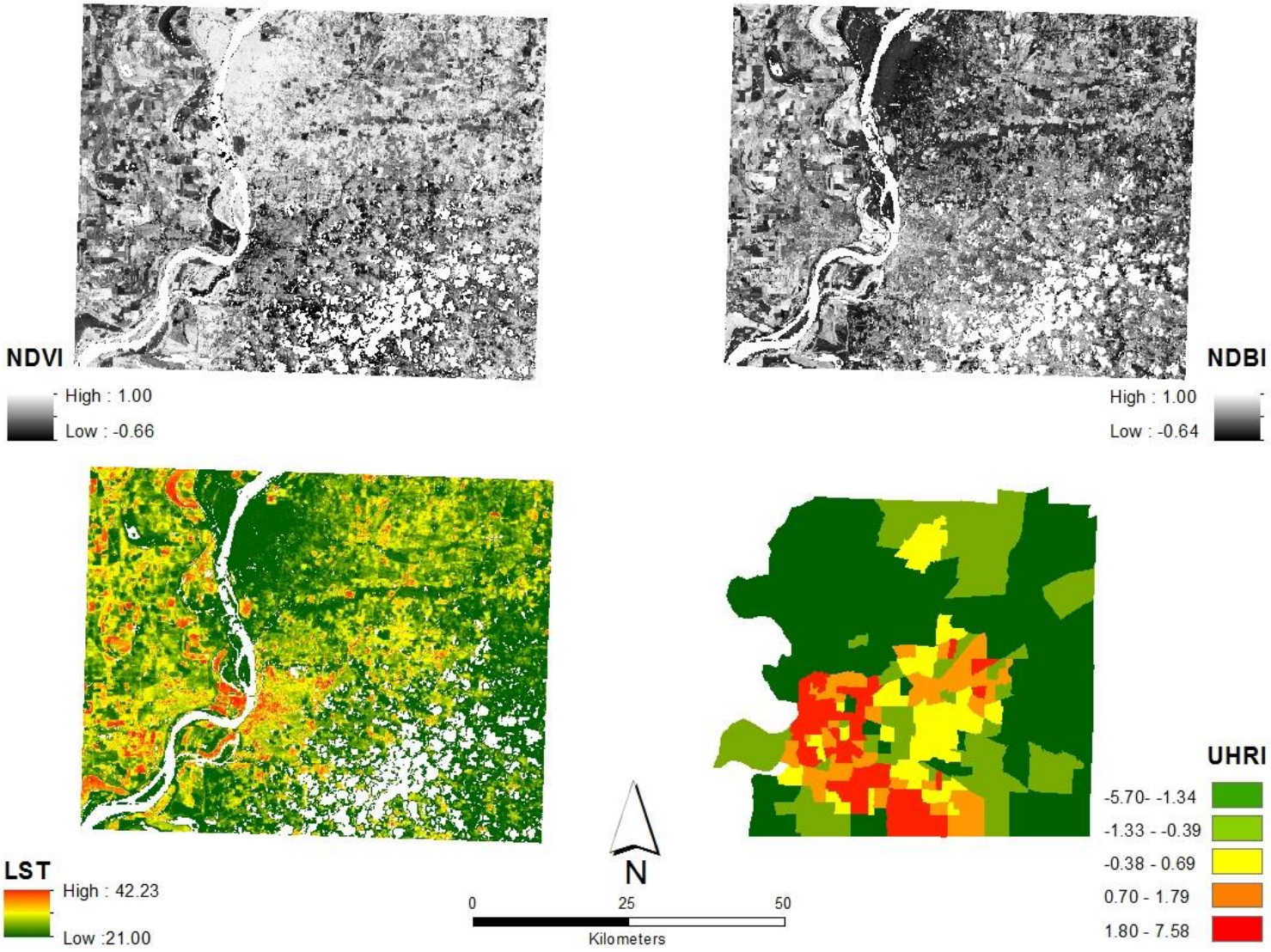

Memphis MSA median household income by quintile; percentage Black, Hispanic, and Asian population by tract

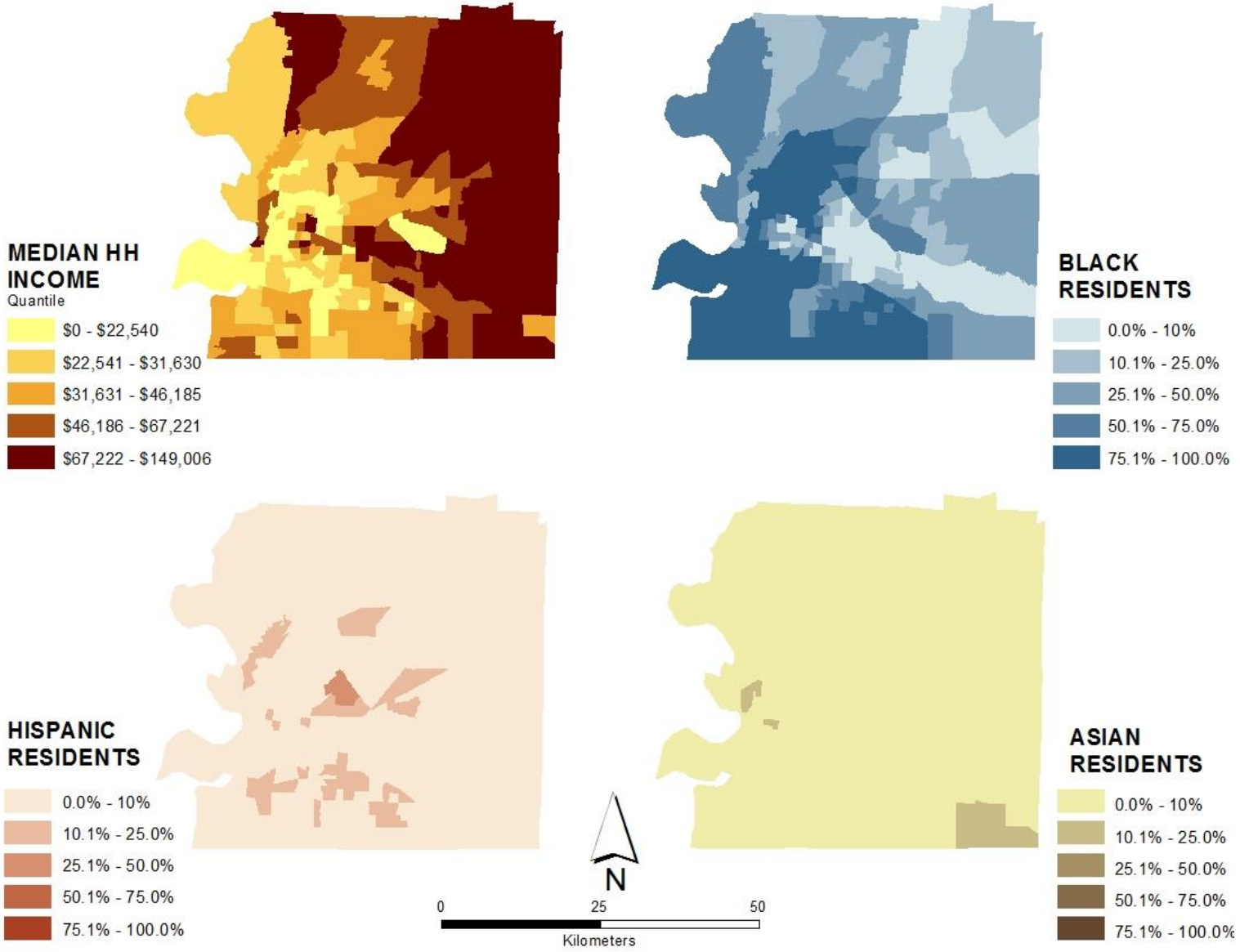

Minneapolis MSA NDVI, NDBI, and LST with UHRI

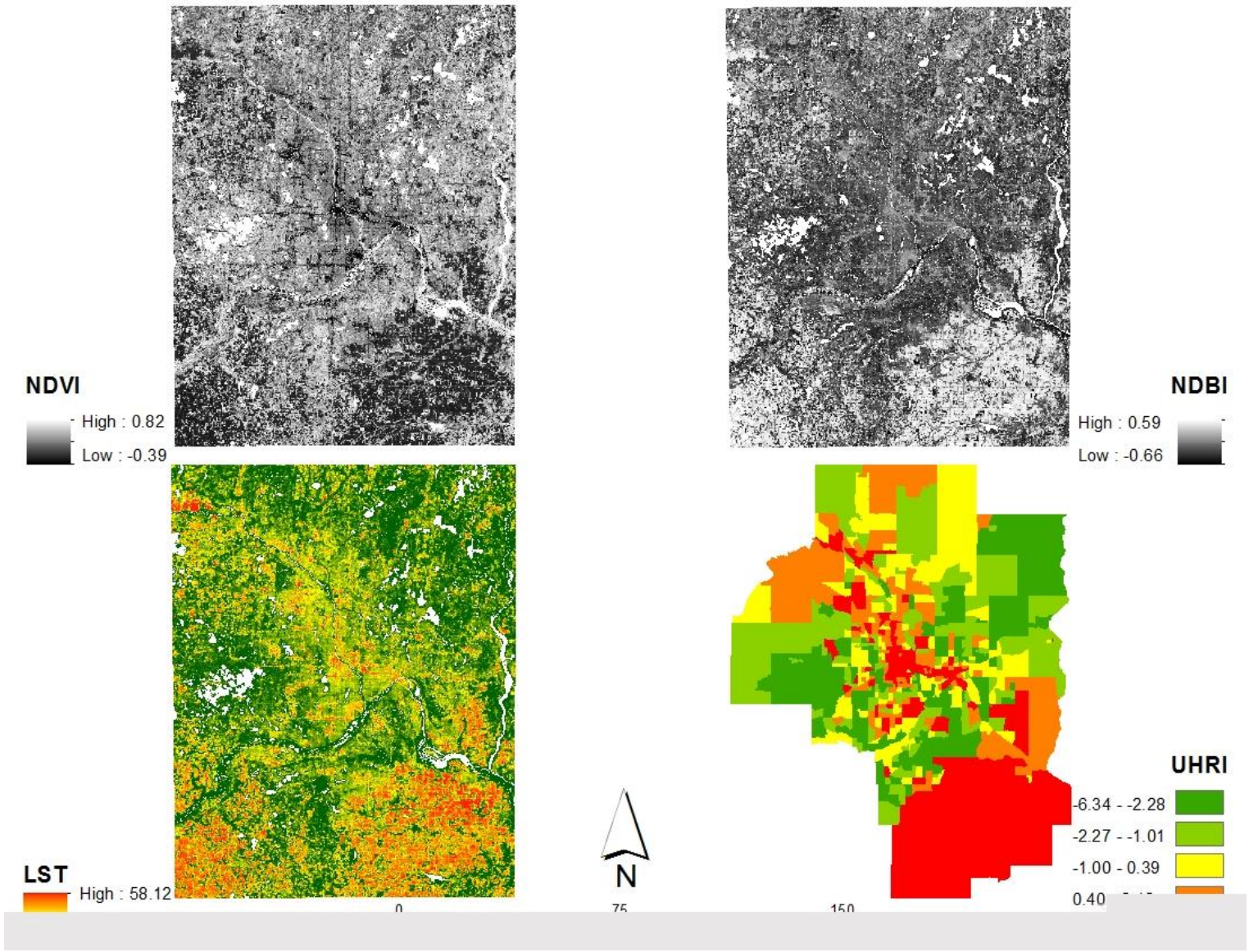

Minneapolis MSA median household income by quintile; percentage Black, Hispanic, and Asian population by tract

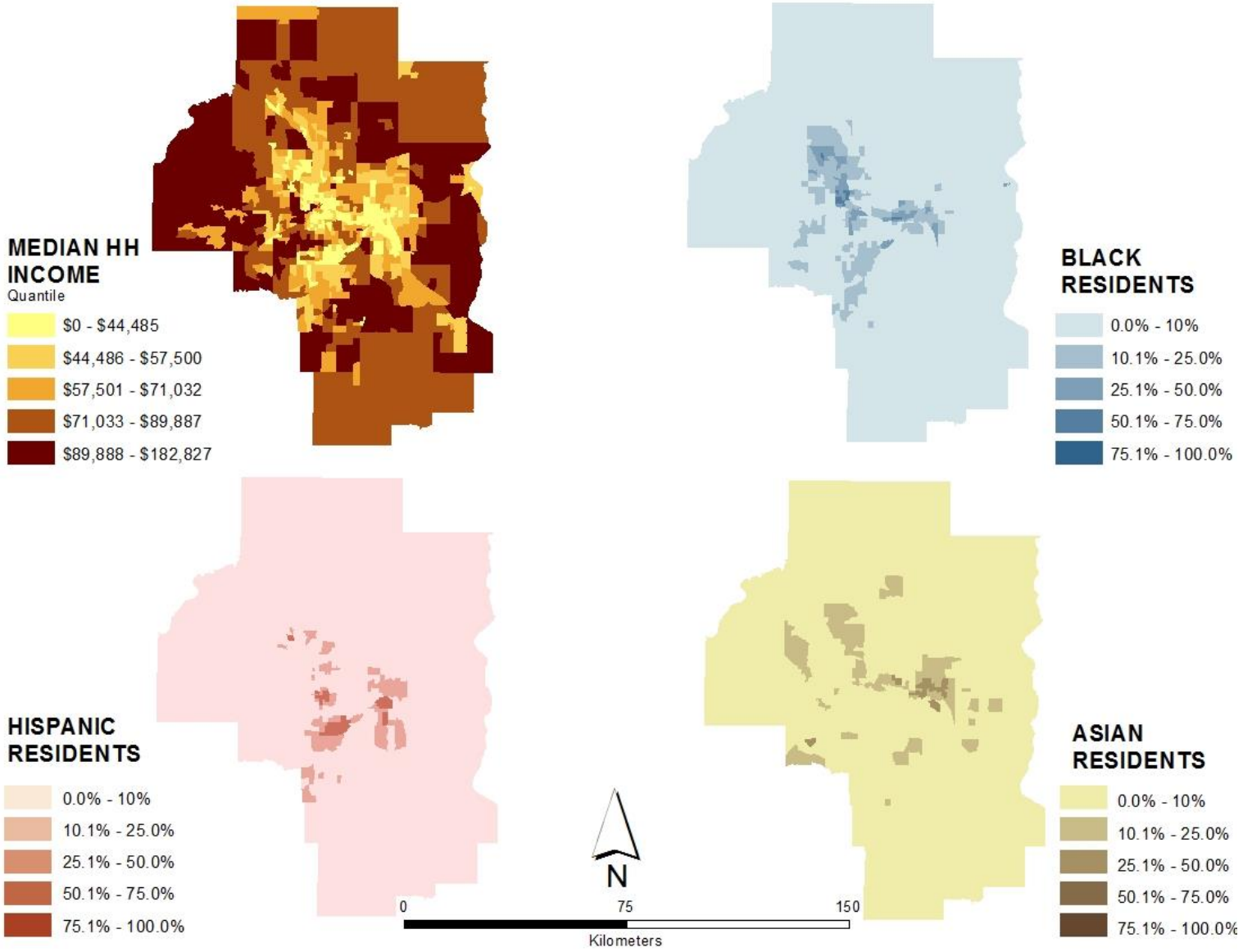

New York City MSA NDVI, NDBI, and LST with UHRI

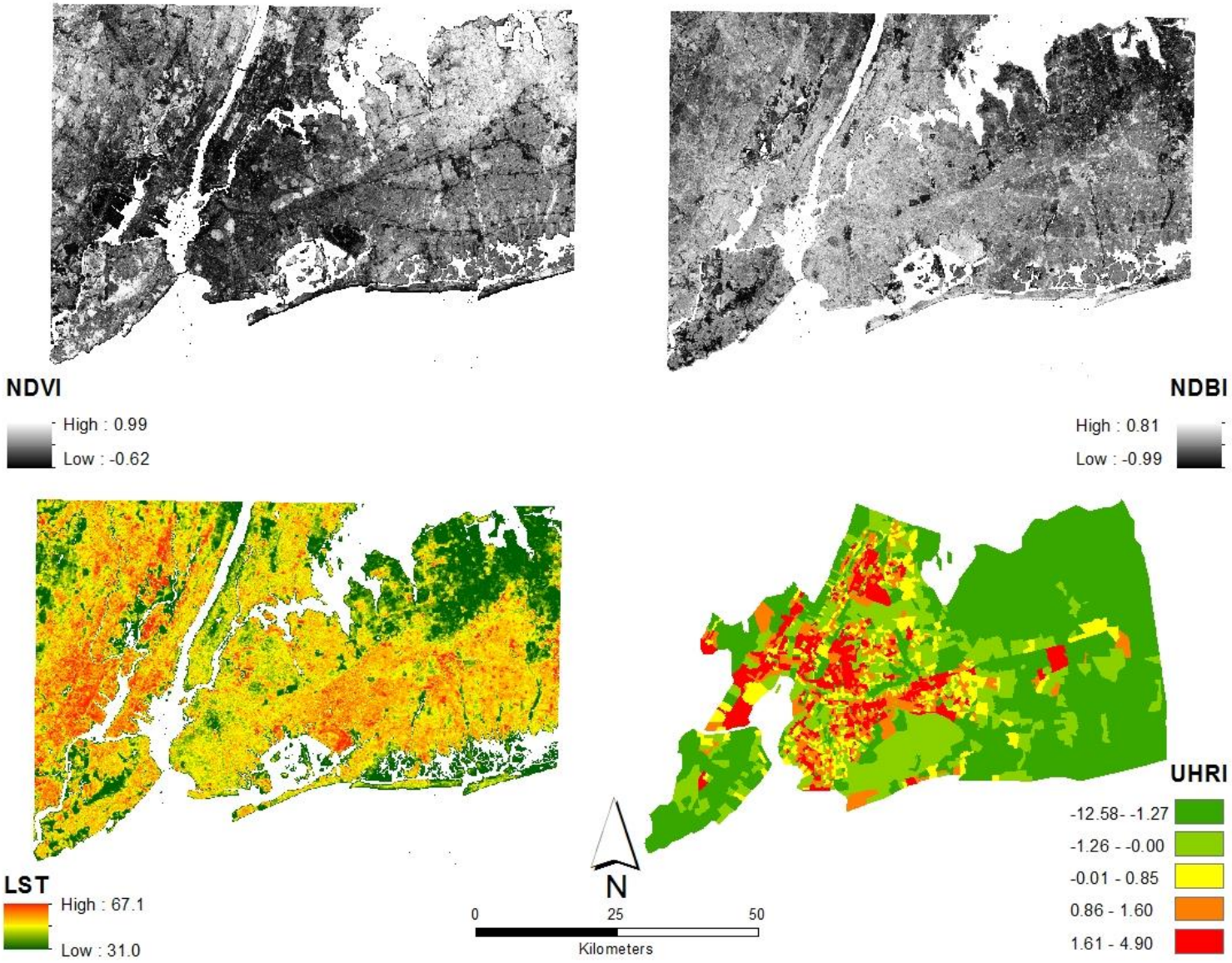

New York City MSA median household income by quintile; percentage Black, Hispanic, and Asian population by tract

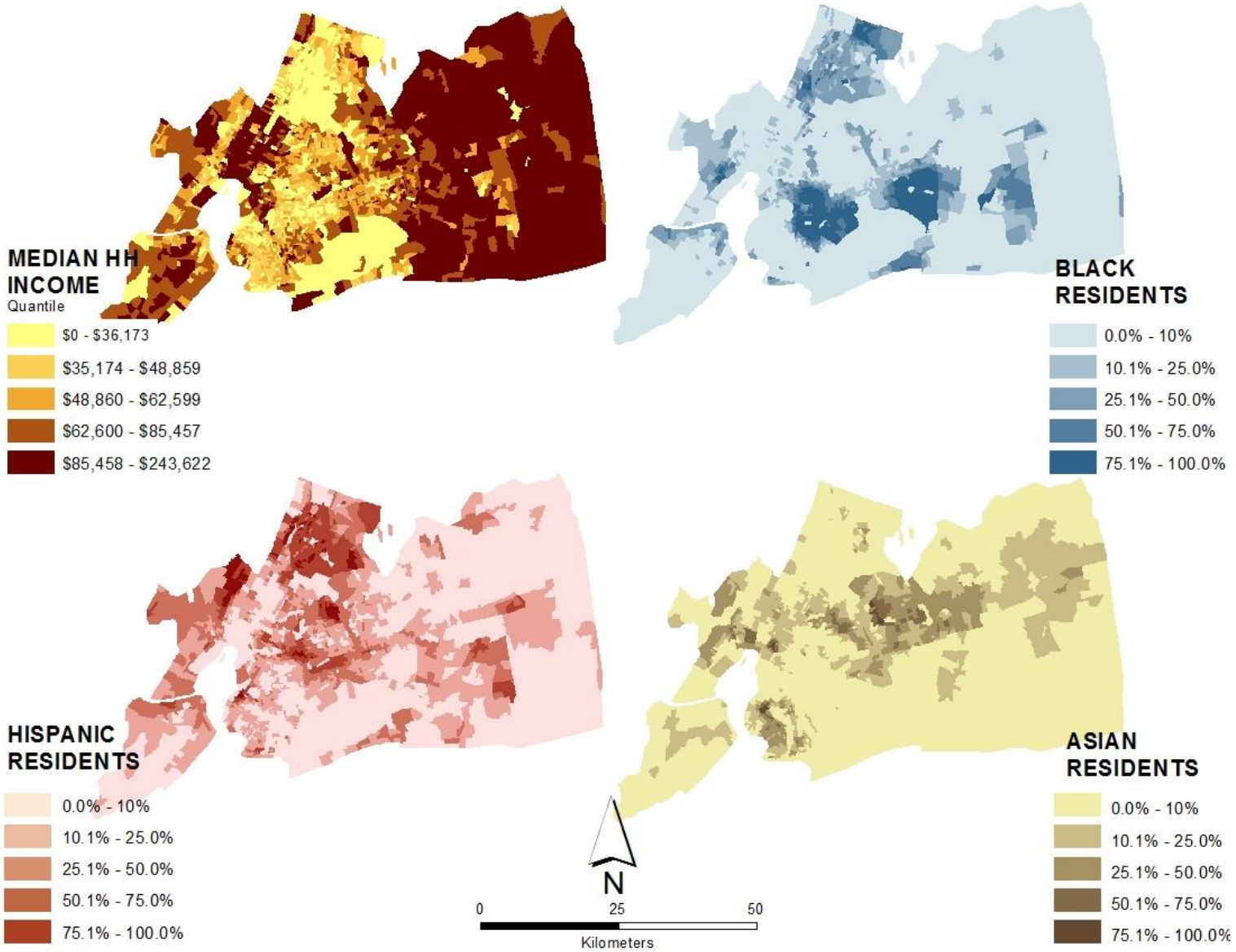

Philadelphia MSA NDVI, NDBI, and LST with UHRI

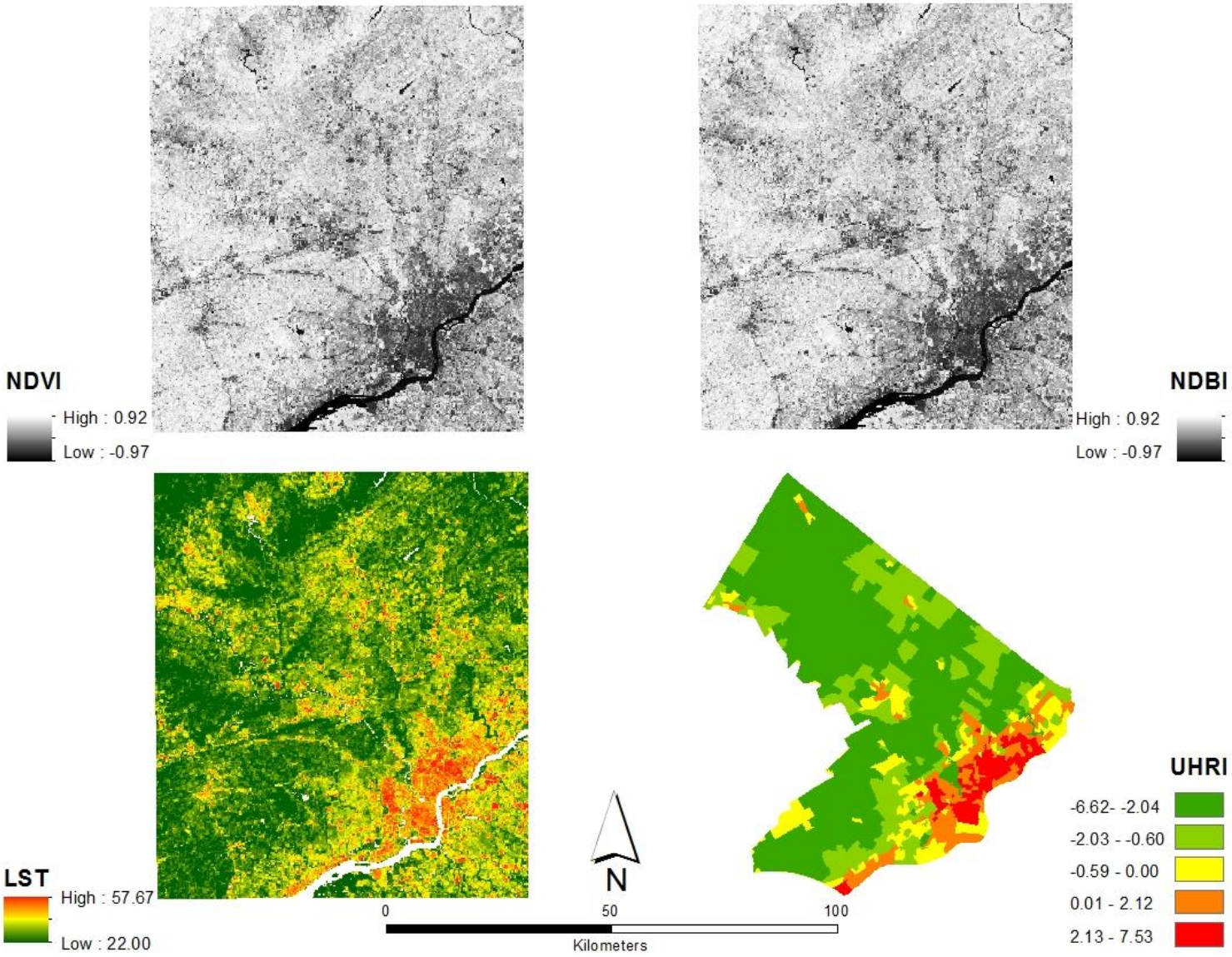

Philadelphia MSA median household income by quintile; percentage Black, Hispanic, and Asian population by tract

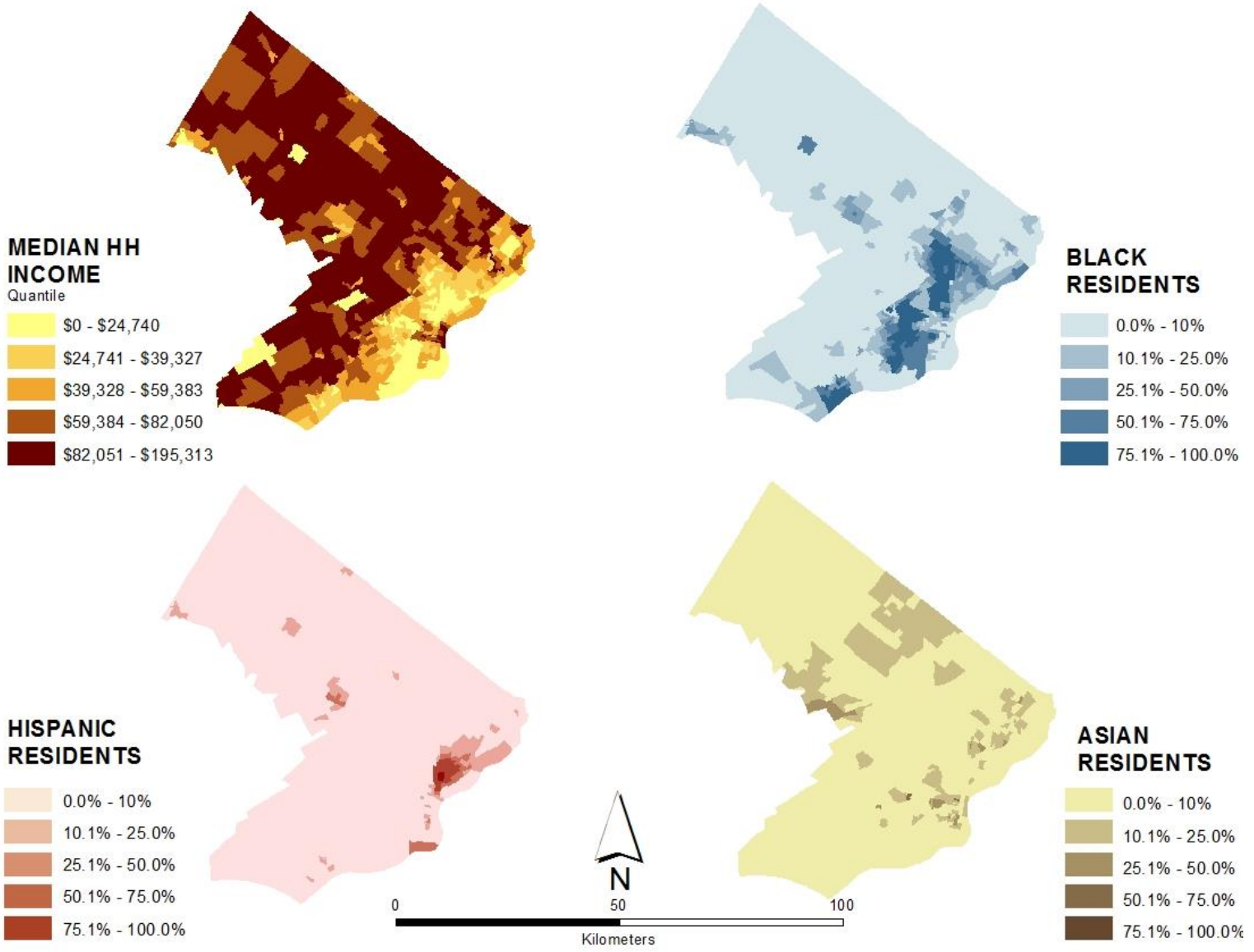

Phoenix MSA NDVI, NDBI, and LST with UHRI

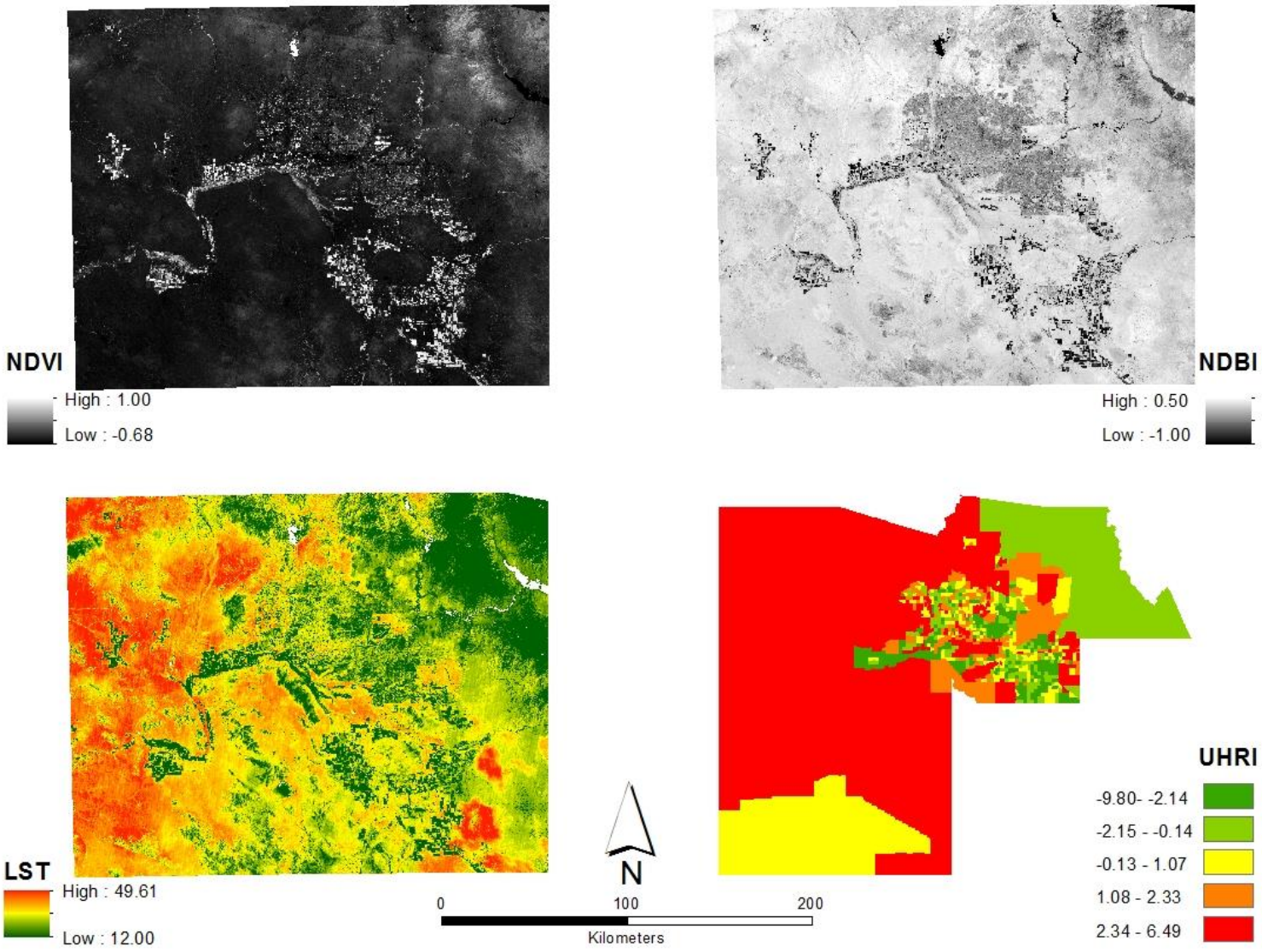

Phoenix MSA median household income by quintile; percentage Black, Hispanic, and Asian population by tract

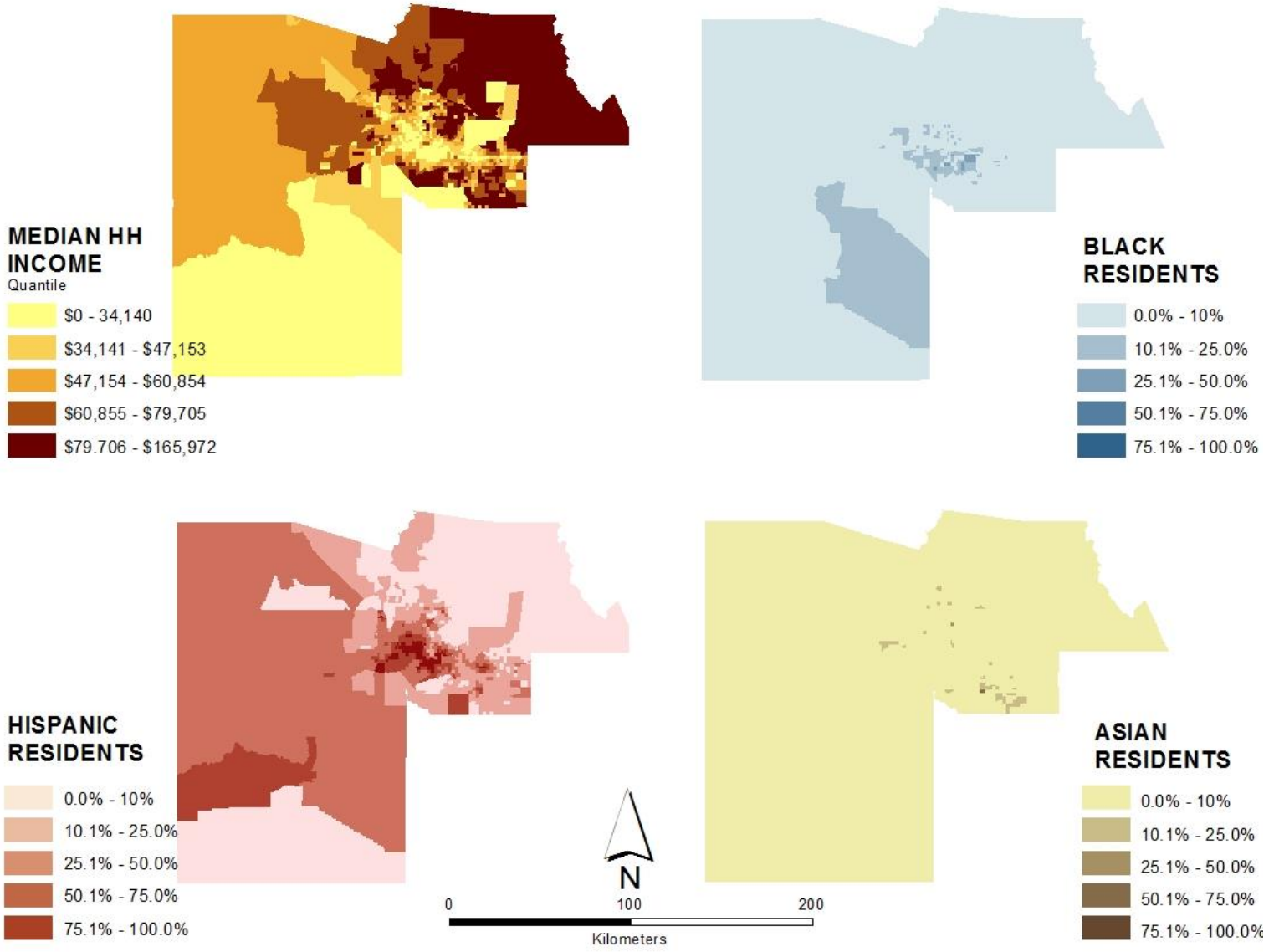

Portland, OR MSA NDVI, NDBI, and LST with UHRI

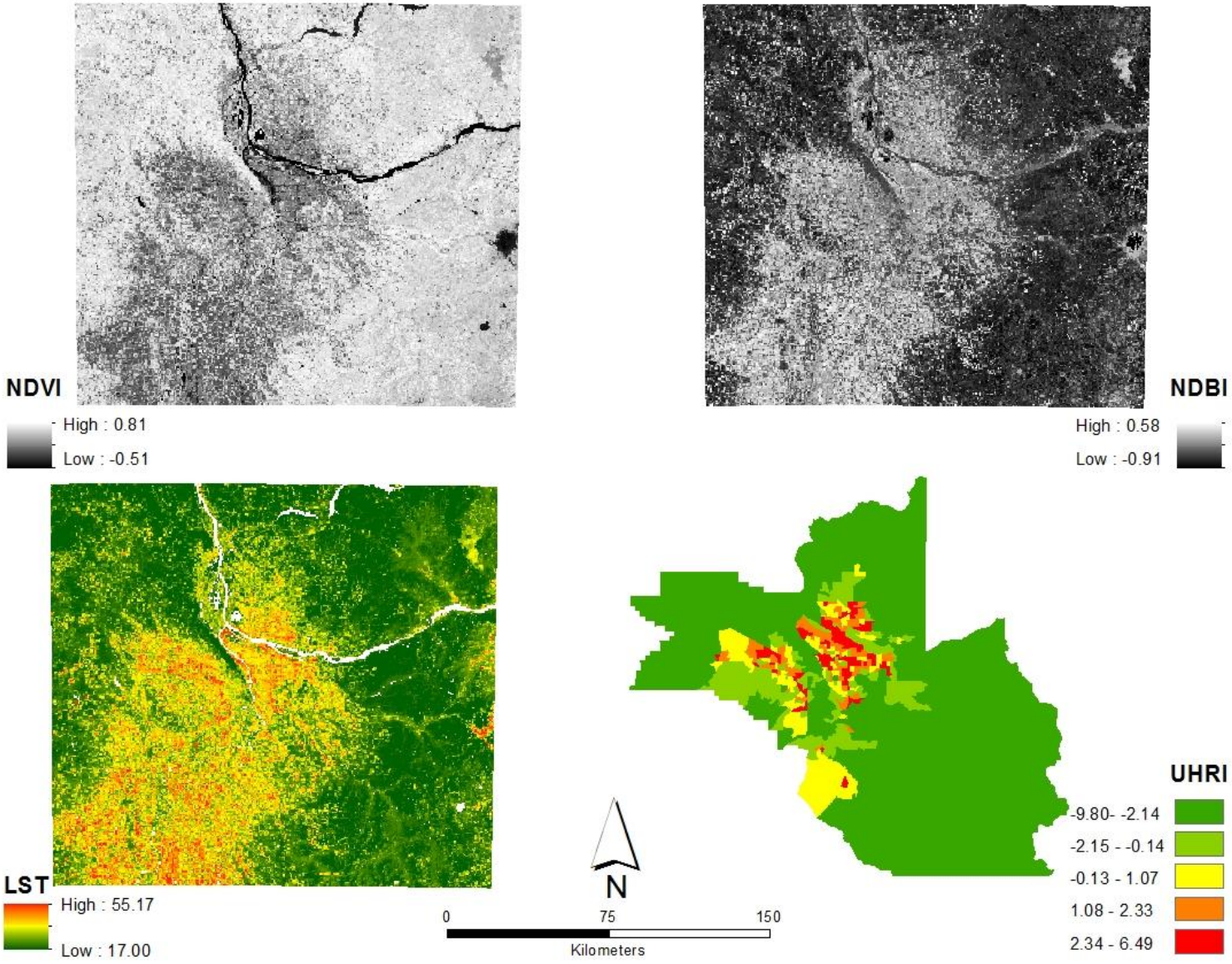

Portland MSA median household income by quintile; percentage Black, Hispanic, and Asian population by tract

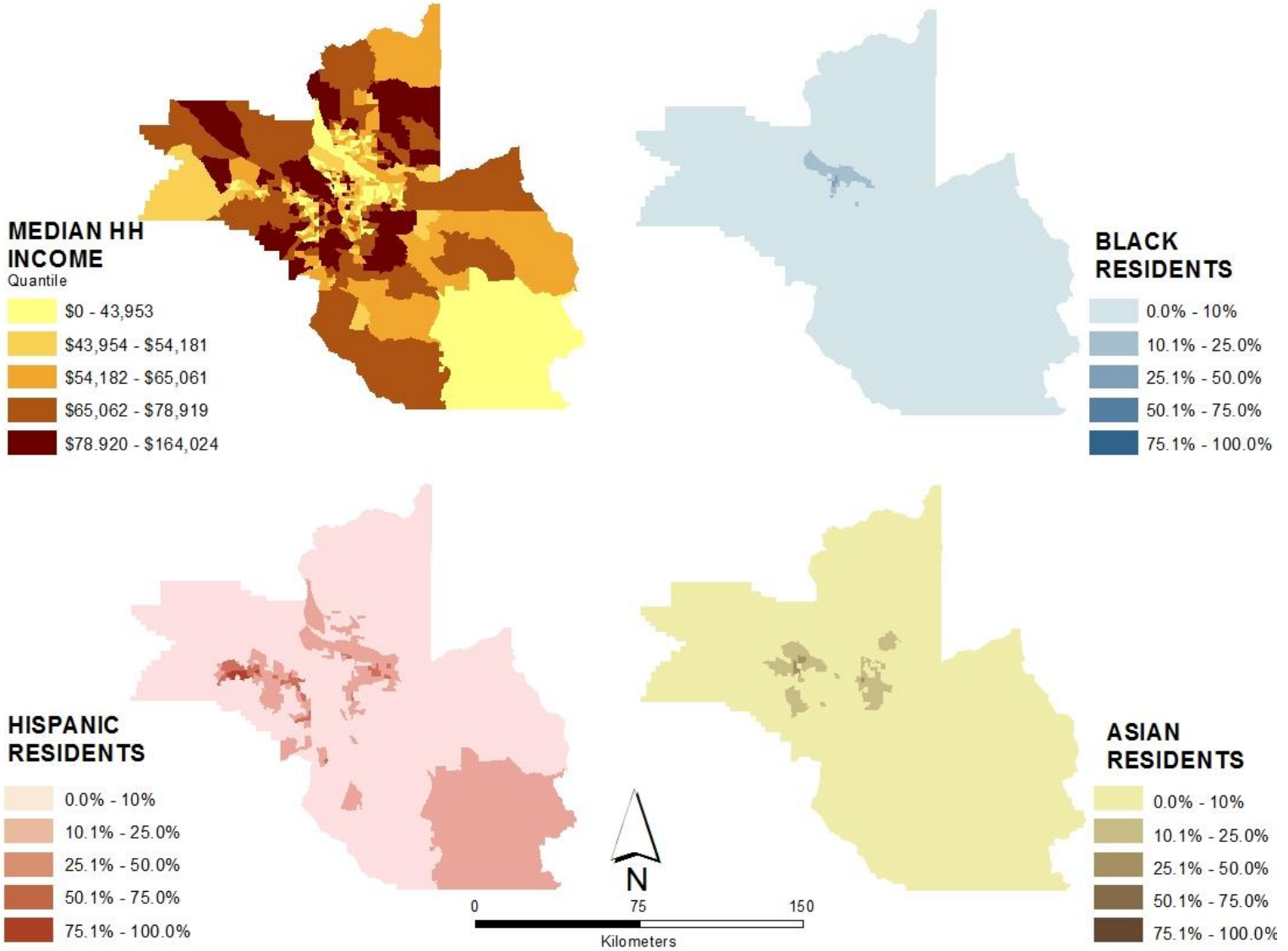

Providence MSA NDVI, NDBI, and LST with UHRI

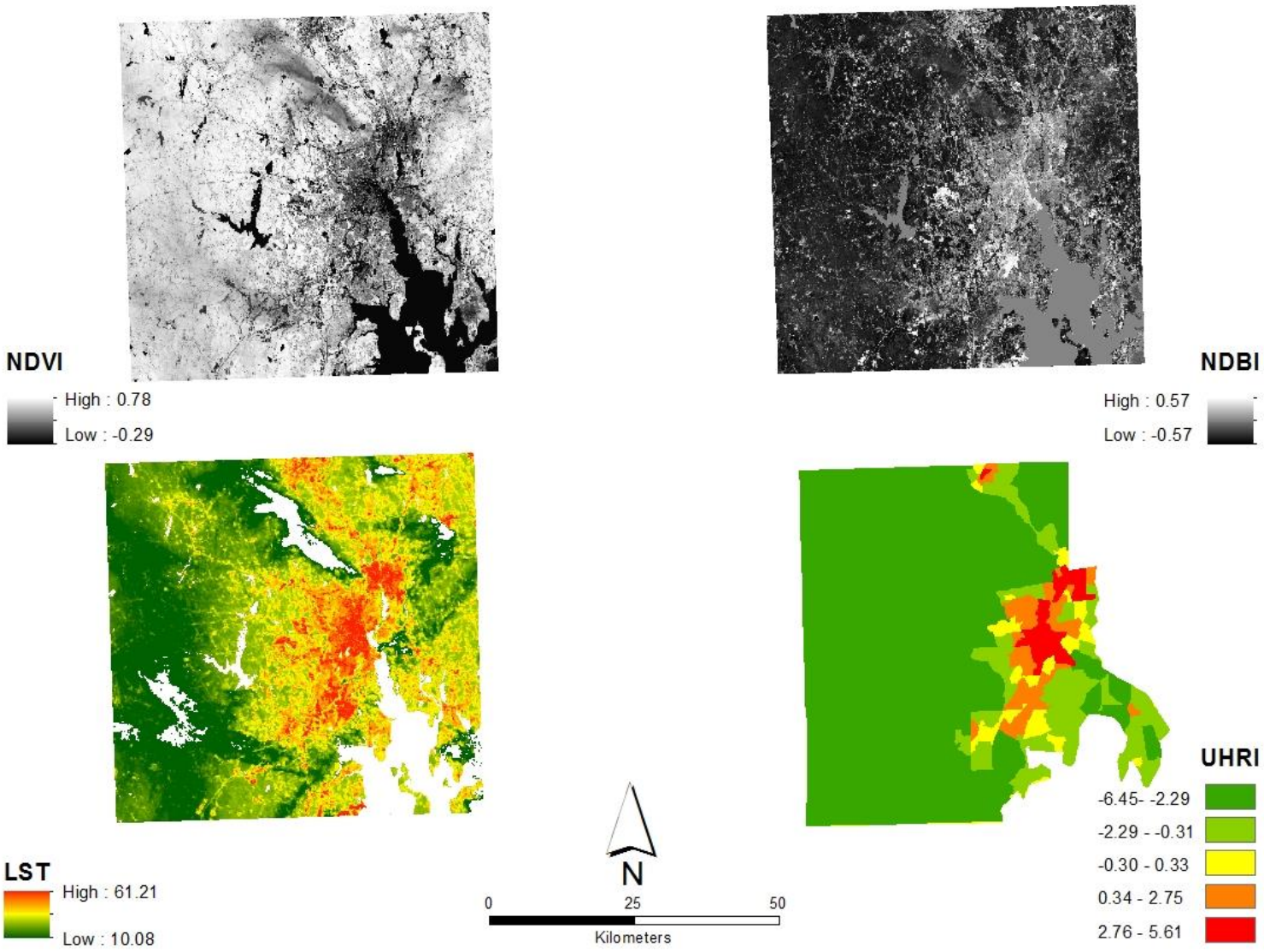

Providence MSA median household income by quintile; percentage Black, Hispanic, and Asian population by tract

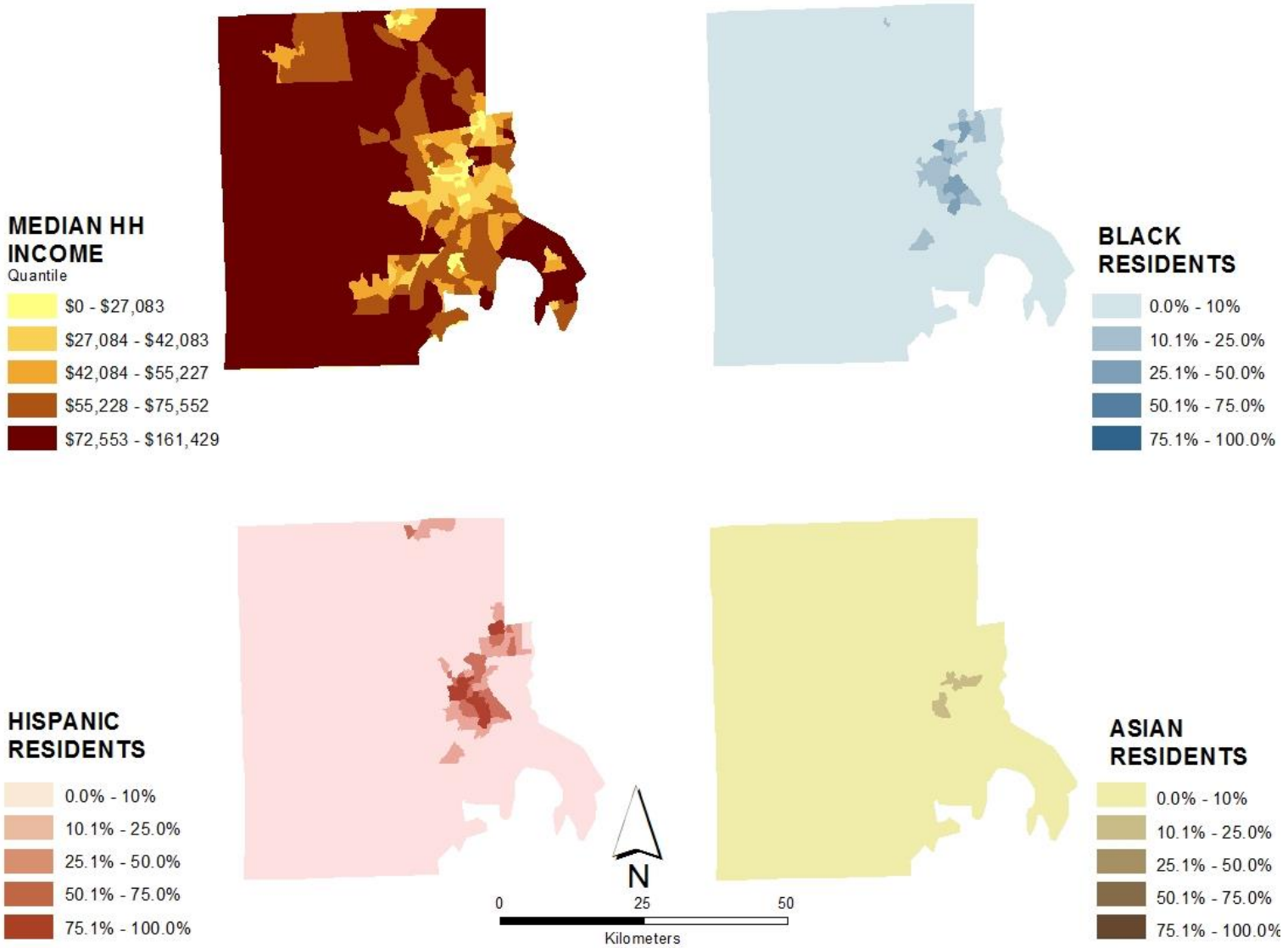

Seattle MSA NDVI, NDBI, and LST with UHRI

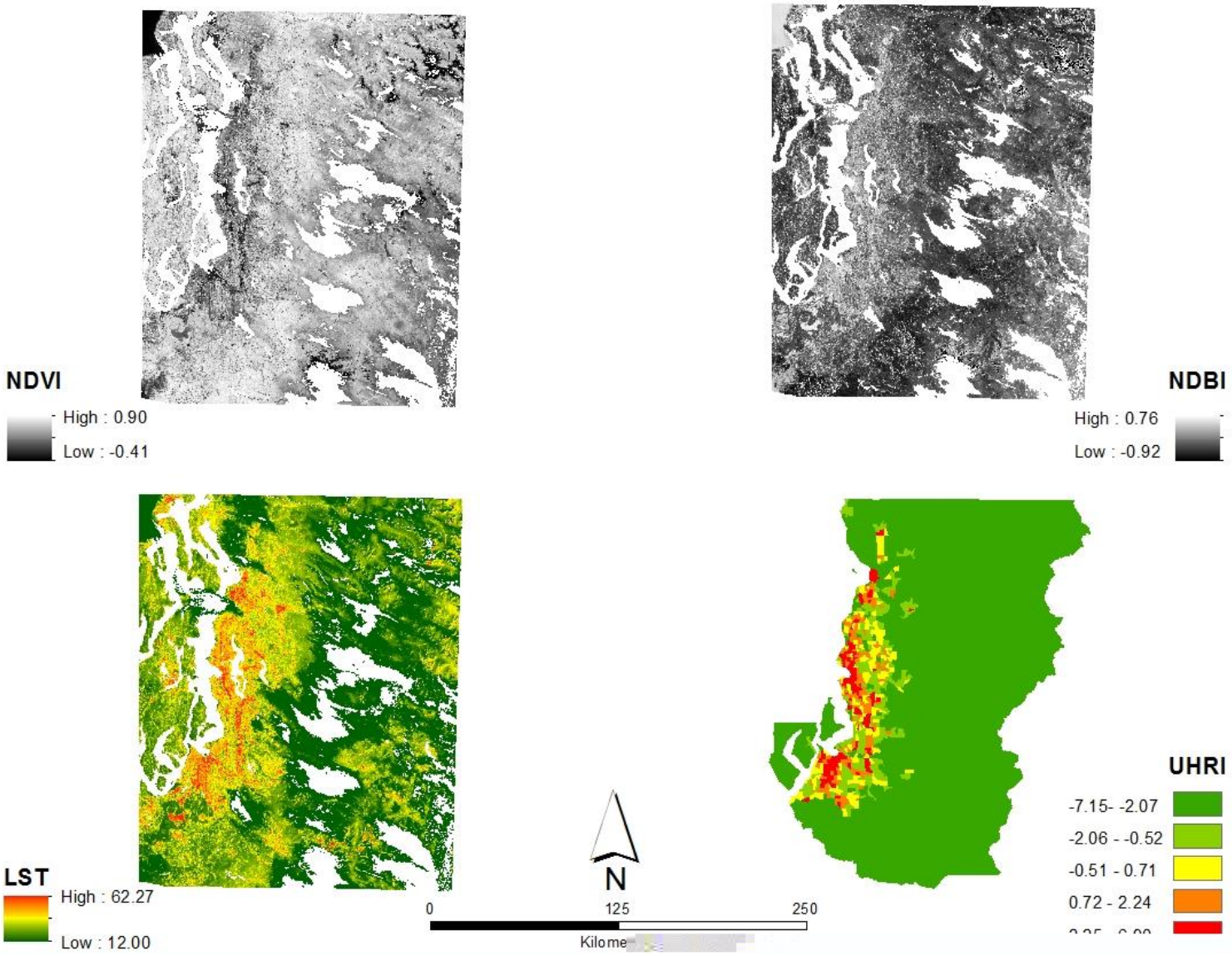

Seattle MSA median household income by quintile; percentage Black, Hispanic, and Asian population by tract

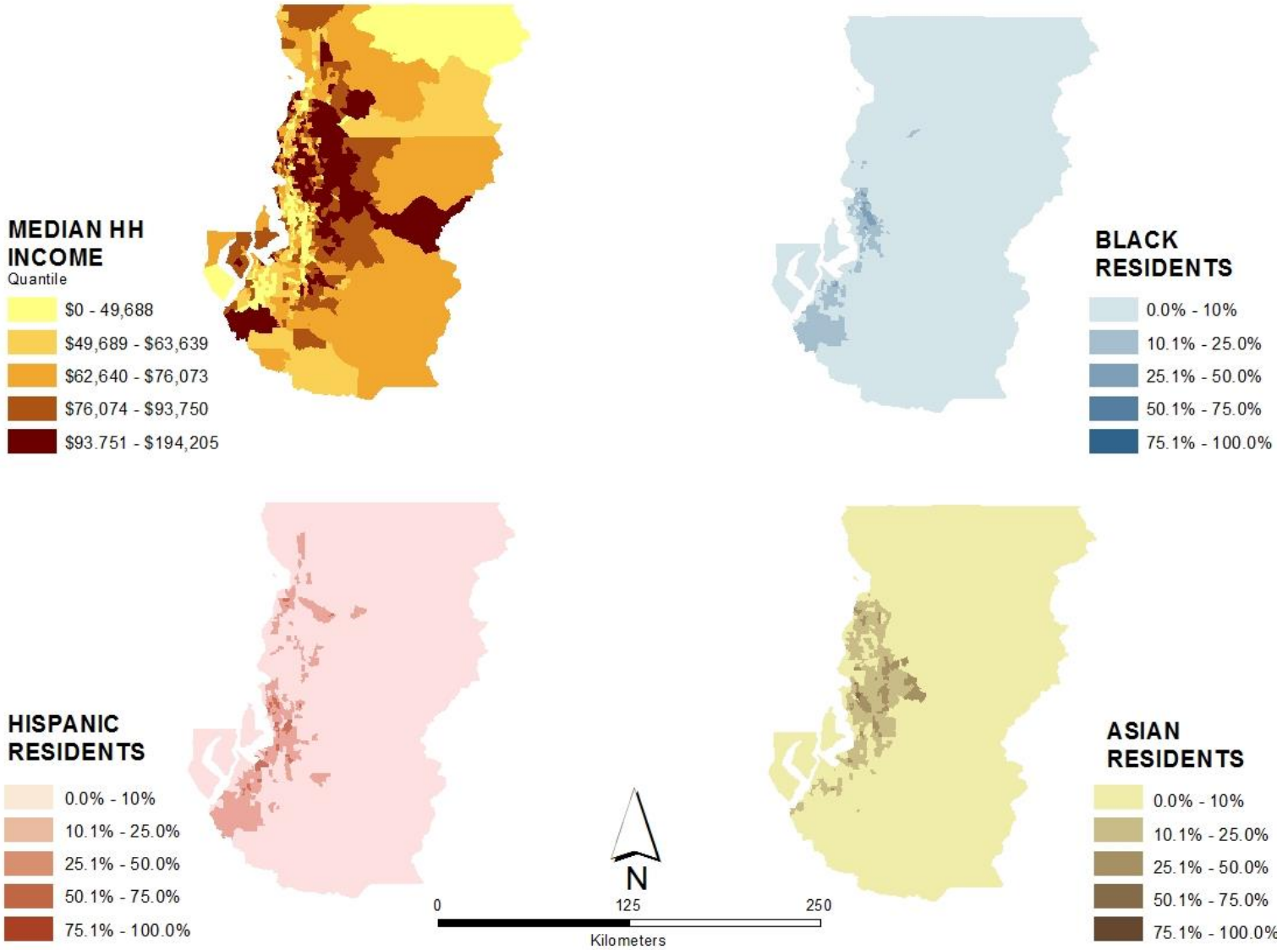

Saint Louis MSA NDVI, NDBI, and LST with UHRI

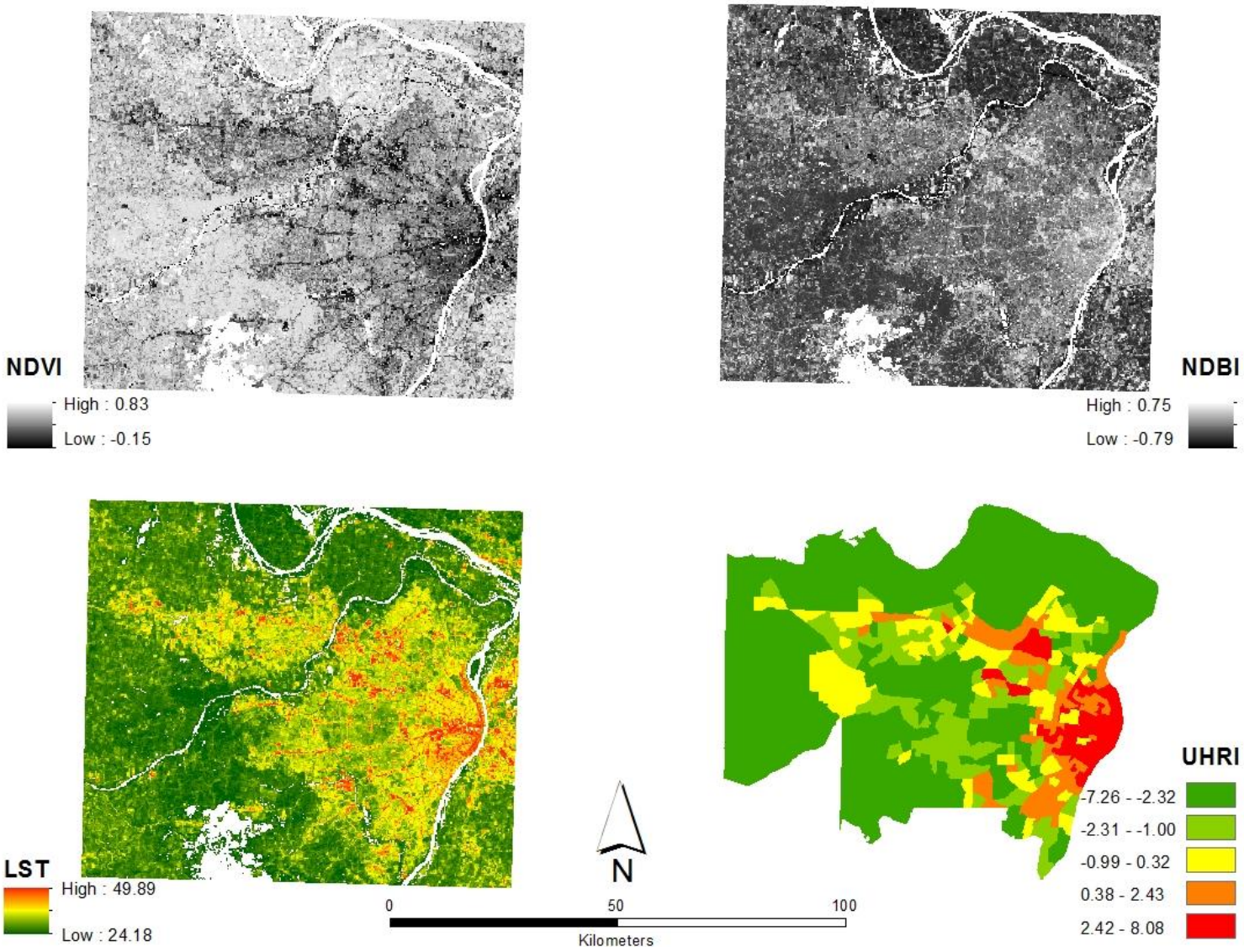

Saint Louis MSA median household income by quintile; percentage Black, Hispanic, and Asian population by tract

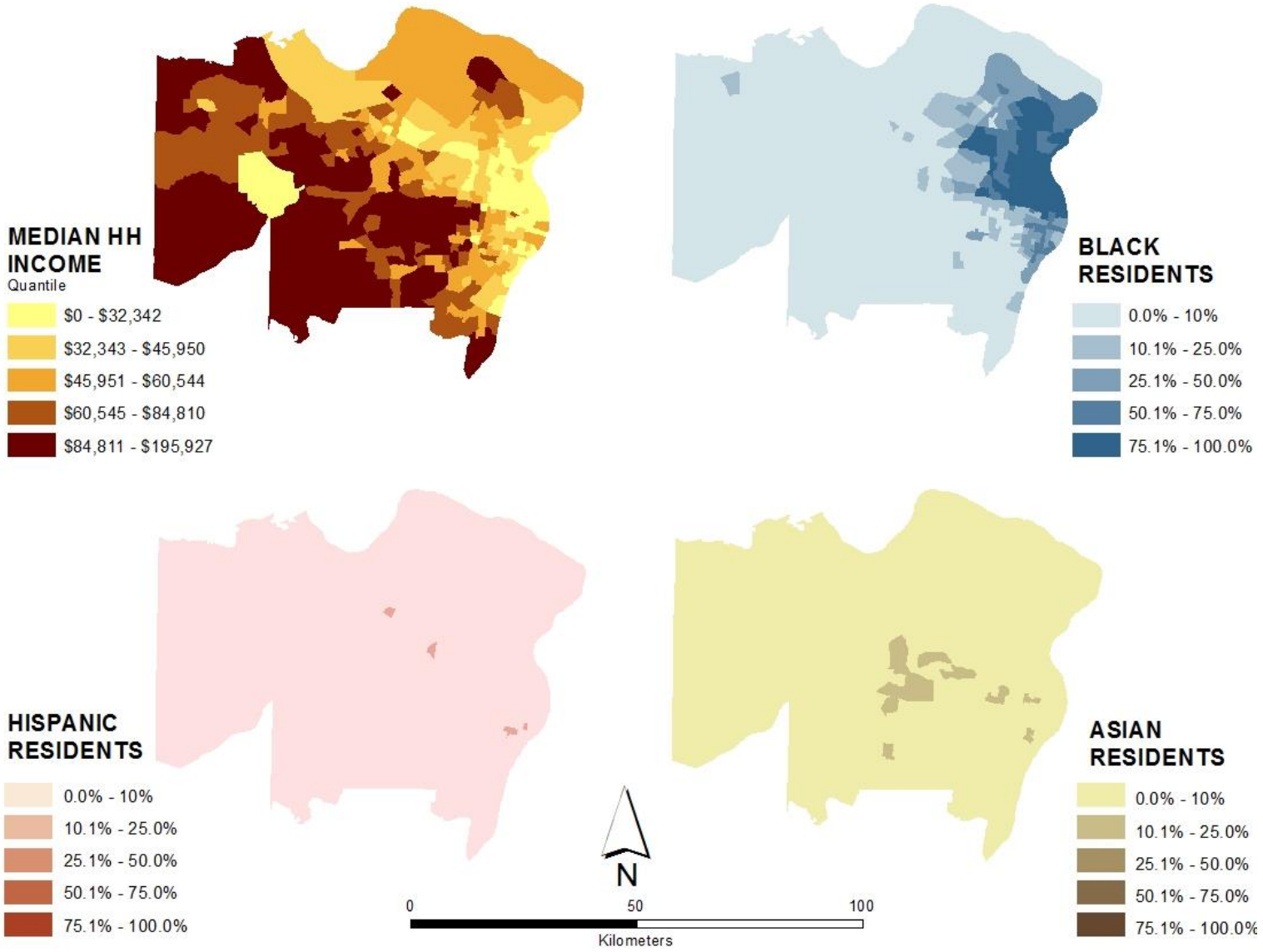

Tampa Bay MSA NDVI, NDBI, and LST with UHRI

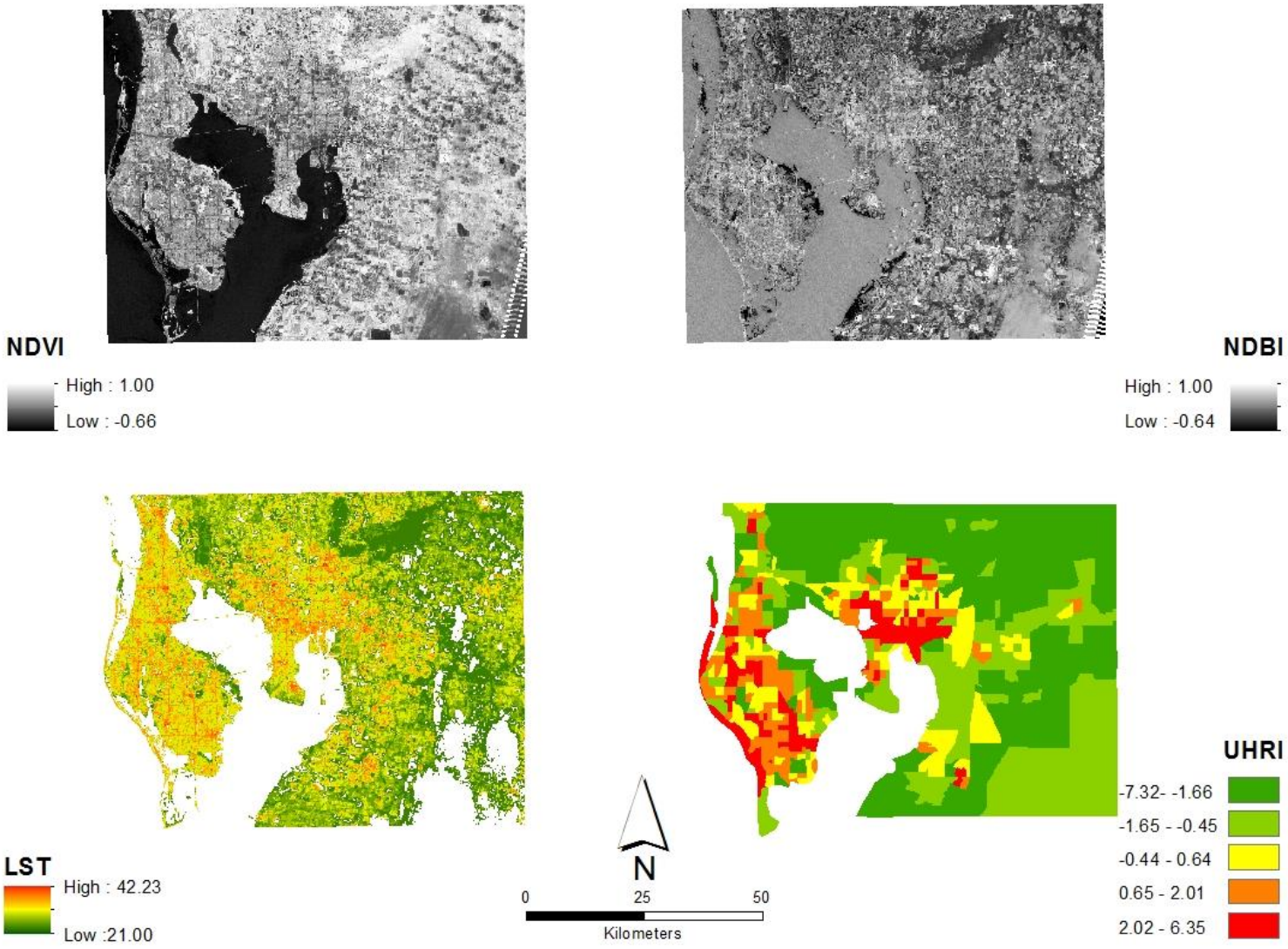

Tampa Bay MSA median household income by quintile; percentage Black, Hispanic, and Asian population by tract

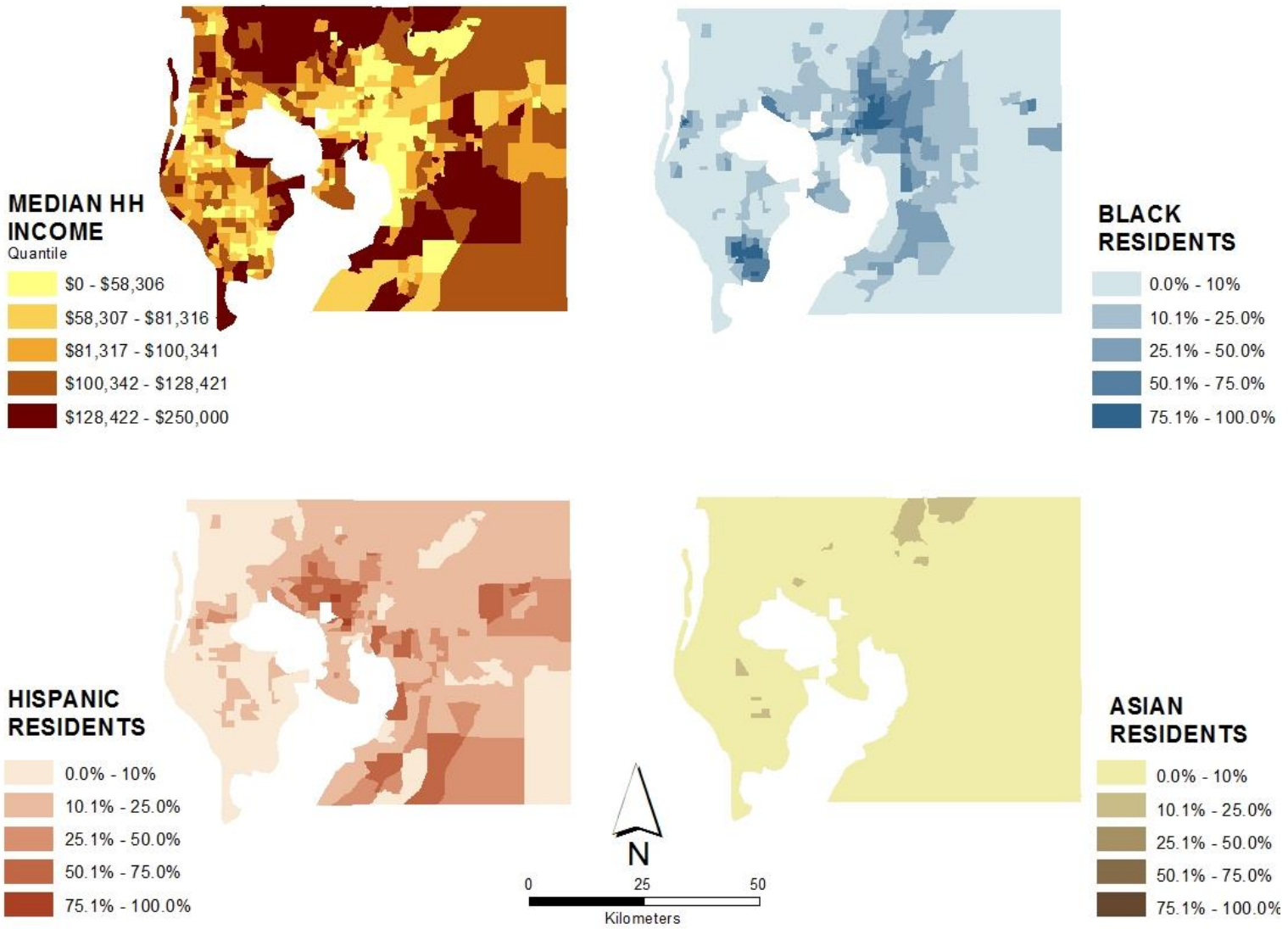

Washington D.C. MSA NDVI, NDBI, and LST with UHRI

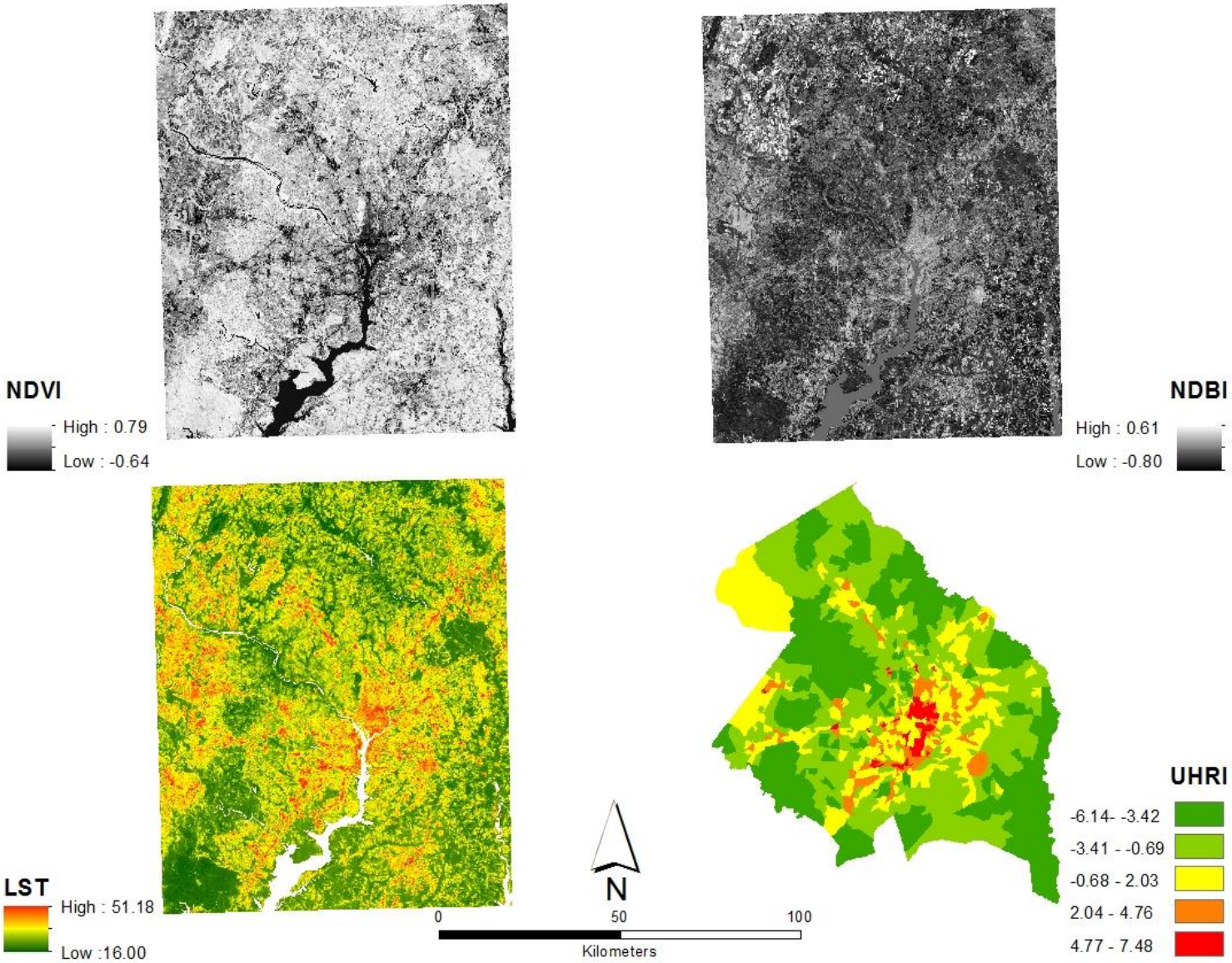

Washington D.C. MSA median household income by quintile; percentage Black, Hispanic, and Asian population by tract